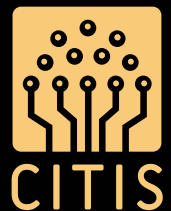Lenin E. Cevallos-Robalino / María Alejandra De La Cruz-Mora
/ Juan Alcides Cárdenas-Tapia sdb
(Coordinators)

X International Conference on Science, Technology and Innovation for Society

Proceedings Papers

CITIS

The Proceedings of the 10th International Conference on Science, Technology, and Innovation for Society (CITIS 2024) capture the transformative discussions and innovative knowledge that drive progress in scientific and technological fields. From the urgent challenges of environmental sustainability to continuous advances in information technology, telecommunications, and mobility, this anthology offers a comprehensive exploration of the most pressing frontiers in science and technology.

The conference, held in July 2024 at the Universidad Politécnica Salesiana in Guayaquil, Ecuador, brought together distinguished academics, researchers, and professionals whose contributions reflect a collective commitment to building a more inclusive, sustainable, and technologically advanced society. These pages stand as a testament to joint efforts to address global challenges and propose innovative solutions for a better future.

Academic research plays a fundamental role in the development of nations, providing the foundation for innovation and continuous improvement. In Ecuador, such efforts are vital to strengthening key sectors such as education, industry, and technology, driving economic growth and enhancing global competitiveness. The works presented at this conference not only highlight the talent and research capacity of academia but also serve as an essential pillar for policy formulation and the creation of solutions that improve the quality of life for all citizens.

Lenin E. Cevallos-Robalino, Ph.D.
July 2024

X International Conference on Science, Technology and Innovation for Society

Proceedings Papers

Lenin E. Cevallos-Robalino
María Alejandra De La Cruz-Mora
Juan Alcides Cárdenas-Tapia sdb
(Coordinators)

X International Conference on Science, Technology and Innovation for Society

Proceedings Papers

CITIS

July 2024

X INTERNATIONAL CONFERENCE ON SCIENCE, TECHNOLOGY AND INNOVATION FOR SOCIETY. PROCEEDINGS PAPERS
Lenin E. Cevallos-Robalino / María Alejandra De La Cruz-Mora /
Juan Alcides Cárdenas-Tapia sdb (Coordinators)

Index

Introduction

Imagine a world where science, technology, and innovation join to create a sustainable future. This was the vision of the Tenth International Congress on Science, Technology, and Innovation for Society (CITIS X). For three days, from July 17 to 19, 2024, Guayaquil became a knowledge hub, where international brilliant minds gathered to share their latest ideas and findings. In this academic record, we invite you to delve into the fascinating discussions and outcomes of this gathering held at the María Auxiliadora campus of the Polytechnic Salesian University in Guayaquil, Ecuador.

CITIS X represented a milestone in national research, with the participation of over a thousand researchers, educators, and students from various national and international institutions that reflected the commitment of our academic community to the generation. Expert lectures addressed relevant topics in fields such as renewable energies, artificial intelligence, and the environment. These lectures enriched the exchange of knowledge and experiences, establishing the congress as a global reference.

With more than 188 presentations, the congress showcased the vitality of research in our country, featuring a high-quality program that included 45 oral presentations, 11 poster sessions, and 7 technical workshops, each being a a valuable elementin research.

This book shows the reflection of a community of researchers who shared their passion at CITIS X. On each page presents a treasure trove of ideas, a testament to the diversity of talents and perspectives that gathered in Guayaquil. We hope this work will be an inexhaustible source of inspiration, a companion for reflection, and an invaluable guide for future research projects.

The Academic Memoir of CITIS X is an invitation to explore new horizons and to use knowledge to tackle global challenges. Immerse yourself in these pages and allow the ideas presented here to resonate you. This book is more than just a collection of words; it encapsulates the essence of a gathering that transcended the boundaries of knowledge. Its pages are a legacy of innovative ideas and a call to continue building a prosperous future. We hope that these memoirs will inspire future generations of researchers and serve as a catalyst for new discoveries and

collaborations that strengthen the scientific community and foster new alliances to address global challenges.

The true value lies in how each reader makes these ideas their own and applies them to transform the world around us. We thank all the participants and collaborators who made CITIS X a memorable event. Thanks to their invaluable contributions, we achieved an enriching gathering that left an indelible mark on our scientific community.

Lenin Estuardo Cevallos-Robalino, Ph.D. and Alejandra De la Cruz MSc
Chairpersons of the Organizing Committee of CITIS 2024

A literature review focused on current trends and practices in web application development

Daniel Patiño-Vásquez
Universidad Politécnica Salesiana, (Ecuador)
Orcid: https://orcid.org/0000-0002-7286-7872

Joe Llerena-Izquierdo
Universidad Politécnica Salesiana, (Ecuador)
Orcid: https://orcid.org/0000-0001-9907-7048

Introduction

As time has progressed, web application development has experienced accelerated growth, becoming an essential component for companies looking to provide high quality technology solutions. The proper use of technologies such as Angular, Node.js, JWT, Bcrypt and MySQL has proven to be essential to create scalable, efficient and secure systems.

Recent studies such as (Effendy et al., 2021) have provided a comparative view of performance between backend and database technologies, highlighting crucial differences that affect overall system performance. The relevance of tools such as MySQL Workbench for the effective management of critical data has also been important (Krogh, 2020).

Despite these advances, there is still a need for a deeper understanding of how these technologies can be synergistically integrated. In this context arises the relevance of exploring and developing a prototype ecosystem that allows an effective integration of these popular technologies in the development of web systems.

Based on the above context, the main objective of this review is to provide a theoretical framework to support the proposed research. It seeks to analyze the evolution of web systems development, examine the relevance of the specific technologies mentioned and review the existing literature on the effective integration of these technologies.

This paper impacts the literature review since it focuses on understanding how these technologies have been used in studies of relevant work, highlighting their advantages and challenges.

Likewise, its rationale seeks to identify success stories and areas where current research can be expanded. This analysis will establish the necessary context for the design and implementation of the prototype, as well as for the subsequent evaluation of its effectiveness in terms of agility, standardization, security, and efficiency in the development of web projects.

Finally, the main objective of this paper is to contextualize and substantiate the proposed research on the development of a prototype ecosystem for the effective integration of popular technologies in the development of web systems, including Angular, Node.js, JWT, Bcrypt and MySQL. This paper arises in response to the fast-paced evolution of web application development and the growing importance of specific technologies in this area.

State of the Art

Historical evolution of web systems development

In the context of the historical evolution of web systems development, a major milestone occurred in November 1990 with the proposal by Tim Berners-Lee and Robert Cailliau of a hypermedia system called "The World-Wide Web". This proposal marked the beginning of the creation of the first web application. Subsequently, in 1991, Tim Berners-Lee implemented the first web server and the first web browser, giving rise to the practical operation of the World Wide Web.

This innovation enabled the creation of the first web pages and laid the foundations for the subsequent development of web systems. The initial web application, although rudimentary compared to today's technologies, introduced the notion of interconnected documents through hypertext links, paving the way for the expansion and continued evolution of web systems over the decades. This historical milestone is crucial to understanding the emergence and transformation of web applications and systems in today's technological landscape (Dene & James, 2021).

The first generation of the Web, which emerged in 1991, was characterized as an information environment where users could only read and share static data. Although it offered advantages such as unique access and autonomy for content creators, it presented technological challenges and interactivity limitations. The inability of users to edit data and lack of participation led to less traffic and advertising. Web 1.0 is considered a closed and less user-friendly stage, marking the beginning of the need to transform to a more interactive and participatory web (Nath, 2022).

Due to the need to interact and share knowledge, Web 2.0 was born around 2003. Web 2.0 was used especially through Virtual Communities of Practice (VCoPs), which are innovative groups that take advantage of information technologies to create and share knowledge. At that time, knowledge management, knowledge creation and the crucial role of information techno-

logies and Web 2.0 in transforming the way people interact and share knowledge in various organizational, educational and political contexts were important (Ziegler, 2022).

In 2007, the well-known Web 3.0 emerged, proposing a change towards a decentralized Internet, where users are the main creators and arbiters of value. It arises as a response to the criticisms of centralization in Web 2.0. Proponents seek a blockchain-based structure, highlighting social, economic, and cultural changes. Socially, it redefines interactions and communities; economically, it introduces user-centric value creation with technologies such as NFT and DeFi; culturally, it empowers creators (Chohan, 2022).

The latest generation is the web 4.0, which has its first impressions at the beginning of 2016, and represents a revolution in the way people interact with online information. Web 4.0 is envisioned as an intelligent and symbiotic network that involves interaction between humans and machines. It is expected to integrate technologies such as big data, augmented reality, machine-to-machine communication, cloud computing and artificial intelligence with intelligent agents. Web 4.0 is perceived as a revolutionary technology that connects the Internet with new objects, enabling advanced interactions in various contexts (Ersöz et al., 2020).

The evolution of web systems, from the conception of "The World-Wide Web" in 1990 to the present day, has marked significant milestones. From Web 1.0, focused on static information, to participatory Web 2.0 and decentralized Web 3.0, each phase reflects the increasing interactivity and transformation of the online experience. Web 4.0, emerging since 2016, promises a revolution by integrating technologies such as artificial intelligence and augmented reality. Together, these generations outline a story of constant innovation and change in the technological landscape.

Methodologies in the development of web systems

In the evolution of software development, methodologies emerged in the 1970s to address problems inherent in the lack of control in the development stages, resulting in deficient products (Molina et al., 2017). With the rise of web applications, the implementation of methodologies has significantly improved the quality of development. The comparison of web methodologies stands out, where OOHDM is identified as the most compliant (Molina et al., 2018). In addition, agile methodologies such as XP and Scrum are being implemented to adapt to changing requirements, bringing flexibility and efficiency to web application development (Carrasco, 2022).

The Extreme Programming (XP) methodology is a response to the growing demand in the software development market, especially in web design, which requires systems that are adaptable and responsive to various devices. The XP methodology, developed by Kent Beck, focuses on addressing the complexity of changing requirements and is based

on proven software engineering principles (Bautista-Villegas, 2022). It is characterized by promoting effective communication, simplicity in design, continuous feedback with the client, respect within the team and the courage to face changes. Its characteristics include a dynamic cycle, work in pairs and 10 to 15 iterations in a typical project. Among its advantages are efficiency in planning and testing, applicability to any programming language and ease of implementation in current technologies, although it may have limitations in long-term and complex projects, as well as the lack of evidence in frequent dynamic changes (Carrasco, 2022).

The Scrum methodology is an agile strategy for project development that seeks to adapt to dynamic environments and encourage team collaboration. It is organized in sprints, development periods of two to four weeks, with planning and review at the end of each one. The methodology is based on roles such as Scrum Master, Product Owner, Stakeholders and Development Team. Scrum is characterized by its focus on team self-organization, flexibility to adapt to changes and systematic risk management. Its advantages include early results, flexibility and adaptation to different contexts, and systematic risk management. However, it can have limitations in small teams and requires intensive task and deadline management, as well as a highly skilled team for successful implementation (Carrasco, 2022). The Scrum methodology has gained widespread acceptance and has been adapted to various disciplines, although these adaptations have generated a variety of modifications and contextual approaches. Its popularity makes it a methodology for adaptations in diverse contexts and objectives, and a key component for other methods. Despite extensive documentation, the lack of integration with a method-centered approach limits the cumulative generation of knowledge (Hron & Obwegeser, 2022).

OOHDM (Object-Oriented Hypermedia Design Methodology) is an object-oriented methodology that follows a five-phase development process, combining UML graphical notations with others specific to the methodology. Initially designed for hypermedia applications, OOHDM was adapted for developing web-oriented hypermedia applications, such as virtual libraries, educational sites and search engines. This methodology focuses on simplifying and improving the efficiency of web application design, using specialized models such as conceptual, navigation and user interface. The five stages of OOHDM include requirements elicitation, conceptual design, navigational design, abstract interface design and implementation, addressing from planning to implementation of the web application (Molina et al., 2018).

Methodologies such as OOHDM, XP and Scrum have been essential in the evolution of software development, improving the quality and adaptability of applications. OOHDM stands out for its focus on hypermedia web applications, simplifying design through phases such

as requirements elicitation and conceptual design. XP, focused on adaptability, promotes effective communication and simplicity. Scrum, with its sprint-based agile management, emphasizes early results. Each methodology contributes uniquely to the dynamic web application development landscape.

MATERIALS AND METHODS

An empirical-analytical research methodology with a quantitative approach is used. The PRISMA data flow is used to select relevant papers.

The definition of the research question is a clear and precise statement that addresses the fundamental PICO (Population, Intervention, Comparison, and Outcome) elements when inquiring about trends and best practices in web application development. The question focuses on the general population of web application development and seeks to understand how different elements, such as architecture, workflows, security and specific technologies such as Node.js, Angular, Bcrypt, JWT, MySQL and other frameworks, impact these processes. The formulation of the research question towards a comprehensive assessment of current practices and trends in the mentioned field is set out in the question: What are the current trends and best practices in web application development, considering aspects such as architecture, workflows, security, and the use of specific technologies such as Node.js, Angular, Bcrypt, JWT, MySQL and other frameworks?

In the process of searching for studies, relevant databases were identified to obtain academic information related to the development of web applications and agile methodologies. A general search was performed from the database provided by Google Scholar, in which some results were obtained from IEE-Explore, Scopus, Dialnet among others. To optimize search efficiency, specific search terms were registered, such as 'web applications', 'agile methodologies', 'application development', 'web frameworks', 'Web Security', among others. In addition, temporal restrictions were implemented to ensure the relevance of the results, limiting the search to studies published in a range of years 2019 - 2023. These steps were essential to ensure that relevant and up-to-date information in the field of interest was obtained (see Table 1).

Table 1
Pre-defined requirements

Criteria	Description
Date of Publication	Studies published in the years 2019-2023 are included. Studies published before 2019 are excluded.
Type of Study	Empirical studies, systematic reviews and case studies are included. Case studies that do not indicate implementation recommendations are excluded.
Methodology	Only studies using a qualitative or quantitative methodology are included. Studies that do not comply with the terms of inclusion are excluded.
Thematic Relevance	Studies that address specific aspects of a topic or technology are included. Studies that are not directly related to the research focus are excluded.
Quality of the Study	Only studies with high methodological standards are included. Studies with significant methodological limitations are excluded.

In the literature review process, pre-defined inclusion and exclusion criteria were applied to select the most relevant studies aligned with the research objectives. Inclusion criteria were established based on specific aspects, such as relevance of content, methodological quality, and date of publication. On the other hand, exclusion criteria were used to discard studies that did not meet the predefined requirements.

The workflow for selecting search was carried out systematically. Initially, a review of the titles and abstracts of the identified studies was conducted, applying the inclusion and exclusion criteria. Subsequently, the selected articles were read for a more detailed evaluation. During this process, a protocol for eliminating duplicates was used, guaranteeing the integrity and uniqueness of the information collected.

Technology integration in web development

Web development projects that highlight the integration of various technologies to address specific challenges are explored. From improving medical records management in healthcare using the Angular framework, to creating complete web applications using Node.js to manage client Internet connections, each project demonstrates the effectiveness of technology integration in web development. In addition, the implementation of MySQL in a CodeIgniter-based application and the use of JSON Web Token (JWT) and bcrypt to secure user authentication in web applications highlight the diversity of approaches and technologies used in modern web development.

In (Ccolque, 2019), the problem of inefficient medical records management in the Peruvian health sector is addressed through the development of a web-based system using the Angular framework and rest, specifically in the city of Juliaca. It is highlighted that most of the managers of health organizations are unaware of the benefits of an adequate administration of medical records. Given the need to manage medical records electronically, it is mentioned that Angular was in-

tegrated into the project as a JavaScript framework that facilitates the creation of web applications. Angular provides features such as data binding, routing, and animations, simplifying the development of modern applications. In addition, it is explained that the adoption of Angular seeks to improve the accessibility and management of information in medical records, optimizing the process of diagnosis and treatment of patients in the Dermacenter Rios Clinic in Juliaca.

On the other hand, Node.js is used by (Kinnunen, 2023), as a JavaScript runtime environment to build secure and versatile web servers. In this case, it was used to develop a complete web application for an Internet service provider. Thanks to its extensive ecosystem, Node.js enabled the construction of a robust and versatile server, along with an API to access the database. The resulting application, designed to run on a variety of devices, was successfully deployed on the company's intranet, giving employees the ability to manage and control customers' Internet connections. This full-stack approach demonstrates the effectiveness of Node.js in creating scalable and secure web applications. MySQL integration plays a key role in the development of the Aplikasi Website Portal Manajemen Informatika, based on the CodeIgniter framework. The application, designed to provide up-to-date information on IT management, leverages the capabilities of MySQL as a database management system to efficiently manage diverse data sets. The implementation of MySQL allows for an organized and accessible structure, thus contributing to the speed and efficiency in

obtaining information for both computer science students and the community at large (Ramadhan et al., 2020).

In relation to user authentication in web applications (Kujala, 2023), used JSON Web Token (JWT) to ensure the security of sensitive data, such as passwords, and implemented bcrypt to hash user passwords. At registration, the application verifies the non-existence of the provided username and email in the database before adding the user with the corresponding password hash. When using bcrypt for password hashing, the developer must determine the number of salt rounds used to calculate the complexity and processing time of the hash operation. The salt rounds represent the cost factor, determining how long it takes to compute a single bcrypt hash, with each additional round increasing the cost factor and doubling the computation time.

Projects that exemplify the integration of various technologies in web development have been explored. From optimizing medical records management with Angular to building complete web applications using Node.js, these cases highlight the effectiveness of combining technologies to address specific challenges. The use of MySQL in CodeIgniter and the implementation of security measures such as JSON Web Token (JWT) and bcrypt reinforce the idea that technology integration is key in modern web development. These examples underscore the versatility and positive impact that the strategic combination of tools can have on problem solving and process improvement in a variety of contexts.

Results

According to the 27 studies analyzed, the following results were obtained.

Figure. 1
Percentage of jobs related to existing thematic areas
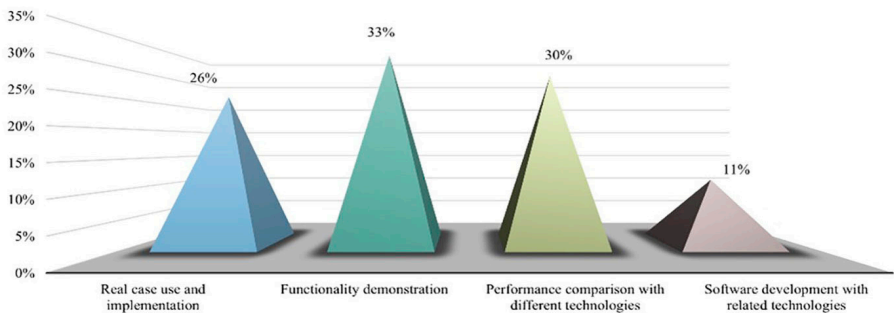
According to the analysis of topics and objectives, the works related to the use and implementation in a real case resulted in 26%, demonstration of functionality 33%, performance comparison with different technologies 30% and software development with related technologies 11% (see Fig. 1).

Figure. 2
Percentage of work related to the formulation of existing problems
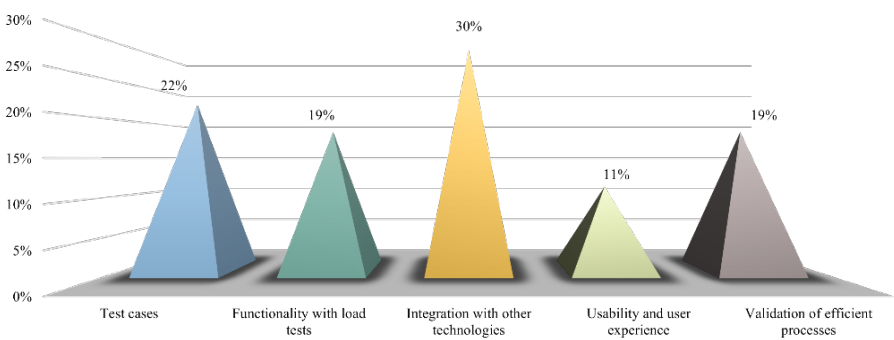
According to the analysis of the problem formulation and data involved, it was obtained that the work related to test cases resulted in 22%, functionality with load testing 19%, integration with other technologies 30%, usability and user experience 11% and validation of efficient processes 19% (see Fig. 2).

Figure. 3

Percentage of jobs that determine an existing constraint
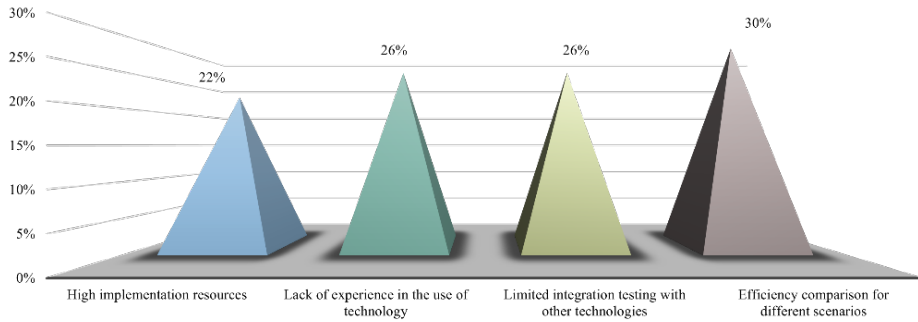
According to the analysis of the limitations encountered, it was found that the works related to high resources for their implementation were 22%, lack of experience in the use of the technologies 26% and comparison of efficiency in different scenarios 30% (see Fig. 3).

Figure. 4

Percentage of related work according to the analysis of proposals and methodologies used
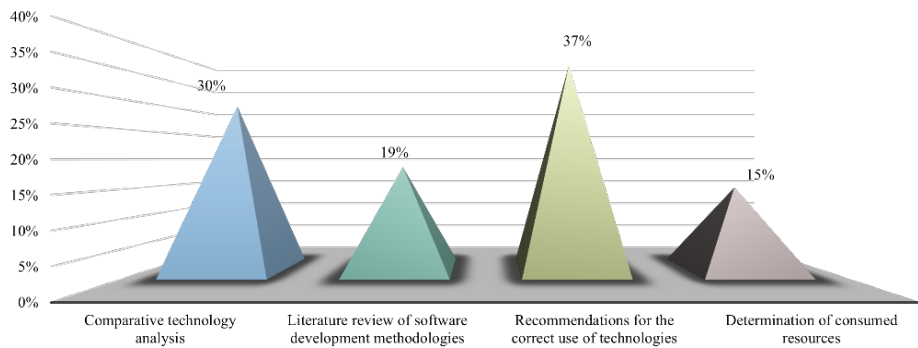
According to the analysis of proposals and methodologies used, it was obtained that the works related to the comparative analysis of technologies were 30%, review of literature on methodologies for software development 19%, recommendations for the correct use of technologies 37% and determination of resources obtained 15% (see Fig. 4).

Figure. 5

Percentage of papers related to the results and challenges encountered
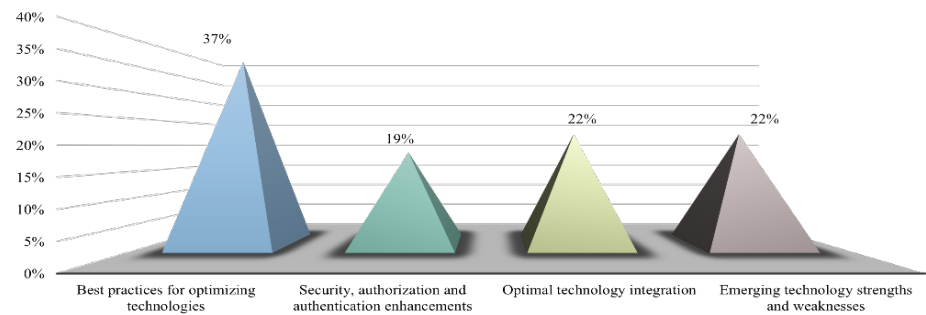
According to the analysis of the solutions found, results and challenges, the works related to best practices for the optimization of technologies were 37%, improvements in security, authorization, and authentication 19%, optimal integration of technologies 22% and strengths and weaknesses of emerging technologies 22% (see Fig. 5).

Finally, the relevant technological trends are presented according to the analysis of the works found (see Table 2).

Table 2

Relevant technological trends

Trends	Relevance	Reference
Angular	It allows the creation of services, directives, and various essential elements for the development of web applications	(Ccolque, 2019;)Cincovic et al., 2019;) (Saini & Jasrotia, 2023)(Ghimire, 2020) (Kaluža et al., 2019)
Node.js	Service implementation follows a separate layered structure for more secure and understandable code	(Kinnunen, 2023)(Pardo et al., 2018) (Sharma et al., 2019)(Huynh, 2020) (Pant et al., 2022)
JSON Web Token	The tokens encode and verify their own assertions, allowing them to be self-contained for short durations and without the need for database access, simplifying design and eliminating database overhead.	(Ramadhan et al., 2020)(Mahindrakar & Pujeri, 2020)
Bcrypt	In a first step, an initial key is established using eks-blowfish and then encrypted with OrpheanBeholder-ScryDoubt using a previously generated 192-bit key. This approach provides additional security by using a structure that makes potential attacks more difficult	(Kujala, 2023)(Giffary & Ramadhani, 2022)
MySQL	Its popularity among programmers is due to its cross-platform capability, ease of use and reliable security system	(Sotnik et al., 2023)(Nagpal et al., 2020)
Scrum	Agile methodology for developing applications that generates a climate of responsibility, progress and effective communication in the work team	(Krogh, 2020)(Dene & James, 2021)(Nath, 2022)(Ziegler, 2022)(Chohan, 2022)(Ersöz et al., 2020) (Molina et al., 2017)(Molina et al., 2018)(Carrasco, 2022)(Bautista-Villegas, 2022)(Hron & Obwegeser, 2022)

DISCUSSION

Web systems development is undergoing a rapid evolution driven by emerging technology trends. The Internet, as a powerful medium of communication and influence, has unleashed significant advances that require continuous adaptation by both users and developers. This dynamism is reflected in the constant search for more efficient and advanced web models and services. The intersection of different programming languages, tools and platforms has given rise to a diversified technological landscape that optimizes speed and precision in the development of web applications. In this context of digital transformation, we explore the most important trends that are shaping the present and future of web systems development.

In relation to JavaScript, it is highlighted its position as the most widely used interpreted language in the construction of web pages, with a syntax similar to Java and C. Its ability to run on the client side is highlighted, which contributes to agility and efficiency in web development. In addition, it is emphasized that, unlike PHP, JavaScript does not involve data exchange with the server, which influences performance (Pardo et al., 2018). HTML is mentioned as a fundamental hypertext markup language for the development of static web applications, although its combination with other languages allows the creation of dynamic applications. HTML5 is introduced as an evolution that introduces dynamic elements to configure the web environment and its contents (Pardo et al., 2018).

Regarding authentication and authorization, JSON Web Token (JWT) is considered especially suitable for serverless applications. Because JWT allows additional information to be stored directly in the token, beyond just the user's credentials, the server no longer needs to look up that information in the database. When a user logs in withhis/her credentials, these are sent to the Authorizer, and the JWT is returned in case of success. The platform validates the JWT before granting access to protected resources. This streamlined process improves security and efficiency in managing user authentication in serverless architectures (Huynh, 2020). Continuing with security, Bcrypt is used as a hashing algorithm in the context of password-based authentication in web applications. This choice of Bcrypt is justified by its ability to add an additional layer of security using "Salt", a random string appended to the password. This procedure strengthens security by preventing direct and indirect attacks on the password stored in the database. When a user attempts to log in, the credentials entered are compared with the information in the database using the comparison function provided by the Bcrypt package. The implementation of Bcrypt ensures that even if someone gains access to the database, passwords remain safe and secure (Pant et al., 2022).

The current landscape of web systems development reflects a dynamic transformation driven by emerging technology trends. The constant evolution, moved by the influence of the Internet, has led to the search for more efficient and advanced models and services. In this context, JavaScript stands out as the most widely used interpreted language, providing agility and efficiency in web development. The combination of HTML and HTML5 continues to be fundamental for creating web applications, offering both static and dynamic structures. In the area of authentication and authorization, JSON Web Token (JWT) is introduced to improve security and efficiency in the management of user authentication. In addition, the implementation of Bcrypt for password hashing reinforces security by adding an additional layer using "Salt", mitigating risks associated with direct and indirect attacks on stored passwords. Thus, these trends reflect a continued commitment to innovation and security in the development of web systems.

CONCLUSIONS

This paper highlights the importance of integrating specific technologies, such as An-gular, Node.js, JWT, Bcrypt and MySQL, for the effective development of web systems. The historical evolution from Web 1.0 to Web 4.0 has demonstrated the constant need to adapt to new technologies to meet the changing demands of the technological landscape. The review of methodologies, such as XP, Scrum and OOHDM, highlights how they have contributed to improving the quality and adaptability of web application development. In addition, current trends in web development, such as the predominant use of JavaScript, HTML5, JWT and Bcrypt, reflect the constant evolution and commitment to innovation and security. The projects reviewed demonstrate that effective integration of these technologies in web development is essential to address specific challenges and improve efficiency in a variety of contexts.

REFERENCES

Bautista-Villegas, E. (2022). Metodologías agiles XP y Scrum, empleadas para el desarrollo de páginas web, bajo MVC, con lenguaje PHP y framework Laravel. *Revista Amazonía Digital*, *1*(1), e168-e168. https://doi.org/10.55873/RAD.V1I1.168

Carrasco, H. C. J. (2022). *Análisis de metodologías ágiles para el desarrollo de aplicaciones Web.* http://dspace.utb.edu.ec/handle/49000/13044

Ccolque, J. L. C. (2019). Desarrollo de un sistema web utilizando angular framework y rest (Transferencia de estado representacional) para la gestión de historias electrónicas. *Universidad Peruana Unión*. https://repositorio.upeu.edu.pe/handle/20.500.12840/3295

Chohan, U. W. (2022). Web 3.0: The Future Architecture of the Internet? *SSRN Electronic Journal*. https://doi.org/10.2139/SSRN.4037693

Cincovic, J., Delcev, S., & Draskovic, D. (2019). *Architecture of web applications based on Angular Framework: A Case Study*. https://www.eventiotic.com/eventiotic/files/Papers/URL/df6b5054-816e-4bee-b983-663fb87be2cd.pdf

Dene, G., & James, O. (2021). Electronic Literature as Digital Humanities. *Bloomsbury Academy*, *2*, 151-162. https://library.oapen.org/bitstream/handle/20.500.12657/58859/1/9781501363481.pdf#page=162

Effendy, F., Taufik, & Adhilaksono, B. (2021). Performance Comparison of Web Backend and Database: A Case Study of Node.JS, Golang and MySQL, Mongo DB. *Recent Advances in Computer Science and Communications*, *14*(6), 1955-1961. https://doi.org/10.2174/2666255813666191219104133

Ersöz, B., Bilimleri, B., & Dergisi, T. (2020). Yeni Nesil Web Paradigması-Web 4.0. *Journal of Computer Science and Technologies*, *1*(2), 58-65. https://dergipark.org.tr/en/pub/bibted/issue/57253/796030

Ghimire, D. (2020). *Comparative study on Python web frameworks: Flask and Django*. https://www.theseus.fi/handle/10024/339796

Giffary, R. S., & Ramadhani, E. (2022). Implementasi Bcrypt dengan SHA-256 pada Password Pengguna Aplikasi Golek Kost. *Jurnal Sistem Komputer Dan Informatika (JSON)*, *3*(4), 543-546. https://doi.org/10.30865/json.v3i4.4285

Hron, M., & Obwegeser, N. (2022). Why and how is Scrum being adapted in practice: A systematic review. *Journal of Systems and Software*, *183*, 111110. https://doi.org/10.1016/J.JSS.2021.111110

Huynh, K. (2020). The development of a web application: The new trend - Serverless application. *Turku Amk*. http://www.theseus.fi/handle/10024/344206

Kaluža, M., Kalanj, M., & Vukelić, B. (2019). A comparison of back-end frameworks for web application development. *Zbornik Veleučilišta u Rijeci*, *7*(1), 317-332. https://hrcak.srce.hr/en/219995

Kinnunen, J. (2023). *Designing a* Node.js *full stack web application*. https://www.theseus.fi/bitstream/handle/10024/793330/Kinnunen_Janne.pdf?sequence=2

Krogh, J. W. (2020). MySQL Workbench. In *MySQL 8 Query Performance Tuning: A Systematic Method for Improving Execution Speeds* (pp. 199-226). Apress. https://doi.org/10.1007/978-1-4842-5584-1_11

Kujala, A. (2023). Development of a modern full stack web application. *Turku Amk*.

Mahindrakar, P., & Pujeri, U. (2020). Insights of JSON Web Token. *International Journal of Recent Technology and Engineering (IJRTE)*, *6*, 2277-3878. https://doi.org/10.35940/ijrte.F7689.038620

Molina, J. R., Zea, M. P., Contento, M. J., García, F. G., Metodologías, C. De, Rolando, J., Ríos, M., Paola, M., Ordóñez, Z., José, M., Segarra, C., Gustavo, F., & Zerda, G. (2018). Comparación de metodologías en aplicaciones web. *3c Tecnología: Glosas de Innovación Aplicadas a La Pyme, ISSN-e 2254-4143, Vol. 7, Nº. 1, 2018, Págs. 1-19*, *7*(1), 1-19. https://doi.org/10.17993/3ctecno.2018.v7n1e25.1-19

Molina, J. R., Zea, M. P., Contento, M. J., García, F. G., Rolando, J., Ríos, M., Paola, M., Ordóñez, Z., José, M., Segarra, C., Gustavo, F., & Zerda, G. (2017). Estado del arte: Metodologías de desarrollo en aplicaciones web. *3c Tecnología: Glosas de Innovación Aplicadas a La Pyme, ISSN-e 2254-4143, Vol. 6, Nº. 3, 2017, Págs. 54-71*, *6*(3), 54-71. https://doi.org/10.17993/3ctecno.2016.v6n3e23.54-71

Nagpal, P., Goel, N., Sangwan, S., & Dixit, H. (2020). Design and Implementation of Hostel Management System Using Java and MySQL. *LC International Journal of STEM (ISSN: 2708-7123)*, *1*(4), 63-74. https://doi.org/10.5281/ZENODO.5149774

Nath, K. (2022). Evolution of the Internet from Web 1.0 to Metaverse: The Good, The Bad and The Ugly. *Tech Rxiv*. https://doi.org/10.36227/TECHRXIV.19743676.V1

Pant, P., Rajawat, A. S., Goyal, S. B., Bedi, P., Verma, C., Raboaca, M. S., & Enescu, F. M. (2022). Authentication and Authorization in Modern Web Apps for Data Security Using Nodejs and

Role of Dark Web. *Procedia Computer Science*, *215*, 781-790. https://doi.org/10.1016/J. PROCS.2022.12.080

Pardo, M. R. V., Tapia, J. A. H., Moreno, A. S. G., & Sánchez, L. F. V. (2018). Comparación de tendencias tecnológicas en aplicaciones web. *3c Tecnología: Glosas de Innovación Aplicadas a La Pyme, ISSN-e 2254-4143, Vol. 7, Nº. 3, 2018, Págs. 28-49*, *7*(3), 28-49. https://doi.org/10.17993/3ctecno.2018.v7n3e27.28-49/30

Ramadhan, W. F., Dewi, W. N., & Nas, C. (2020). Aplikasi Web Portal Manajemen Informatika Berbasis Website Dengan Menggunakan Framework Codeigniter Dan Mysql Pada Universitas Catur Insan Cendekia. *Jurnal Digit*, *10*(2), 124. https://doi.org/10.51920/jd.v10i2.164

Saini, S. S., & Jasrotia, A. (2023). A Survey Based on Current Technologies of Web Development. *TIJER*, *10*(6). https://www.tijer.org/papers/TIJER2306278.pdf

Sharma, V., Verma, R., Pathak, V., Paliwal, M., & Jain, P. (2019). Progressive Web App (PWA)-One Stop Solution for All Application Development Across All Platforms. *International Journal of Scientific Research in Computer Science, Engineering and Information Technology © 2019 IJSRCSEIT |*, *5*(2), 2456-3307. https://doi.org/10.32628/CSEIT1952290

Sotnik, S., Manakov, V., & Lyashenko, V. (2023). Overview: PHP and MySQL Features for Creating Modern Web Projects. In *International Journal of Academic Information Systems Research* (Vol. 7, Issue 1, pp. 11-17). IJAISR. https://openarchive.nure.ua/handle/document/21601

Ziegler, M. G. (2022). Web 2.0 and Knowledge Sharing. A Literature Review. *Intech Open*, *2022*, 1-14. https://doi.org/10.5772/ACRT.03

Antimicrobial activity of secondary metabolites from *Bacillus* and *Trichoderma* against pathogens of red pitaya (*Hylocereus undatus*)

Bonifáz Játiva Pamela Annabell
Universidad Politécnica Salesiana, (Ecuador)
Orcid: https://orcid.org/0009-0007-0759-2626

Rubio Zurita Tatiana Nicole
Universidad Politécnica Salesiana, (Ecuador)

Pacheco Flores de Valgaz Angela Vanessa
Universidad Politécnica Salesiana, (Ecuador)
Orcid: https://orcid.org/0000-0002-7417-7218

Espinoza Lozano Rodrigo Fernando
Universidad Politécnica Salesiana, (Ecuador)
Orcid: https://orcid.org/0000-0002- 2051-2682

Introduction

The exportation of pitaya has distinguished Ecuador as a leader in the exportation of the yellow variety and a prestigious producer of the red variety. However, the losses caused by phytopathogenic fungi in pitaya destined for exporting are significant to both the agricultural industry and the national economy. It is estimated that these losses can reach up to 50% in developing countries and 25% in developed countries (Andrés Cadena, 2020).

Various phytopathogenic fungi have been identified in pitaya crops, such as *Fusarium* sp., *Botrytis* spp., *Curvularia* sp., *Lasiodiplodia* sp., and *Neoscytalidium* sp., causing pathological deterioration. To address this problem, it is essential to implement post-harvest management strategies that minimize the risk of fungal infections. One of the alternatives for controlling phytopathogens is to use biological control, which involves employing organisms or their natural antagonistic by-products to reduce plant damage (Martínez, 2017).

The production of secondary metabolites through liquid fermentation using microorganisms such as *Trichoderma* sp. and *Bacillus* sp. has been studied due to their potential as biocontrol agents to combat pathogens in crops and preserve quality during storage or transportation (INIAP, 2020).

The combined use of *Trichoderma* sp. and beneficial bacteria such as *Bacillus* sp. and *Pseudomonas* has shown promising results in the development of synergistic microbial inoculants for sustainable agriculture (Daniel Eugui, 2022). *Bacillus* sp. and *Trichoderma* sp. are important due to their ability to synthesize antifungal metabolites and other bioactive substances that promote plant growth and control pathogens; *Bacillus* sp. produces antibiotics such as bacilysin, iturin, and fengycin, while *Trichoderma* sp. produces trichodermin, 6-pentyl-2H-pyran-2-one, and viridin, which have inhibitory properties against certain phytopathogenic fungi (Tingting Li, 2020).

Materials and Methods

Obtaining conidia from microorganisms

Isolates of *Bacillus* sp. previously isolated from the rhizosphere of rice plants were used. Additionally, two strains of rice phytopathogenic fungi, *Fusarium* spp. and *Curvularia cactivora*, were obtained from the fungal culture collection of the Laboratory of the Biotechnology Research Center of Ecuador (CIBE), within the Phytopathology Area of the Life Sciences Faculty at the Escuela Superior Politécnica del Litoral. Before conducting the antagonism study, the growth capacity of the bacterial strains on Potato Dextrose Agar (PDA) medium was evaluated for its use in dual culture.

For the subculturing process of *Trichoderma* sp. derived from the C9 strain (mother strain of *Trichoderma* sp.), the following method was used to obtain an aqueous conidial solution (Pedraza, 2022). Nine days after the initial subculture of the C9 strain, spores were washed using autoclaved water to produce a *Trichoderma* C9 solution. Subsequently, three progressive dilutions of this solution were made in 15 ml Falcon tubes, with concentrations of 1×10^{-1}, 1×10^{-2} and 1×10^{-3}, respectively, until reaching a final volume of 10 ml. Finally, the conidia were counted under a microscope using a Neubauer chamber. During this stage, a concentration of $3{,}17 \times 10^7$ spores/ml and 1×10^9 spores/ml was obtained in the Neubauer chamber.

Liquid fermentation

Liquid fermentation (LF) is characterized by the use of dissolved nutrients, which provides extensive control over culture factors. This capability is essential as it allows us to adapt and improve the development conditions of the microorganisms (Arango, 2015).

For the preparation of the *Bacillus* sp. culture medium, a 1000 ml flask containing a commercial medium was used. During this process, 10 ml of the specific commercial medium for *Bacillus* sp. was extracted, to which the bacterial inoculum was added to reach a concentration of 1x108 on the Mc-Farland scale. This resulted in a final volume of 990 ml in the flask. The remaining 10 ml of the medium along with the inoculum were reintroduced into the original 1000 ml flask containing a saline solution. This led to liquid fermentation for a period of 24 hours, with constant agitation and at an ambient temperature of 30 °C.

Filtration sterilization

The cold syringe filtration technique is used to separate solid particles or impurities from a liquid. Filters composed of two layers are used: an overlay of polypropylene prefilters with pores of 10 μm and 5 μm, followed by a membrane for efficient separation. To simplify and avoid rapid filter saturation, the samples are centrifuged beforehand. The supernatants are then filtered with a 5 ml syringe and 0,22 μm filters under sterile conditions. 20 ml of each supernatant are stored at 6 °C, labeled as "sterile supernatant of *Trichoderma* sp." and "sterile supernatant of *Bacillus* sp."

Mixture of sterile supernatants for the preparation of treatments and respective controls, with these antimicrobial tests being evaluated.

A mixture called "M" was created by combining equal parts of the sterile supernatant of *Trichoderma* sp. in PDB and the sterile supernatant of *Bacillus* sp., in a 50/50 ratio. This mixture will be used in one of our treatments.

Petri dishes with PDA were prepared for each of the strains isolated from the symptoms of pitaya fruits, totaling 99 Petri dishes (11 strains, 4 treatments, and 4 controls). Each Petri dish was divided into four sectors for each treatment and control.

Finally, *in vitro* tests were evaluated using the modified agar well diffusion method on PDA medium, where each well contained 90 μl of solution. The main objective of this study was to analyze the efficacy of various treatments in *in vitro* models. These qualitative methods are easy to standardize and are suitable for studying microorganisms, as they do not require very specific conditions and allow rapid reproduction of results.

The purpose was to determine the compatibility and growth of the evaluated microorganisms (Peña, 2017). After a period of 5 days, the antimicrobial capacities of each treatment and control were qualitatively evaluated by measuring the distance in millimeters between the inhibition halo of the microorganism and the wells containing different solutions: sterile supernatant of *Trichoderma* sp. in PDB, sterile supernatant of *Trichoderma* sp. in deionized water, sterile supernatant of *Bacillus* sp., and a mixture of sterile supernatant of *Trichoderma* sp. in PDB and sterile supernatant of *Bacillus* sp. each test was replicated four times per strain.

Figure. 1

Methodological description of the research process
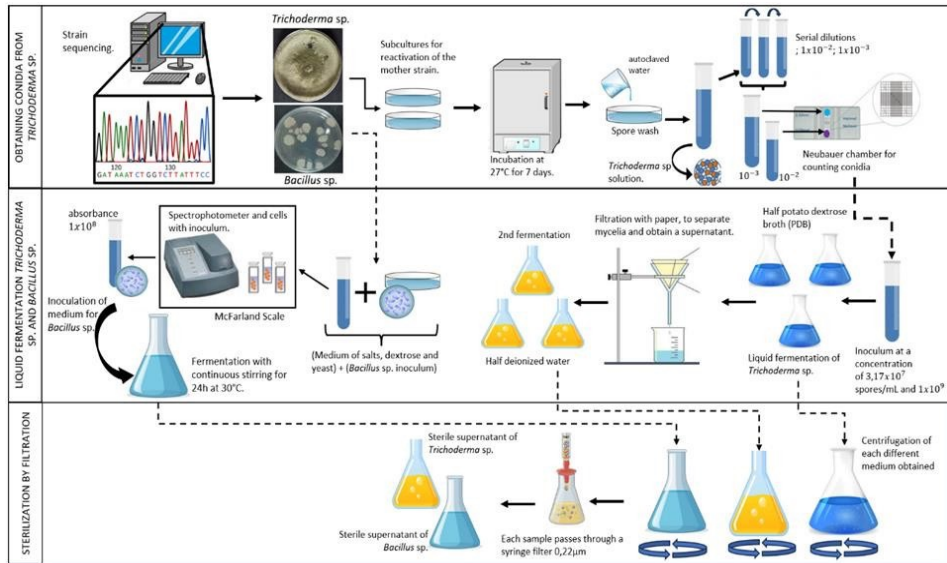
Note. The diagram illustrates the systematic steps involved in obtaining sterile supernatants of the different microorganisms used in this project.

Isolation and sequencing of microorganisms with the molecular identification of strains isolated from the symptoms of red pitaya fruit.

Finch TV software was used to edit the sequences, selecting the optimal parts of the chain. Consensus sequences were then generated for each isolation sample by aligning the ITS1 and ITS4 sequences in Geneious Prime. These consensus sequences were used to identify the isolated strains using the BLAST (Basic Local Alignment Search Tool) algorithm, successfully identifying the strains associated with the symptoms of red pitaya.

For the molecular identification of the strains isolated from the symptoms of red pitaya fruit, DNA was extracted from fungal mycelium obtained from pure cultures on PDA medium, following the Cenis protocol. Amplification of the ITS1, 5.8S, and ITS2 regions was performed by PCR using universal primers ITS-1. The PCR reaction volume and amplification conditions were detailed according to the protocol of Suárez (2021), and the products were visualized on 2% agarose gel.

For this study, experiments were conducted under controlled conditions to analyze the antimicrobial activity of filtered supernatants; eleven culture plates were used, each replicated four times to evaluate the *in vitro* interaction between bacteria and fungi. Four different treatments were applied: two sterile filtered supernatants of *Trichoderma* sp., one of *Bacillus* sp., and a mixture

Antimicrobial activity of secondary metabolites from Bacillus and Trichoderma against pathogens of red pitaya (Hylocereus undatus)

27

of the sterile supernatant of *Trichoderma* sp. in PDB medium with *Bacillus* sp., to test against 11 pathogens, with four control groups corresponding to each treatment. The objective was to obtain data to statistically evaluate the results and observe the efficiency of each treatment.

Results

Molecular identification of isolated strains

Table. 1
Molecular identification of the sequencing of the ITS1, 5.8S, ITS2 region of strains isolated from red pitaya fruit using the BLAST database

Code	Strain	Identification number in Gen Bank	Identify percentage (%)
PIT1-H2	*Fusarium dimerum*	EU 926267.1	98,87
PIT2-6	*Fusarium verticillioides*	MK790046.1	92,90
PIT2A-6	*Fusarium verticillioides*	MK790046.1	92,90
PIT2-H6	*Fusarium falciforme*	MG189935.1	99,81
PIT2-H9	*Fusarium verticillioides*	MK790046.1	92,90
PIT5-21	*Fusarium dimerum*	EU926267.1	98,57
PIT2-8	*Curvularia cactivora*	KJ909775.1	95,56
PIT3-H10	*Curvularia cactivora*	MN688803.1	99,81
PIT3-H12	*Curvularia cactivora*	MN688803.1	99,81
PIT4-H19	*Curvularia cactivora*	MN688803.1	99,81
PIT5-H25	*Curvularia cactivora*	MN688803.1	99,81

According to Crespo (2022), regarding morphological identification, two parameters must be considered: the e-value, which should approach a value of 0,0 and genetic similarity, which should range between 90% and 100%.

Based on this, it can be confirmed that all isolates show genetic similarity above 90% and an E-value of 0,0 in the ITS region.

Antimicrobial activity

Bacillus *sp. and* Trichoderma *sp. vs.* Fusarium dimerum

The measurement of the inhibition halo diameter of the replicates indicates that the halo of the fungus *Fusarium dimerum* was found above the wells with sterile supernatant containing the secondary metabolites produced by *Bacillus* sp. (B) and the mixture of sterile

supernatants of *Trichoderma* sp. and *Bacillus* sp. (M). This suggests that the secondary metabolites of *Trichoderma* sp. and *Bacillus* sp. were not effective in inhibiting the growth of the fungus *Fusarium dimerum*.

Bacillus *sp. and* Trichoderma *sp. vs.* Fusarium verticillioides

The measurement of the inhibition halo diameter of the replicates indicates that the halo of the fungus *Fusarium verticillioides* extended to the edges of the wells containing the sterile supernatant of *Bacillus* (B) and the mixture of sterile supernatants of *Trichoderma* and *Bacillus* (M). This indicates that, although to a lesser extent, the antimicrobial activity of the produced secondary metabolites exerted an inhibitory action on the growth of the fungus *Fusarium verticillioides*.

Bacillus *sp. and* Trichoderma *sp. vs.* Fusarium falciforme

The measurement of the inhibition halo diameter of the replicates indicates that the halo of the fungus *Fusarium falciforme* was found above the wells with sterile supernatant containing the secondary metabolites produced by *Bacillus* sp. (B) and the mixture of sterile supernatants (M). However, despite the absence of manifested antimicrobial activity by the secondary metabolites, an effect impacting its growth or evolutionary process was observed.

Figure. 2
Pathogen inhibition test replicate 2
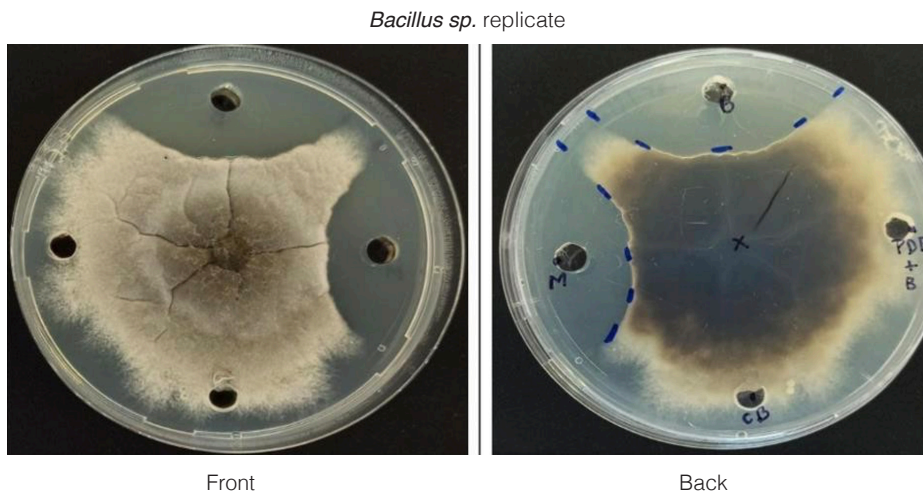
Bacillus sp. replicate

Front   Back

Note. Antimicrobial activity (modified agar well diffusion method) of the sterile supernatant of *Bacillus* sp. (B) and the mixture of sterile supernatants of *Trichoderma* sp. and *Bacillus* sp. (M) against *Curvularia cactivora* with sample code PIT2-8.

Antimicrobial activity of secondary metabolites from Bacillus and Trichoderma against pathogens of red pitaya (Hylocereus undatus)

29

Figure. 3
Pathogen inhibition test replicate 1

Bacillus sp. replicate 1
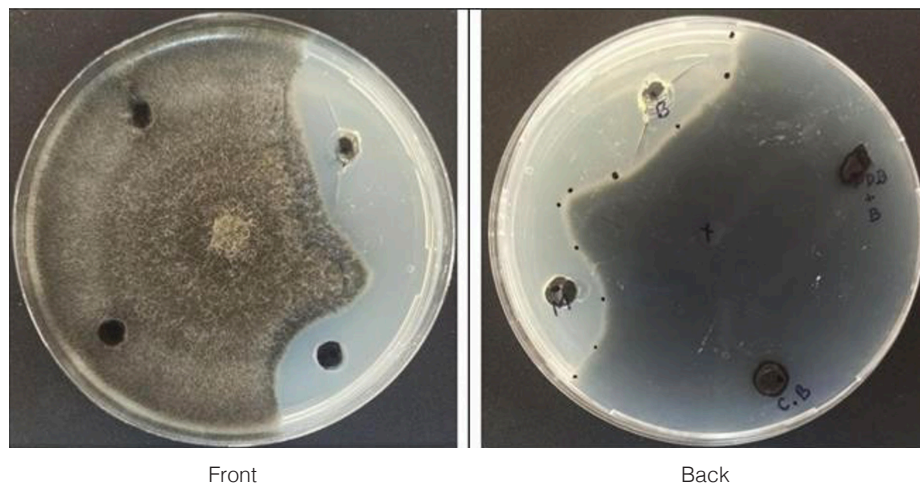
Front   Back

Note. Antimicrobial activity (modified agar well diffusion method) of the sterile supernatant of *Bacillus* sp. (B) and the mixture of sterile supernatants of *Trichoderma* sp. and *Bacillus* sp. (M) against *Curvularia cactivora* with sample code PIT5-H25.

The measurement of the inhibition halo diameter in each of the replicates indicates that the secondary metabolites produced by *Bacillus* sp. (B) and the combination of secondary metabolites from *Trichoderma* sp. and *Bacillus* sp. (M) caused a significantly high inhibition in the growth of the fungus *Curvularia cactivora*. This suggests that the secondary metabolites have a potent effect in suppressing the growth of this fungus.

The readings of the inhibition halos of the isolated strains are presented, where we can observe and interpret the effectiveness of treatments T3 and T4.

Table. 2
Results of the antimicrobial activity of treatments and controls with Bacillus sp. against the isolated strains

Isolated strains	Treatments and controls	
	T3	T4
Code	Bacillus sp. (mm)	Mix (mm)
PIT2-6	14,4166	12,6667
PIT2A-6	11,4375	6,5

Isolated strains	Treatments and controls	
	T3	T4
Code	Bacillus sp. (mm)	Mix (mm)
PIT2-H9	13,125	8,6667
PIT2-8	16,0833	11,9167
PIT3-H10	14,875	14,125
PIT3-H12	15,8125	11,3125
PIT4-H19	16,375	14,5625
PIT5-H25	18,8125	16,5

Note. The values detailed in this table correspond to the diameter of the inhibition zones observed in the two different treatments with bacillus and "mixture" against the pathogens.

Average inhibition halo (mm)

Treatments 3 and 4, corresponding to the sterile supernatant of *Bacillus* sp. (B) and the mixture of sterile supernatants (M), showed antimicrobial activity against the isolated fungi from red pitaya. Meanwhile, treatments 1 and 2 with *Trichoderma* sp. did not show antimicrobial activity in any of the isolated strains from red pitaya.

The table presents the average inhibition halo (mm) found in various isolated strains symptomatic of pathogens from red pitaya fruit, highlighting the strain of the fungus *Curvularia cactivora* with code (PIT5-H25), which presented the highest average inhibition halo in treatments 3 and 4, being 18,8125mm and 16,5mm respectively. This indicates that treatments with *Bacillus* sp. are effective as antimicrobial agents in controlling the fungus *Curvularia cactivora*.

According to Heydrich (2012) in their study of the antagonism of *Bacillus* sp. against phytopathogenic fungi in rice cultivation, the inhibitory capacity of *Bacillus* sp. members against species of the genus *Curvularia* was demonstrated.

On the other hand, the strain of *Fusarium verticillioides* with code (PIT2A-6) presented the lowest inhibition averages in treatments 3 and 4.

These results differ from the claims of Ariza Yesid and Sánchez Ligia (2012), who affirm that *Bacillus* sp. is very effective as biological control against *Fusarium* sp. with inhibition rates ranging from 70 to 100%. Therefore, it is inferred that the performance of sterile supernatants of *Bacillus* sp. in our treatments could be linked to the concentration in each of them.

Antimicrobial activity of secondary metabolites from Bacillus and Trichoderma against pathogens of red pitaya (Hylocereus undatus)

31

Statistical analysis

For the presentation and evaluation of the results, a statistical analysis of the data obtained was performed using the Infostat program version 2017, with a focus based on the analysis of variance (ANOVA). A Tukey test was applied, which shows the differences between the means and allows for a detailed observation of the results to analyze the inhibitory activity of the pathogens in the samples.

Table 3 presents the average values of the inhibition halos observed in the treatments of *Bacillus* sp. and in the mixture, used as biological control agents against the pathogens. A normality test was performed to determine the suitability of the statistical analysis, confirming the applicability of the one-way ANOVA.

Table. 3

Standard deviation of the inhibition percentage of Bacillus sp. and mixture

Strain	Bacillus	Desve	Mix	
C1	14,4166667	1,04748376	12,6666667	0,82495791
C2	11,4375	0,625	6,5	0,93541435
C3	16,0833333	1,47667043	11,9166667	0,82495791
C4	13,125	1,76186454	8,66666667	0,96465308
C5	14,875	0,66143783	14,125	1,88745861
C6	15,8125	0,55433895	11,3125	1,32876823
C7	16,375	2,25924029	14,5625	0,875
C8	18,8125	0,625	16,5	1,5411035

Note. Values are detailed that represent the inhibition percentage of the *bacillus* and the "mixture" sample against the pathogen. With this analysis, the probability value $P = 0.001$ which is less than 0,05 was obtained.

ANOVA analysis revealed significant variability among the means of the samples, highlighting two representative values: one of 18,8125 for the inhibition halo of Bacillus sp. and another of 16,5 for the mixture in strain 8 indicating effective suppression of the phytopathogenic fungus.

The Tukey test was applied to identify the most representative differences between the means of the samples in terms of the inhibition halo. Noticeable variations were observed among the strains, with strain 8 being the most effective in control, while strain 2 showed a lower variation. The Tukey test applied to the mixture also demonstrated its effectiveness as a method of biological control

Figure 4

Tukey histogram, Bacillus sp. assay
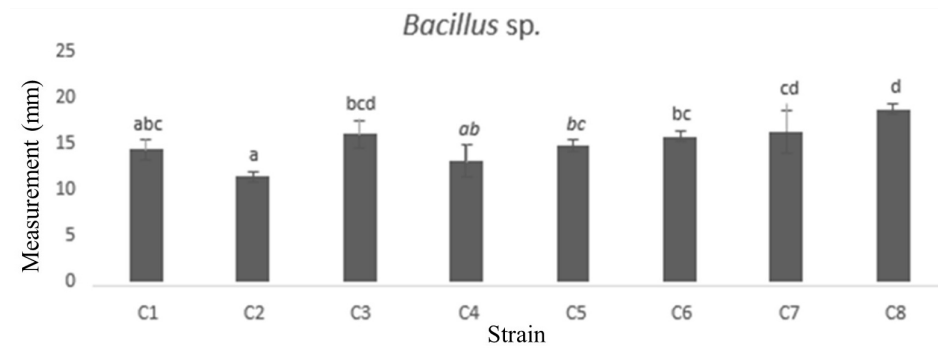
Note. As seen in the histogram, it details the highest peak of the clusters obtained, the most prominent being that of sample 8 in terms of the *bacillus* test.

Figure 5

Tukey histogram, mixture assay
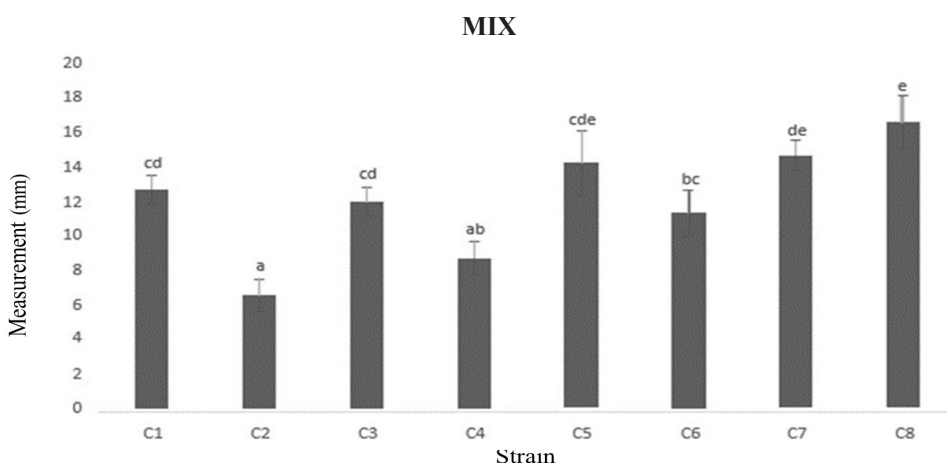
Note. The variations in the means between the samples are evident, with one of the greatest variations observed in the mixture compared to strain 8. In comparison with the *bacillus* assay, the "mixture" strain represents a greater prominence in clusters values.

Conclusions

This study has conducted the molecular identification of strains isolated from red pitahaya, employing bioinformatics tools such as Geneious Primer, FinchTV, and NCBI. This analysis is crucial for a profound understanding of the diversity of pathogens affecting red pitahaya, as well as for the design

Antimicrobial activity of secondary metabolites from Bacillus and Trichoderma against pathogens of red pitaya (Hylocereus undatus)

33

and implementation of specific control strategies in this crop.

The focus of this research was on analyzing the inhibition halos, determining the capacity of secondary metabolites produced through liquid fermentation of *Trichoderma* sp. and *Bacillus* sp. to inhibit and/or control the proliferation of fungi isolated from red pitahaya (*Hylocereus undatus*).

It can be concluded that the secondary metabolites produced by *Bacillus* sp. exhibit a greater inhibitory action on pathogens, showing one of the most representative inhibition halos with 18,8125mm and 16,5mm respectively against strains of *Curvularia cactivora.*

The methods used in this study facilitated the production of a substantial number of metabolites, supporting the effectiveness of liquid fermentation as a viable strategy for generating na-tural antimicrobial agents for pathogen control in agriculture. Finally, this study yielded positive results regarding the capacity of secondary metabolites produced by *Bacillus* sp. to inhibit the growth of *Curvularia cactivora* and *Fusarium* spp. These findings suggest that these metabolites could play a significant role in controlling specific fungal pathogens affecting red pitahaya. On the other hand, further evaluation of the potential of secondary metabolites from *Trichoderma* sp. is suggested. Although this study did not observe effectiveness in inhibiting the growth of strains of *Curvularia cactivora* and *Fusarium dimerum*, it is important to consider that the efficacy of these metabolites could be influenced by specific environmental conditions or genetic characteristics of the strains. Therefore, additional research could provide insight into their true potential as antifungal agents.

References

Andrés Cadena, K. M. (2020). Evaluation of gene expression involved in the biosynthesis of antimicrobial lipopeptides in Bacillus megaterium using RT- qPCR. *Universidad Politécnica Salesiana Ecuador*, 91.

Arango, C. S. (2015). Use of liquid fermentation of Lentinula edodes (shiitake) for the production of bioactive secondary metabolites and evaluation of its potential use in the production of a functional food. *Universidad Nacional De Colombia*.

Ariza Yesid, S. L. (2012). Determination of secondary metabolites from Bacillus subtilis with bio-control effect on Fusarium sp. *Journal scielo.*

CRESPO, J. B. (2022). Isolation, characterization, and identification of filamentous fungi associated with cancer symptoms in dragon fruit plantations. (Hylocereus spp.). *Escuela Superior Politécnica del Chimborazo*.

Daniel Eugui, J. P. (2022). Combined use of Trichoderma and beneficial bacteria (mainly Bacillus and Pseudomonas): Development of microbial synergistic bio-inoculants in sustainable agriculture. *ELSEVIER*, 19.

Heydrich, M. (2012). Antagonism of Bacillus spp. against phytopathogenic fungi in rice cultivation (Oryza sativa L.). scielo.sld.cu.

INIAP. (2020). Biological Control: A tool for sustainable agriculture, a viewpoint on its benefits in Ecuador. *Journal scielo*.

Martínez, H. O. (2017). Biological control of phytopathogens using Trichoderma spp. *Agro Productivity*.

Pedraza, A. P. (2022). Isolation and identification of metabolites produced by the native strain SGP 321 of Mucor circinelloides and evaluation of its antimicrobial activity. Obtenido de https://doi.org/10.11144/javeriana.10554.651/

Peña, D. &. (2017). Antimicrobial effect of the essential oil of Minthostachys mollis on microorganisms commonly found in lower respiratory tract infections. *Journal of Science and Technology*, 13 (3), 55-66.

Suárez Contreras, L. &. (2021). Molecular identification of filamentous fungi and their biotechnological potential. *Biotechnology in the Agricultural and Agroindustrial Secto*, 194-206.

Tingting Li, J. T. (2020). Co-culture of Trichoderma atroviride SG3403 and Bacillus subtilis 22 improves the production of antifungal secondary metabolites. *ELSEVIER*, 8.

Calibration of cocoa orchard (*Theobroma cacao* L.) with different reproductive methods and their effect on climate change

Jaime Fabián Vera Chang

Facultad de Ciencias de la Industria y Producción, Carrera de Ingeniería en Alimentos,
Universidad Técnica Estatal de Quevedo, (Ecuador)
Orcid: https://orcid.org/0000-0001-6127-2307

Luis Humberto Vásquez Cortez

Facultad de Ciencias Agropecuarias, Carrera de Agroindustria,
Universidad Técnica de Babahoyo, (Ecuador)
Orcid: https://orcid.org/0000-0003-1850-0217

María Fernanda Jumbo Tejena

Facultad de Ciencias de la Industria y Producción, Carrera de Ingeniería en Alimentos,
Universidad Técnica Estatal de Quevedo, (Ecuador)
Orcid: https://orcid.org/0009-0003-8811-9136

Sanyi Lorena Rodríguez Cevallos

Facultad de Ciencias de la Industria y Producción, Carrera de Ingeniería en Alimentos,
Universidad Técnica Estatal de Quevedo, (Ecuador)
Orcid: https://orcid.org/0009-0003-4684-9587

Matteo Radice

Departamento de Ciencias de la Tierra, Universidad Estatal Amazónica, Puyo, (Italia)
Orcid: https://orcid.org/0000-0002-4771-8912

Introduction

The cocoa plant is crucial for the economy and livelihoods of millions of farmers in tropical regions, but its production is threatened by climate change. Traditional propagation practices, such as seed planting, fail to ensure the necessary uniformity and resilience against these changes, highlighting the need to explore alternative methods like grafting and cloning. These methods could enhance cocoa's adapta-tion to adverse climate conditions and reduce its carbon footprint. This study aims to compare different reproductive methods in terms of production, disease resistance, and climate adaptation (Vera et al., 2023).

The top eight cocoa-producing countries, ranked by their annual production, are Ivory Coast (38%), Ghana (19%), Indonesia (13%), Nigeria (5%), Brazil (5%), Cameroon (5%), Ecuador

(4%), and Malaysia (1%). Together, these countries account for 90% of the world's cocoa production. In Ecuador, most of the cocoa cultivation is concentrated in the provinces of Los Ríos, Guayas, Manabí, and Sucumbíos. The primary export markets for Ecuadorian cocoa are Europe (55%), the United States (35%), Asia (9%), with the remainder distributed within Latin America (Vásquez et al., 2022).

Climate change, evidenced by a 1 °C increase in global temperature since the pre-industrial era, affects cocoa production, with projections of a 3 °C to 5 °C increase by 2100 (BBC News World, 2018). ICTA (International Center for Tropical Agriculture) has developed a climate change impact gradient for cocoa, predicting that a temperature increases of 2.1 °C will result in decreased production due to moisture loss. This could lead to a cocoa shortage and an increase in prices for the product and its derivatives, such as chocolate. Therefore, studying orchard calibration in cocoa and its relationship with climate change is crucial for understanding and mitigating these effects. The main objective of the research study is to determine the calibration of cocoa orchards (*Theobroma cacao* L.) Nacional, Forastero, and Trinitario as a diagnostic tool for climate change.

Materials and Methods

Location

This research was conducted at the Experimental Farm "La María" located at the Technical State University of Quevedo. Bromatological evaluation took place at the Bromatology Laboratory of the same institution (Campus La María, Los Ríos Province, Ecuador). Organoleptic evaluation was conducted at the Comprehensive Cocoa Quality Laboratory of the National Institute of Agricultural Research - Pichilingue (Quevedo, Los Ríos Province, Ecuador) (Erazo et al., 2023).

Methods

A Completely Randomized Design (CRD) was employed, comprising 12 treatments classified into 3 distinct types, each replicated 4 times as indicated in Table 1. Experimental units consisted of 20 plots, and repetitions were conducted monthly during harvests to assess differences among treatment means. Statistical analysis included the Tukey test for multiple comparisons with a significance level of P<0.05 (Vera, 2018).

The Tukey test, or Tukey's honestly significant difference (HSD) test, is a statistical procedure used to make pairwise comparisons between means of different groups following the detection of significant differences in an analysis of variance (ANOVA). This test calculates confidence intervals for the differences between all possible combinations of treatment means (Vera et al., 2022).

Calibration of cocoa orchard (Theobroma cacao L.) with different reproductive methods and their effect on climate change

37

Table 1
Identification and coding of the 12 treatments to be evaluated

Block	Treatment	Number of replications	Total number of units
2	T0 (Forastero)	4	24
2	T1 (Trinitario)	4	24
2	T2 (Nacional)	4	24
Total		12	72

Number of healthy pods (NHP) and number of diseased pods (NDP)

The total number of healthy and physiologically mature pods per tree will be counted according to the harvest frequency. Similarly, for the healthy pods, the diseased pods were counted and separated into different containers (Vera & Salazar, 2021).

Total pods (TP)

In this variable, all pods (healthy and diseased) were counted during the harvest period. For this, a harvest record was used, which involved counting the number of pods from selected plants in each experimental unit, and then averaging the data (Quezada et al., 2017).

Performance

Equation 1. Perfomance cocoa

$$P = (\frac{Nm}{IM}) \times Np$$

It was determined using the following formula:

Where:

P= Performance
Nm= Number of cobs per plant
IM = Ear Index.
Np = Number of plants per hectare.

Cob morphology evaluations

This is the number of mature and healthy pods of each genotype needed to obtain one kilogram of dry cocoa. The following formula was used for its calculation:

The Cob index was determined by assessing 20 physiologically mature cobs, free from any disease symptoms, in each sample (randomly selected). Following almond extraction, the almonds were subjected to fermentation and drying until they reached 7% humidity (Vásquez et al., 2023). The Cob index was calculated using the specified formula

Equation 2. Cacao cob index (CCI)

$$IM = \frac{Number\ of\ 20\ cobs \times 100}{Weight\ (g) of\ dried\ almonds}$$

Cob weight was recorded with a digital scale. Length and diameter were recorded with a ruler (diameter from furrow to groove from the equatorial diameter). Cob ridge and spine thickness were recorded with a caliper. The Seed index were performed taken at random 300 fermented and dried almonds; all almonds were weighed, and averages were calculated. The following formula was applied:

Equation 3. Seed index

$$SI = \frac{\text{Weight in grams of 300 fermented and dried seeds}}{300}$$

Cobs Length

Ten cobs randomly selected from each treatment are measured using a caliper to calculate the average (Lagunes et al., 2018).

Cobs Width

After harvesting, 20 cobs were randomly selected from each treatment and then weighed using a precision scale, and the weight was recorded (Chacón et al., 2007).

Principal Component Analysis (PCA)

Principal Component Analysis (PCA) was applied to obtain scatter plots (biplots) of the quantitative variables grouped according to their optimal components of the productive and physical profiles, using the following formula:

Equation 4. Component Analysis

$$rij = \frac{cov(F1,Fj)}{\sqrt{var(Fi)\,var(Fj)}}$$

Where:

Cov. X, Y = Covariance of Fi and Fj
S²Fi = Variance of X
S²Fj = Variance of Y

Principal Component Analysis (PCA) and biplots are used in dimension reduction, allowing for the visualization of all generated data in a lower-dimensional space. Artificial axes, known as Principal Components, are constructed to analyze and synthesize the variability or dispersion with their original characteristics. Biplots graphically express this information to identify associations. The new principal components or factors are linear combinations of the original variables and are independent of each other. The results are presented in graphical form (biplot) (Vera et al., 2014).

Results

Climatic variables

This comparison of the means of the climatic data for the three years indicates the following: The average air temperature in degrees Celsius for the year 2017 is 24.9 °C, higher than for the year 2018 at 24.55 °C, and lower than for the year 2019 at 24.97 °C, making it the highest average temperature of the three years. For the maximum temperature, 2017 recorded 30.06 °C, the highest of the three years, with 2018 being the lowest at 29.53 °C, and 2019 at 29.85 °C. Similarly, the minimum temperature for 2017 is 22.18 °C, followed by 21.71 °C for 2018, the lowest minimum of the three years, and 22.07 °C for 2019. The temperature range for 2017 is 7.89

Calibration of cocoa orchard (Theobroma cacao L.) with different reproductive methods and their effect on climate change

39

°C, the highest value, followed by 7.81 °C for 2018, and 7.19 °C for 2019, the lowest value (Table 2).

The average relative humidity for the year 2017 was 85.58%, for 2018 it was 84.33%, the lowest average, and for 2019 it was 85.83%, indicating the year with the highest average value. Con-sequently, the maximum humidity for the years 2017 and 2019 was 96.83%, while for 2018 it was 96.33%. Finally, the minimum humidity for 2017 has a value of 62.25%, the lowest, followed by 62.75% for 2018, and 64.50% for 2019, indicating the highest minimum humidity (Table 2).

Table 2
Annual climatic conditions during the years (2017-2019) of T. cacao progeny evaluation in the Quevedo area of Ecuador

Weather Conditions		Experimental Farm 'La Represa			Average
		2017	2018	2019	
Air Temperature (°C)	Mean	24.90	24.55	24.97	24.81
	Maximum	30.06	29.53	29.85	29.81
	Minimum	22.18	21.71	22.07	21.98
	Oscillation	7.89	7.81	7.19	7.63
Relative Humidity	Mean	85.58	84.33	85.83	85.25
	Maximum	96.83	96.33	96.83	96.67
	Minimum	62.25	62.75	64.50	63.17
	Annual Sunshine Duration	73.38	67.10	66.96	69.15
	Evaporation (mm)	86.54	92.41	81.27	86.74
	Precipitation (mm)	272.56	144.22	249.98	222.25

Note: Three-year averages of the weather conditions are displayed

Production metrics variables

In the obtained results, regarding the number of healthy cobs, number of disea-sed cobs, and total cobs presented in Table 3, it was observed that there was no sig-nificant difference ($p \leq 0.05$) between the treatments for the aforementioned varia-bles. Regarding the yield, due to signifi-cant difference ($p < 0.05$), it was demons-trated that T2 achieved the highest yield with 2245.42 kg/ha/year, while T3 showed a lower yield of 1681.60 kg/ha/year

Table 3

Statistical averages of cocoa (T. cacao) production parameters

Treatments	NHP	NDP	TP	Yield per hectare per year calibrated	Production per hectare per year
T0	12.02[a]	2.65[a]	14.67[a]	1864.25[b]	1219.52[b]
T1	14.06[a]	2.62[a]	16.43[a]	2245.42[a]	1284.14[a]
T2	11.69[a]	2.36[a]	14.31[a]	1681.60[c]	1015.52[c]
Average	12.59	2.54	15.14	1930.42	1173.06
C.V.	0.10	0.06	0.07	0.15	0.12

Note: The calibrated yield is shown compared to the yield per hectare per year.

Fruit parameters

In the cob index, no significant difference ($p \geq 0.05$) was found among the studied treatments; however, the highest value was observed in T3 (23.17), while T2 had the lowest value (20.87). Regarding the seed index variable, there was no statistical significance ($p \geq 0.05$) between treatments T0 and T2 with a value of 1.17, which, unlike T2, indicates statistical significance with a higher value (1.22). In relation to cob weight, it was observed that there was no statistical significance among the treatments.

Table 4

Parameters of Nacional, Forastero, and Trinitario cocoa fruit (PI; Pod Index, SI; Seed Index, PW; Pod Weight)

Treatment	PI	SI	PW
T0	21.49[a]	1.17[a]	701.38[a]
T1	20.87[a]	1.22[b]	749.50[a]
T2	23.17[a]	1.17[a]	691.38[a]
Average	21.18	1.39	714.09
C.V.	2.1%	24%	4.4%

Fruit

Calibration

Regarding the length of the cocoa pod, in the first and fourth months of growth, there was no statistical significance ($p \geq 0.05$) among the studied treatments. However, in the second month, it was demonstrated that T2 with 10.39 was statistically different ($p \geq 0.05$) from T0, which had the smallest size. Additionally, in the fifth month (harvest month), there was statistical significance indicating the highest value in T0 with 24.15 and the lowest value in T2 with 22.30.

Calibration of cocoa orchard (Theobroma cacao L.) with different reproductive methods and their effect on climate change

41

In relation to the width of the cocoa pods, in the first, fourth, and fifth months, the treatments did not present significant differences (p≥0.05). However, in the second month, the treatments showed significant differences (p≥0.05), with the highest value in T2 (4.88) and the lowest value in T1 (2.81), with an average of 3.58 and a coefficient of variation of 31.7%. As for the third month, it was determined that T0 and T2 with 7.9 were statistically different (p≥0.05) from T2 with 6.28, which obtained a lower value.

Principal Component Analysis (PCA)

Through PCA, a comparison was made between physical, productive, and climatic parameters. It was found that physical quality parameters such as IS (Seed Index), IM (Pod Index), and AM (Pod Weight) have a greater influence, while temperature and humidity have a lesser influence on Nacional variety. In contrast, Forastero variety shows a higher contribution from temperature, humidity, and the number of pods. Regarding the Trinitario variety, pod weight is related to calibrated yield, closely followed by actual yield and pod length. Considering the sum of these two components, total of 100% of the existing total variability was obtained, allowing for a more comprehensive relationship.

The climate exhibits a moderate range for cocoa cultivation; however, certain months of the year experience high peaks of temperature and maximum precipitation, which have influenced the presence of pests such as monilia. The terrain in all analyzed systems shows flat surfaces, with slopes less than 2%, indicating a low risk of soil erosion (Albiño, 2020). Despite Criollo cocoa being a variety with a unique genotype known for its fine flavor chocolate, more vigorous hybrids with higher agronomic yield and lower susceptibility to diseases, such as Trinitario, have been introduced (Mejía et al., 2018).

Table 5

Fruit calibration of Nacional, Forastero, and Trinitario in each of their stages

Treatments	COBS									
	1° Month		2° Month		3° Month		4° Month		5° Month	
	Length	Width	Length	Width	Length	Width	Length	Width	Length	Width
T0	6.30[a]	2.05[a]	8.55[b]	3.04[ab]	15.28[a]	7.90[a]	18.58[a]	8.29[a]	24.15[a]	9.70[a]
T1	6.48[a]	1.95[a]	9.39[ab]	2.81[b]	14.99[a]	7.88[a]	19.59[a]	8.45[a]	23.59[ab]	10.33[a]
T2	6.16[a]	1.89[a]	10.39[a]	4.88[a]	14.52[a]	6.28[b]	19.55[a]	8.54[a]	22.30[b]	9.13[a]
Average	6.313	1.96	9.44	3.58	14.93	7.35	19.24	8.43	23.35	9.72[a]
C.V. (%)	2.5%	4.1%	9.8%	31.7%	2.6%	12.6%	3.0%	1.5%	4.1%	6.2%

Note: This table shows the calibration or measurement of pods during the five months of the stud

Discussion

Climatic variables

The climatic conditions, as determined in the study, are within the parameters established by Zamora, (2018), who, in their research, emphasize the importance of considering climatic conditions in order to prevent and reduce soil erosion, both in the agricultural sector and in deforestation

Production metrics variables

The data reported on the number of healthy cobs is similar to what was determined by Erazo et al. (2023), who indicated a small production (30-194 healthy cobs) in clones T23, INIAP 484, and T13 during the months of March-April, with a peak in September. Clones T11, T8, and T1 demonstrated the highest production of healthy cobs, while the least productive clones were T23, INIAP 484, and T13. Microorganisms used as control methods have been found to be highly efficient in reducing the two most devastating diseases in cocoa crops (moniliasis and witches' broom), as evidenced by the literature. Villamil et al. (2015) indicate that the most commonly used biocontrol agents are fungi (*Trichoderma* sp.) and bacteria (*Bacillus* sp.), which undergo metabolic processes and can be used for biological control.

In the study conducted by Tezara et al. (2020), it was reported that the most vulnerable clones with the highest rate of diseased cobs were T23, INIAP 484, T24, and T13 (50-60%).

Meanwhile, the least susceptible clones were T11, PMA 12, T8, and T1 (5-27%). In contrast, clones CCN51 and T1 had the highest number of diseased cobs, as found by Cortez et al. (2017), while those showing the lowest number of diseased cobs were clones T8, PMA 12, and T11 respectively. According to Vera & Goya, (2015),there are manyFactors that affect the final number of fruits, including "cherelle wilt" or premature death, which can destroy fruits in their early stage and reduce them by 20 to 90%.

According to the National Institute of Forestry Research (2019), the Chocotab hybrid has been statistically superior to its parents, with an average of 45 fruits/plant/year over five years of evaluation. Its fruit index is 22, similar to UF 273, but higher than PA 169 with 26 fruits. (Vera et al., 2023) affirm that the number of present cobs is not a good indicator of yield because many cobs from some trees produce more cocoa seeds than others.

Fruit parameters

The cob index is a significant trait in the industry and in the selection of material for genetic improvement, with a preference for materials with an index lower than 20 cobs (Vera et al., 2022).

According to Vera et al. (2019), the physical quality of almonds in twenty-one interclonal cocoa crosses in Ecuador ranged from 1.41 to 0.97, with an average of 1.25. Intriago et al. (2023) indicate that there is variability among

Calibration of cocoa orchard (Theobroma cacao L.) with different reproductive methods and their effect on climate change

43

genotypes related to this index; Trinitario-type cocoas have a lower seed index than Forastero type.

Seed weight is related to findings by (Garcia et al., (2019), where the average cob weight and percentage of shell were 732.8 g and 81.8%, respectively. It is worth noting that the cocoa shell percentage can vary from 52% to 76%. According to the National Institute of Forestry Research, average weights range from 261g to 454g. On the other hand, Álvarez et al. (2020), mention a relationship between the degree of cob ripeness and grain weight; the riper the cob, the heavier the grains.

Fruit calibration

According to Quevedo Guerrero, (2018), in their studies conducted on fifth-month cocoa pods in the phenotypic characterization, they determined an average fruit length of 20.8 ± 0.88, indicating similar results to those obtained in this study. Additionally, they reported a fruit width of 9.10.

Conclusions

The productive parameters based on NMS, NME, and MT of each variety did not present significant differences according to the Tukey test (p≥0.05), obtaining average values of 12.59, 2.54, and 15.14, respectively. With these data, a calibrated yield was provided, which showed statistical significance among its treatments, with the highest value in T2 (2245.42 kg/ha/year) and the lowest value in T2 (1681.60 kg/ha/year). These results were obtained when the environment had a maximum temperature of 29 °C, a minimum of 22.07 °C, and an average of 24.97 °C, with an average humidity of 85.83%.

The evaluation based on the physio-phenological characteristics of cocoa revealed an average total pod count of 15.14, including healthy and diseased pods across treatments. It is worth mentioning that there was moderate to low production during the study months. Regarding calibration, it was determined that in the second month, pods showed statistical significance among treatments in length and width, with the highest value in T2 (10.39 - 4.88), the lowest value for length in T0 (8.55), and for width in T1 (2.81). For the third and fourth months, there was no significant difference, but in the fifth month, pods indicated the following: for length, the highest value was in T1 (24.15) and the lowest in T2 (22.03), and for width, the highest value was in T1 (10.30) and the lowest in T2 (9.13).

To validate this calibration process, a PCA was conducted to compare the physical, productive, and climatic parameters. It was found that calibration tends to be more accepted by the Trinitario variety, while the variety most related to climate is Forastero, as obtained in this research. Each treatment was rigorously selected to identify the evaluated varieties, determining their accuracy and reliability in the entire process.

References

Albiño. (2020). Los sistemas de producción de cacao del cantón Shushufindi y su resiliencia al cambio climático. *Revista Latinoamericcana de Estudios SocioAmbientales*, *27*, 90-114.

Álvarez, Vera, J., Vallejo, C., & Tuarez, D. (2020). Aprovechamiento de almendras de jackfruit adicionado manteca de cinco clones experiemntales de cacao extraída apartir de mazorcas infecadas con moniliasis para la obtención de crema de chocoalte blanco. *Universidad, Ciencia y Tecnología*, *1*, 61-68.

Chacón, Gómez, C., & Márquez, V. (2007). Caracterización morfológica de frutos y almendras de plantas de cacao (Theobroma cacao L.) en la región suroccidental de Venezuela. *Revista de La Facultad de Agronomía de La Universidad Del Zulia*, *24*(1), 202-207.

Erazo, Vera, J., Tuarez, D., Vásquez, L., Alvarado, K., Zambrano, C., Mindiola, V., Mora, R., & Revilla, K. (2023). Caracterización fenotípica en flores de cacao (theobroma cacao l.) en 40 híbridos experimentales en la finca experimental La Represa. *Revista Bionatura*, *8*(3), 1-9. https://doi.org/http://dx.doi.org/10.21931/RB/2023.08.03.11

Garcia, Serna, A., Códoba, D., Marín, J., Montalvo, C., & Ordoñez, G. (2019). Estudio de la fermentación espontanea de cacao (Theobroma Cacao l.) y evaluación de la calidad de los granos en una unidad productiva a pequeña escala. *Revista Colombiana de Investigaciones Agroindustriales*, *6*(1), 41-51. https://doi.org/https://doi.org/10.23850/24220582.1635

Intriago, Chávez, G., Vásquez, L., Alvarado, K., Escobar, R., Vera, J., Radice, M., & Raju, M. (2023). Evaluación del contenido de cadmio y caracterización fisicoquímica de almendras y pasta de cacao (Theobroma cacao). *Innovaciencia*, *11*(1), 1-11. https://doi.org/https://doi.org/10.15649/2346075X.3411

Lagunes, Ramírez, M., Ortiz García, C. F., & Gutiérrez, O. A. (2018). VARIACIÓN MORFOLÓGICA DE FRUTOS Y SEMILLAS DE CACAO (Theobroma cacao L.) DE PLANTACIONES EN TABASCO, MÉXICO. *Revista Fitotecnia Mexicana*, *41*(2), 117-125. https://doi.org/10.35196/rfm.2018.2.117-125

Mejía, Coronel Niño, R., Gálvez López, D., Rosas Quijano, R., & Vásquez Ovando, A. (2018). *Efecto de la fermentación y del tostado sobre el contenido de aminas biogénicas en semillas de cacao*. *3*(12), 958-979. https://doi.org/10.19230/jonnpr.2778

Quevedo Guerrero. (2018). *Calidad físico química y sensorial de granos y licor de cacao (Theobroma cacao L.) Usando cinco métodos de fermentación*.

Quezada, Quevedo, J., & García, R. (2017). Determinación del efecto del grado de madurez de las mazorcas en la producción y calidad sensorial de (Theobroma cacao L.). *Revista Cientiífica Agroecosistemas*, *5*(1), 36-46.

Tezara, Valencia, E., Reynel, V., Bolaños, M., & Flores, H. (2020). Photosynthetic activity of ten national cocoa clones and their relationship to yield. *Espam Ciencia Para El Agro*, *11*(1), 19-27.

Vásquez, Intriago, F., & Alvarado, K. (2023). Extracto de (banano y manzana) con micoorganismos eficientes y su efecto en la disminución de cadmio en almendras de cacao (Theobroma cacao L.). *CCIUTM*, *6*, 1-941.

Vásquez, Vera, J., Erazo, C., & Intriago, F. (2022). Induction of rhizobium japonicum in the fermentative mass of two varieties of cacao (Theobroma Cacao L.) as a strategy for the decrease of cadmium. *International Journal of Health Sciences*, *3*(April), 11354-11371. https://doi.org/https://doi.org/10.53730/ijhs.v6nS3.8672 Induction

Vera. (2018). *Resumen de principios de diseños experimentales* (Compás, Ed.).

Vera, & Goya, A. (2015). Comportamiento agronómico, calidad física y sensorial de 21 líneas híbridas de cacao (Theobroma cacao L.). *Revista La Tecnica*, *15*, 26-37. https://doi.org/https://doi.org/10.33936/la_tecnica.v0i15.539

Calibration of cocoa orchard (Theobroma cacao L.) with different reproductive methods and their effect on climate change

45

Vera, Intriago, F., Alvarado, K., & Vasquez, L. (2022). Inducción anaérobica de bradyrhizobium japonicum en la postcosecha de híbridos experimentales de cacao y su mejoramiento en la calidad fermentativa. *Journal of Science and Research*, *7*(2), 50-69. https://doi.org/https://doi.org/10.5281/zenodo.7723254 AUTORES:

Vera, Ramos, R., Sánchez, F., Chévez, H., Veliz, B., & Pinargote, J. (2019). Caracterización física y sensorial de treinta materiales élites de cacao (Theobroma cacao L.) en la cuenca alta de rio Guayas - Ecuador. *CONAMTI*, *5*(22), 115-124.

Vera, & Salazar, M. (2021). Aplicación de siete bioles sobre el desarrollo agronómico en cacao (Theobroma cacao L.) De origen sexual y asexual en etapa productiva en la finca experimental la represa. *Centrosur*, *1*(1), 1-43.

Vera, Torres, A., Vásquez, L., Alvarado, K., & Intriago, F. (2023). Extraction of cocoa powder for the preparation of a drink by adding mucilage and guava. *Sarhad Journal of Agriculture*, *39*(2), 1-10. https://doi.org/https://dx.doi.org/10.17582/journal.sja/2023/39/s2.10.18

Vera, Vallejo, C., Párraga, D., Morales, W., Macias, J., & Ramos, R. (2014). Physical-chemical and sensory atributes of the cocoa Nacional (Theobroma cacao L.)n fifteen clones beans in Ecuador. *Science and Technology Magazine*, *7*(2), 21-34. https://doi.org/https://doi.org/10.18779/cyt.v7i2.139

Villamil, Viteri, S., & Villegas, W. (2015). Aplication of microbial ntagonist for the biological control of Moniliophthora roreri Cif & Parc in Theobroma cacao L. under field conditions. *Journal of the National Faculty of Agronomy Medellin*, *68*(1), 7441-7450. https://doi.org/https://doi.org/10.15446/rfnam.v68n1.47830.

Zamora. (2018). Cambio Climático. *Revista Mexicana de Ciencias Forestales*, *6*(31), 4-7.

Comparative analysis of microstructure and hardness of Isobloc W360 steel with tempering and Austempering heat treatment

Gabriel Usiña
Universidad Politécnica Salesiana, (Ecuador)
Orcid: https://orcid.org/ 0009-0004-2460-4690

Cristian Leiva-González
Universidad Politécnica Salesiana, (Ecuador)
Orcid: https://orcid.org/ 0000-0002-8255-1337

Erika Pilataxi
Universidad Politécnica Salesiana, (Ecuador)
Orcid: https://orcid.org/ 0009-0009-2633-0407

William Quitiaquez
Universidad Politécnica Salesiana, (Ecuador)
Orcid: https://orcid.org/ 0000-0001-9430-2082

Introduction

In the Ecuadorian industry, the sector focused on taps and fittings is linked to the elaboration of dies for creating new brass elements or pieces, through the forging process that allows the production of a great number of equal products. This process presents as an advantage good mechanical property such as resistance to corrosion, fatigue, great tenacity and ductility (Quitiaquez et al., 2022). Due to the properties obtained by this process in the manufacturing field, forging accounts for 20-30 % of the value of all goods and products produced (Moreno & Adames, 2022).

The materials used in forging dies involve aspects that must be taken into account, such as the plastic deformation obtained by cold forging, to increase the ductility of brass, forging is carried out in hot forging (Penghui et al., 2020), Zuno et al. (Zuno-Silva et al., 2023) detail for hot forging works an addition of vanadium plus boron to be potentially used in dies obtaining an improvement in wear resistance, which translates into

an extension in the useful life of forging dies. The addition of vanadium and boron produced a stable wear factor at a temperature of 22 and 400 °C.

When mentioning hot forging, factors such as working temperatures of approximately 1050 °C, are contemplated as the problems presented by forging dies. These problems are wear, mechanical fatigue, breakage, plastic deformation, and cracks due to thermal fatigue (Fernádez-Tamayo et al., 2022), and can be found in different parts of the cavity of the dies, thus dominating different failure mechanisms. Peñaloza (Peñalosa, 2022) details that the metal is heated to high temperatures before being worked to reduce its resistance to deformation. In the case of steel (depending on the alloy and carbon content), the temperature ranges between 800 and 1250 °C, being higher than the recrystallization and phase transition temperature, facilitating the forming of the alloy and the working of the dies in forging.

Tchiquendja et al. (Tchiquendja-Eleno et al., 2020) detail that the material used for tooling usually has 0.47 % carbon, 0.70 % manganese, and other alloys that should contain the steels for forging that are treated at high temperatures and for determining the appropriate type of cooling, obtaining an improvement in the mechanical properties to be used in hot forging processes. It is observed by microstructural analysis if the material improves its deformation strength or changes its structure. Ishtiaq et al. (Ishtiaq et al., 2022) mention that when tempering steel with a carbon content ranging between 0.37 and 0.54 %, it is evident in its microstructure the presence of martensite, which determines that the material acquires high hardness but increases its brittleness, thus being dismissed in hot forging works due to the presence of cracks.

Chien et al. (Huang et al., 2023) detail that not only does the amount of carbon interfere when a material is exposed to a heat treatment such as quenching. Described for 631 stainless steel, the working temperature in quenching is around 500 °C; treated with austempering at 720 °C, it is possible to obtain a higher tensile and impact strength than 631 stainless steel under normal quenching conditions. Properties are improved by the influence by the chemical composition, in this case, the amount of chromium (Cr) which is 16.99 %. Sabzalipour and Rashidi (Sabzalipour & Rashidi, 2023) performed the heat treatment of tempering and austempering, and the variation of hardness goes from 50 % of the hard phase of ferrite and martensite to different from those composed of ferrite-bainite phases, which goes from 80 % in volume of hard phase.

Lee et al. (2022) discuss nanostructured high-carbon bainitic steels austempered at 200, 250 and 300 °C. It is observed that all steels have mostly plate-like transformation products such as bainite. Plate-type bainite may contain retained austenite and martensite transformed from metastable austenite after quenching, especially in the steels austempered at 200 and 250 °C, which

Comparative analysis of microstructure and hardness of Isobloc W360 steel with tempering and Austempering heat treatment

49

means that the austempered steels have a higher martensite fraction compared to the steel austempered at 300 °C. Brown et al. (2023) detail that bainitic steels exhibit strain hardening by improving the properties of ultimate tensile strength and hardness 600 to 670 HV compared to quenched and tempered steels.

Su et al. (2022; 2023) describe that for an M50 steel, a heat treatment of quenching plus three times tempering is applied, in which the solution temperature ranges between 1070 and 1110 °C and the tempering temperature is between 540 and 550 °C. After heat treatment, the microstructure of M50 steel consists mainly of quenched martensite and a small amount of retained austenite, hardness at room temperature can reach 60-63 HRC. The processes result in multiscale microstructure refinement that can improve the yield strength of martensitic steels (Wang et al., 2023). When considering the limits of a martensite microstructure, it is observed that an austempering contributes to improving the mechanical properties of the steels, García et al. 2022) detail the austempering heat treatment on a 0.41 % carbon (C) steel, which starts with an austenitizing at 950 °C for 72 min, followed by a molten salt bath at 310 °C for 120 min and then air-cooled. The salts used were a mixture of 45 % NaNO3 and 55 % KNO3. It has characteristics such as resistance, toughness, wear resistance, corrosion resistance, and shock absorption (Zhou et al., 2020).

Behzadifar et al. (describe that an increase in the austempering time increases the carbon content of the retained austenite, regardless of the temperature and the microstructure obtained, which consists of bainitic ferrite plates with an average thickness of 53 nm surrounded by carbon-rich retained austenite with a hardness of 561HV, yield strength of 1614 MPa and a total elongation of 9 %. Varshney et al. (2020) similarly mention that the amount and size of carbides in the samples austempered at 350 and 400 °C are smaller than in the samples austempered at 300 °C.

This research aims to carry out a comparative analysis of the heat treatment quenching-reviving with tempering-reviving, to determine the treatment that avoids the presence of cracks in dies used in forging that is used in taps and fittings. The introduction describes the importance of heat treatment in stainless steel and mechanical properties that are improved with the heat treatments performed. The materials and methods section presents the heat treatments performed, the microstructure obtained, as well as the resulting hardness in each case. In the results section, the comparative analysis between the two treatments is detailed, analyzing the microstructure and the hardness obtained, thus determining which heat treatment is the most suitable to avoid the presence of cracks in the material when it is subjected to forging work.

Materials and Methods

In the heat treatment process, the chemical composition of the material and the temperatures recommended by the manufacturer for the heat treatments to be carried out must be clearly known, in addition to the Temperature, Time, Austen-ite Transformation (TTT) diagrams to determine the correct time and temperature for the experiment, as well as the microstructure obtained. Figure 1 indicates the procedure to be followed to carry out this research.

Figure 1

Procedure for evaluating the quenching and tempering process of Isobloc W-360
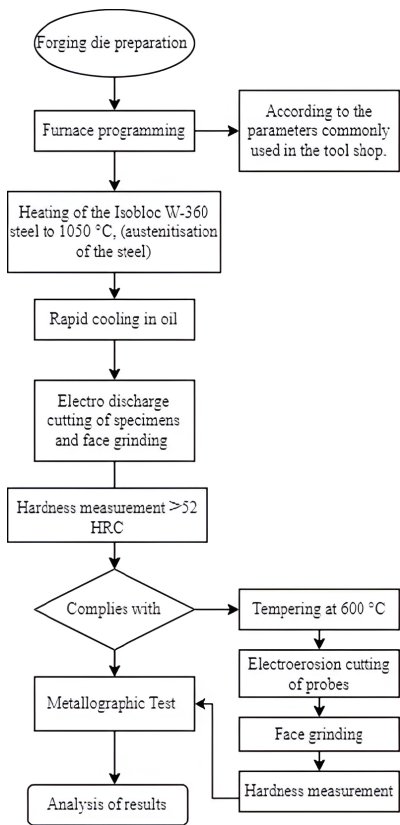
The Isobloc W-360 steel samples with dimensions of length, width and thickness of 50, 20 and 10 mm respectively, were the result of cutting with wire, avoiding that the material would modify its microstructure by the pre-heating of the cut. The chemical composition of the steel is detailed in table 1,where it is observed that it is a material that possesses a high content of Chromium as of Molybdenum can be exposed to works of high temperatures (Rodríguez-Cabrera, Ruíz Mondragón, Macías-López, 2019).

Table 1

Chemical composition of Isobloc W360 steel (%wt) (Bohler, 2021)

Carbon (C)	Silicon (Si)	Manganese (Mn)	Chrome (Cr)	Molybdenum (Mo)	Vanadium (V)
0.5	0.2	0.25	4.5	3	0.6

The processes for austempering, which is a heat treatment in which the surface of the low carbon steel is carburized and when a sudden cooling is applied, is subjected to an isothermal cycle, favoring the formation of a bainite base in the decarburized layer transforming it into a solid solution of quenching and austempering (Ríos-Diez et al., 2020). For the austempering, the curve 'S' of the TTT diagram corresponding to the Isobloc W-360 steel is used, from which the temperature and time for the phase transformation to Baini-

te is obtained, which is 300 °C and 30 min respectively, as shown in Figure 2.

Curve 'b' is the one that resembles the cooling carried out in thermal oil.

Figure 2

Continuous quenching TTT curves of Isobloc W-360 steel (Bohler, 2021)

The process carried out for the quenching heat treatment starts with the furnace at a temperature of 650 °C heating for a set time of 35 min, generating nucleation and growth of acicular ferrite. Once it was kept in that time interval to reach austenitisation 1050 °C is applied on the samples without removing from the furnace, maintaining the time limit of 35 min continuously. When the determined temperature and time intervals are met, a rapid and uniform cooling in thermal oil is carried out until the fluid temperature is reached. Finally, the specimens are removed from the oil tank, leaving the specimens to reach room temperature. As seen in Figure 3, a temperature vs. time graph is shown, considering time cumulatively.

Figure 3

Flow diagrams for tempering heat treatment
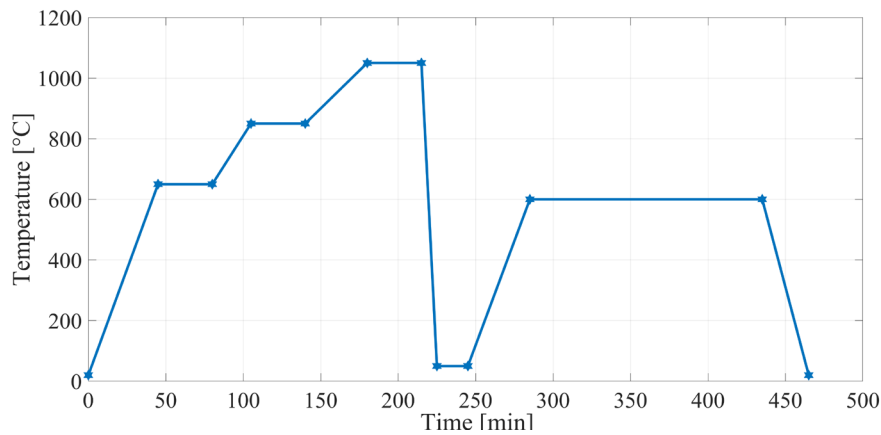
Figure 4 shows the temperature vs. time curve for the austempering treatment where the specimens are heated to a temperature of 650 °C and held for 35 min, continuing with an increase of 850 °C at the same time range where the temperature continues to increase to 1050 °C for 35 min, thus obtaining austenitisation. Unlike quenching, to obtain austempering, the samples are cooled in oil for 3 minutes so that they immediately reach a temperature of 300 °C, the samples enter the furnace which is preheated to 300 °C and is maintained for 30 minutes. Once this time has elapsed, they are cooled until they reach room temperature.

Figure 4

Flow diagrams for Austempering

Comparative analysis of microstructure and hardness of Isobloc W360 steel with tempering and Austempering heat treatment

53
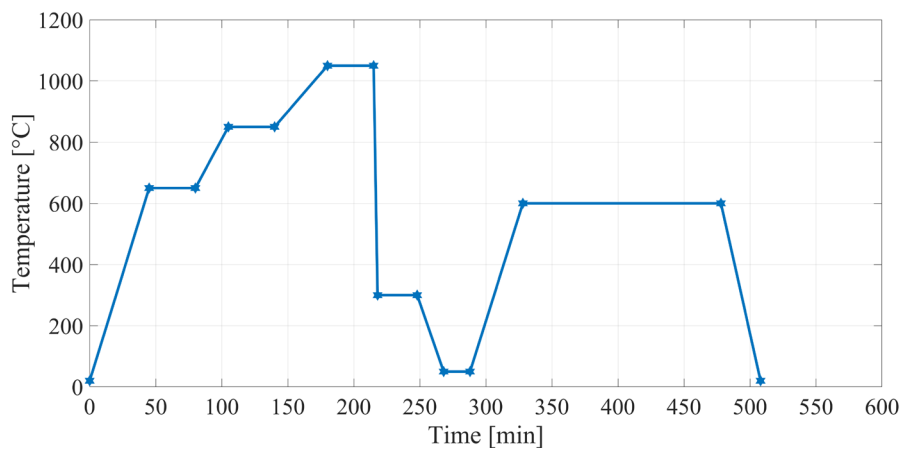
As it is true that by performing only the heat treatment of quenching or austempering, an increase in the hardness of the material is obtained but this modification affects its brittleness and to prevent this from happening, a stabilisation tempering must be performed which should consist of a temperature of 600 °C and keep the specimens for 2 hours and 30 min. Leading to the Isobloc W-360 steel to balance its hardness as well as the microstructure to avoid causing brittleness in the material. Continuing with the analysis and to detail the existence of changes in the material we proceed to measure the hardness of the samples in the different stages of heat treatment, such as supply, quenching, austempering and tempering. In each of the cases, the measurements are taken in Rockwell (digital hardness tester TINIUS OLSEN FH 1-5) on HRC scale according to ISO 6508 or ASTM E18 (Require- et al., 2014). Five specimens were used for these measurements. Figure 5 shows the arrangement of the 7 points where the hardness measurements were taken.

Figure 5

Diagram of hardness measurements on the specimens
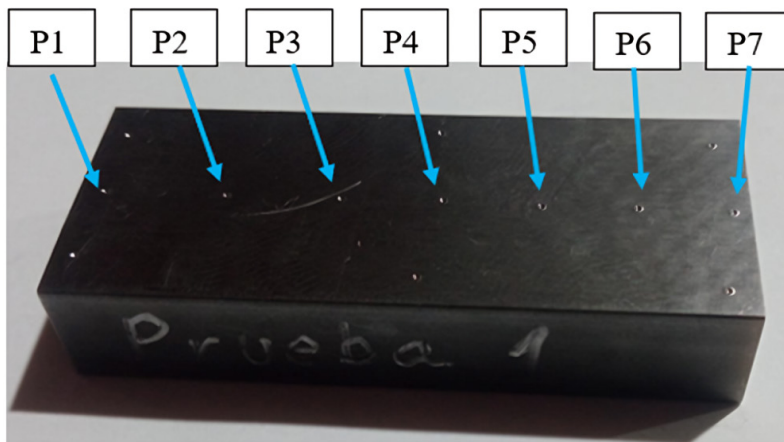
Once the hardness of the specimens that have been cut by wire EDM, the faces of the specimens are ground to obtain a uniform surface with the help of a flat grinder, obtaining a suitable surface finish to proceed with the mirror polishing of the specimens. The polishing of the samples is carried out with fine grain sandpaper under a water jet, and then followed by polishing with a cloth to obtain a mirror finish. Once each of the samples have these finishings, the chemical is applied to each of the test specimens. Nital_4 is applied for 11 minutes for the specimens that are only tempered and austempered, unlike the specimens that are tempered, Nital_4 is applied for 3 minutes and then prical for 40 seconds to obtain a clearer visibility of the microstructure of the material.

The qualitative metallographic analysis is performed with a NIKON TS2-S-SM optical microscope. It is a microscope designed to observe the microstructure of a material after being exposed to all the steps involved in a metallographic analysis. It is an inverted microscope with high resolution objective lenses 10X, 20X, 50X and 100X with very short working distances. To analyze the results, the 100X magnification lens is used to clearly appreciate the microstructures obtained by the thermal treatments applied to the specimens tested.

Results

Microstructure

As a first parameter of analysis, the microstructure is observed in each case of heat treatment in Figure 6. The microstructure of the tempered specimens is shown, which are constituted by a microstructure with a retained austenite base that are white areas that generate the visibility of the grain size. The presence of carbides dispersed in an intergranular way is observed leading the material to a phase where its hardness increases and the martensite sheets in black colour that like the carbides provide an increase in the hardness, but it goes hand in hand with the fragility generated in the material. In such a way that a stabilisation tempering is carried out in each of the cases.

Figure 6
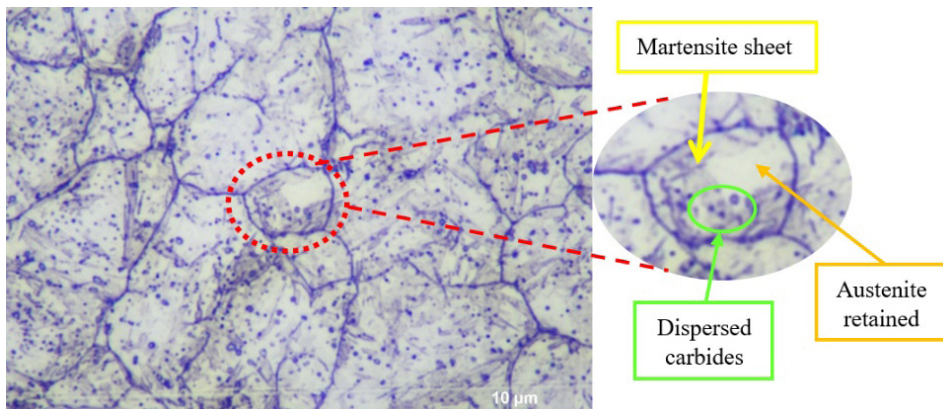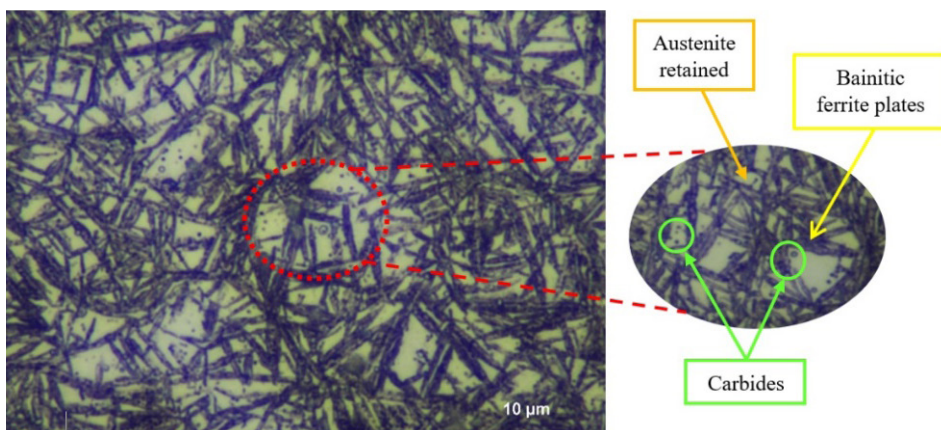*Micrograph obtained after hardening*

Figure 7. shows the microstructure of the austempered specimens, where it is clearly observed that the combination of intercritical austenitisation followed by the application of low temperatures (300 °C) generates the formation of bainitic ferrite sheets, which is more stable than the presence of austenite blocks, even so, the presence of retained austenite is evident, causing the release of nano-sized carbides which are formed by diffusion towards the austenite.

Comparative analysis of microstructure and hardness of Isobloc W360 steel with tempering and Austempering heat treatment

55

Figure 7
Micrograph obtained after austempering

As seen in Figure 8 in the specimens that were applied a stabilisation tempering for both tempered and austempered samples, in each case the tempering contributes with a stabilisation to the material. achieving structural homogeneity. In Figure 8 (a) a tempering can be seen after tempering, where the martensite sheets are refined by the plastic deformation of the martensite, generating a partial dissolution of carbide particles. The presence of dislocations and formation of carbon clusters contributes to the presence of nucleation of fine carbides during a subsequent tempering, as it is true that the influential factors for this phenomenon are temperature and residence time, but observing the presence of austenite retained as a base microstructure determines that the material improves the hardness. The low temperature in the shrinkage of the structure generates that the carbon atoms that are dispersed in the martensite and retained austenite jump to neighbouring dislocations and act as sites for the formation of carbides. Also, during tempering the high presence of Cr, Mo and W generate the significant presence of retained austenite as observed in the microstructure (Miranda, 2020). Figure 8 (b) corresponds to the application of tempering after austempering, and it is observed in the first phase that there is the presence of bainitic ferrite that when passing to a tempering of 600 °C, leaving a dwell time of 2 hours and 30 min, leading the cementite to precipitate into the bainite, thus generating ferrite plates which proceed to form segments parallel to the refined bainite. The form of precipitation of the carbides influences the stresses associated with the dysfunctional growth of the bainite, since the carbides in the bainite are extremely thin. As a consequence, bainitic ferrite tends to be more tenacious than refined bainite, despite being tougher, the sharp cementite particles of refined bainite act as nucleation points for crack dissociations (Ríos-Diez et al., 2020).

Figure 8

Micrograph obtained after tempering (a) quenched, (b) austempered
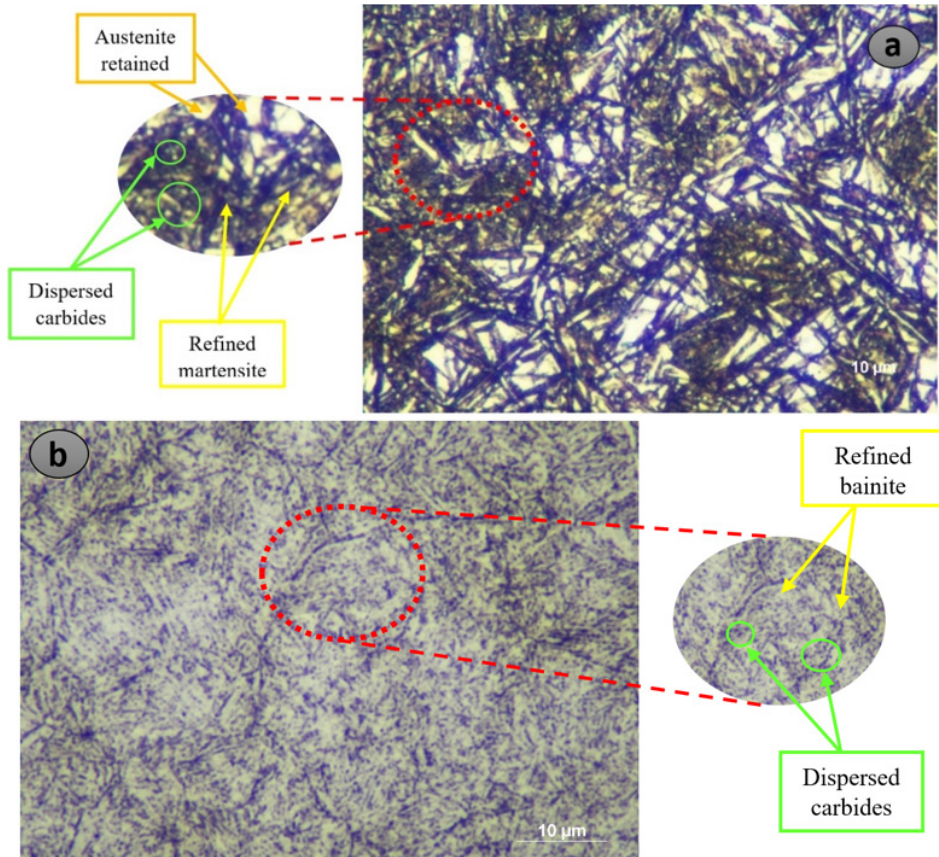
When observing the microstructure, the bainite is the result of an isothermal transformation. The size of bainitic ferrite plates and retained austenite is based on the application temperature, achieving considerable stability in the material when applying a heat treatment. Based on the study of the microstructure of the treated material, another parameter of analysis is observed. As for the hardness obtained from the samples after each thermal process, it is modified according to the time of permanence in conjunction with the exposure temperature. The supply hardness ranges from 5 to 7. 5 Rockwell hardness (HRC), when carrying out respectively the thermal treatment of tempering and austempering. It is observed that the hardness acquires the values of 62 HRC in the samples that are exposed to tempering, unlike the austempering specimens which decrease the hardness in a 12 % giving as value 54 HRC (Figure 9.), although it is true that the hardness is increased but the fragility of the material is high for forging works; there-

Comparative analysis of microstructure and hardness of Isobloc W360 steel with tempering and Austempering heat treatment

57

fore, the application of a stabilization tempering leads the material to present a homogeneous microstructure that goes hand in hand with a hardness of 56 HRC, achieving that the mechanical properties of the material can withstand high temperatures, avoiding the presence of cracks.

Figure 9

Micrograph obtained after tempering (a) quenched, (b) austempered
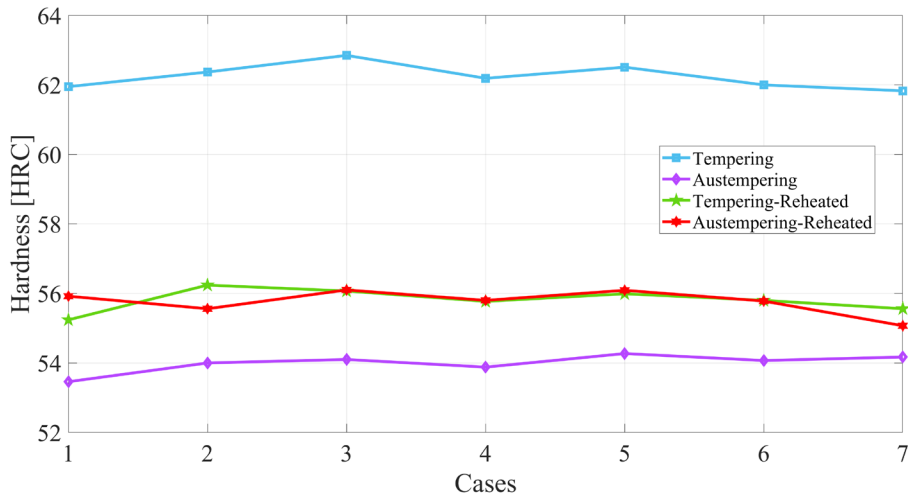
Conclusions

It is important to highlight that when heat treatments such as quenching and tempering are carried out, each one with a stabilization tempering in steels such as M50, W303, Isobloc W-350 of low carbon content, these contribute to carbide dispersions, but by containing alloys such as chromium and molybdenum these contribute to a uniform distribution of retained austenite as the base microstructure of the heat treatment of quenching and tempering, as well as in austempering and tempering. The presence of these alloys contributes to a homogeneous distribution of retained bainite, generating a significant improvement in the toughness of the material.

When a heat treatment is performed, the microstructure is obtained according to the amount of temperature and time exposed in the sample. A a change is generated in the Isobloc W-360 steel, when a tempering is performed. The presence of martensite as a base microstructure causes a hardness of 62 HRC, generating greater tensile strength but decreasing its ductility. Unlike only being exposed to an austempering with a hardness of 53 HRC obtaining a bainitic ferrite base microstructure as well as maintaining the mechanical properties of the material, when performing a stabilization tempering for both tempering and austempering it is evident

that the hardness is matched both in the tempering-retempering and austempering-retempering, obtaining a hardness of 56 HRC; this value enters the range for hot forging work.

When performing the stabilization tempering in the two cases, it is evident that there is a decrease in hardness in the tempered-reduced of 9.5 %, which goes hand in hand with a microstructure of refined martensite base in conjunction with retained austenite, thus generating a stabilization of the mechanical properties improving its ductility. Unlike the austempering-reduced one, it presents an increase in hardness of 3. 6 %, with a microstructure of refined bainite and dispersion of carbides, thus stabilizing the mechanical properties and avoiding the fragility of the material, achieving in both cases an admissible hardness but with a microstructure in austempering-reduced avoiding a fragile structure, due to the temperatures used for the thermal treatments which must be established according to the properties to be improved.

References

Behzadifar, J., Mohammad-Ali Boutorabi, S., & Saghafian Larijani, H. (2024). Effects of austempering on the microstructure and mechanical properties of high-strength nanostructured bainitic steel containing 3.5 wt% aluminum. *Journal of Materials Research and Technology*, *29*(December 2023), 344-352. https://doi.org/10.1016/j.jmrt.2024.01.054

Bohler, E. (2021). *Manual de Aceros Especiales BOHLER* (p. 120).

Brown, C. S., Speer, J. G., & De Moor, E. (2023). Influence of retained austenite on abrasive wear performance of bainitic steels. *Wear*, *522*(December 2022), 204720. https://doi.org/10.1016/j.wear.2023.204720

C. RODRÍGUEZ-CABRERA, J.J. RUÍZ-MONDRAGÓN, F. MACÍAS-LÓPEZ, A. H.-H. (2019). Caracterización Microestructural de Cupones de Matrices para Forja de Acero AISI/SAE l6 Reparados Mediante el Proceso "Flood Welding". *4 to Foro de Ingeniería e Investigación En Materiales*, *16*, 543-551.

Fernádez-Tamayo, M. L., Mondelo-García, F., Parada-ExpÃ\textthreesuperiorsito, A., & Pino, A. S. (2022). Influencia del tratamiento térmico sobre microestructura y dureza de esteras en acero Hadfield con cromo. *Ingenieria Mecánica*, *25*, 17-28.

García, A; Lopez, V; Saucedo, M ;Garcia, J; Meza, E. (2022). *Phase Transformations during heat treatment of austempering of a steel 0.41 % C - 0.7 % Mn - 2.15 % Si - 0.013 % Al. 10*, 125-128.

Huang, C.-T., Hung, F.-Y., Zhao, J.-R., & Hsieh, H.-Y. (2023). Microstructure and mechanical properties of 631 Stainless Steel: Study of Yield Slip and Strain Rate Mechanism with Austempering and Martempering. *Journal of Alloys and Metallurgical Systems*, *2*, 100015. https://doi.org/https://doi.org/10.1016/j.jalmes.2023.100015

Ishtiaq, M., Inam, A., Tiwari, S., & Seol, J. B. (2022). Microstructural, mechanical, and electrochemical analysis of carbon doped AISI carbon steels. *Applied Microscopy*, *52*(1). https://doi.org/10.1186/s42649-022-00079-w

Lee, S.-I., Lee, J.-M., Kim, S.-G., Song, Y.-B., Kim, H.-K., Shim, J.-H., & Hwang, B. (2022). Influence of austempering temperature on microstructure and mechanical properties of high-carbon nanostructured bainitic steels. *Materials Science and Engineering: A*, *848*, 143334. https://doi.org/https://doi.org/10.1016/j.msea.2022.143334

Miranda, G. A. (2020). *Revista CIENCIA Y TECNOLOGÍA. 16*(1), 9-20.

Comparative analysis of microstructure and hardness of Isobloc W360 steel with tempering and Austempering heat treatment

59

Moreno, B., & Adames, J. (2022). Proceso del Forjado y sus Materiales más Utilizados en la Industria. *Facultad de Informática, Electrónica y Comunicación, Escuela de Mecatrónica*, 11.

Peñalosa, D. (2022). *Análisis y evaluación del proceso de forja en la fabricación de tornillos y tuercas de acero inoxidable 304 en SISPRO S.A.*

Penghui, Y., Hanguang, F., Guolu, L., Jinhai, L., & Xuebo, Z. (2020). Microstructures and properties of carbidic austempered ductile Iron containing Fe3C particles and superfine ausferrite. *Materials and Design*, *186*, 108363. https://doi.org/10.1016/j.matdes.2019.108363

Quitiaquez, P., Cocha, J., Quitiaquez, W., & Vaca, X. (2022). Investigation of geometric parameters with HSS tools in machining polyamide 6 using Taguchi method. *Materials Today: Proceedings*, *49*, 181-187. https://doi.org/https://doi.org/10.1016/j.matpr.2021.08.002

Require-, G., Re-, G., Bar, R., Vessels, P., & Plate, N. A. (2014). *Standard Test Methods for Rockwell Hardness of Metallic Materials 1, 2.* 1-38. https://doi.org/10.1520/E0018-14.2

Ríos-Diez, O., Serna Giraldo, C. P., & Aristizábal-Sierra, R. (2020). Desarrollo de aceros fundidos para ser tratados térmicamente mediante carbo-austemperado. *Ingeniare. Revista Chilena de IngenierÃ\-A*, *28*, 718-730. http://www.scielo.cl/scielo.php?script=sci_arttext&pid=S0718-33052020000400718&nrm=iso

Sabzalipour, M., & Rashidi, A. M. (2023). Machinability of martensitic and austempered ductile irons with dual matrix structure. *Journal of Materials Research and Technology*, *26*, 6928-6941. https://doi.org/https://doi.org/10.1016/j.jmrt.2023.09.054

Su, Y., Hu, B., Wang, S., Yu, X., Yang, S., Wang, S., & Liu, H. (2023). Effect of cooling rate after isothermal stage of vacuum austempering on microstructure and hardness of M50 bearing steel. *Journal of Materials Research and Technology*, *26*, 8748-8756. https://doi.org/10.1016/j.jmrt.2023.09.162

Su, Y., Yang, S., Yu, X. F., Zhou, C. B., Liu, Y. B., Feng, X. C., Zhao, Q., & Wu, J. D. (2022). Effect of Austempering Temperature on Microstructure and Mechanical Properties of M50 Bearing Steel. *Journal of Materials Research and Technology*, *20*, 4576-4584. https://doi.org/https://doi.org/10.1016/j.jmrt.2022.09.002

Tchiquendja-Eleno, F., Alfonso-Brindis, E., Quiza-SardiÃ\pmas, R., GonzÃ!`lez-Quintero, O., & Rivas-Santana, M. (2020). Optimización multiobjetivo del endurecimiento por tratamiento mecánico-térmico reiterado en acero AISI 1045. *Ingeniería Mecánicanica*, *23*.

Varshney, A., Sangal, S., Pramanick, A. K., & Mondal, K. (2020). On the extent of transformation of austenite to bainitic ferrite and carbide during austempering of high Si steel for prolonged duration and its effect on mechanical properties. *Materials Science and Engineering: A*, *793*, 139764. https://doi.org/10.1016/j.msea.2020.139764

Wang, K., Hu, F., Zhou, W., Zhang, D., Yin, C., Yershov, S., & Wu, K. (2023). Effect of refined multi-scale microstructures on the ultra-high impact toughness of bainitic steel austempered below Ms temperature. *Journal of Materials Research and Technology*, *26*, 5773-5785. https://doi.org/10.1016/j.jmrt.2023.09.003

Zhou, H., Li, Y., Yin, Z., Ran, M., Liu, S., Huang, Y., Zhang, W., Zheng, W., & Liu, J. (2020). Microstructure and mechanical behaviors of grinding balls produced by dual matrix structure two-step austempering process. *Journal of Materials Research and Technology*, *9*(3), 4672-4681. https://doi.org/10.1016/j.jmrt.2020.02.095

Zuno-Silva, J., Bedolla-Jacuinde, A., Ortiz Dominguez, M., Borja-Soto, C., Ruiz-Lopez, I., & Rodriguez-Muñoz, J. L. (2023). Mejora de la resistencia al desgaste de troqueles para forja en caliente utilizando aceros grado herramienta aleados con Vanadio y Boro. *Ingenio y Conciencia Boletín Científico de La Escuela Superior Ciudad Sahagún*, *10*(20), 75-78. https://doi.org/10.29057/escs.v10i20.10846

Development of an intelligent system for fruit detection and cutting using computer vision

Mayra Comina
Universidad de las Fuerzas Armadas-ESPE, (Ecuador)
Orcid: https://orcid.org/ 0000-0002-1541-4850

Alexandra Verdugo
Universidad de las Fuerzas Armadas-ESPE, (Ecuador)
Orcid: https://orcid.org/ 0000-0001-9328-0248

Jorge Comina
Universidad Politécnica Salesiana, (Ecuador)
Orcid: https://orcid.org/ 0009-0004-0402-2474

Walter Verdugo
Universidad Politécnica Salesiana, (Ecuador)
Orcid: https://orcid.org/ 0000-0002-0656-0135

Introduction

In the food industry, process automation is essential for improving efficiency, productivity, and ensuring product quality. Computer vision has emerged as a powerful tool for the automated detection, classification, and manipulation of fruits and other foods (Fan et al., 2024). This technology enables precise and rapid identification of characteristics such as type, ripeness, and quality, facilitating processes like classification, packaging, and quality control (Patil et al., 2023).

Computer vision utilizes artificial intelligence and machine learning algorithms to analyze images and extract relevant information, allowing high-precision classification of fruits based on shape, color, and texture (Del Castillo et al., 2021). Recent studies have highlighted the potential of this technology to enhance efficiency and quality in food production, such as defect detection in fruits and vegetables, grain and seed classification, and fish species identification (Kang & Chen, 2020).

The relevance of computer vision and artificial intelligence algorithms for object detection has expanded across various fields, including industrial processes, quality control, and automation,

proving indispensable in Industry 4.0. Applications extend beyond industry to scientific and security sectors, significantly improving processes in various companies (Sucari et al., 2020).

Research has demonstrated substantial improvements in process quality through the implementation of computer vision systems. These include systems for recognizing Latin American tropical fruits, using advanced techniques to enhance precision and efficiency in object identification and classification (Fan et al., 2020). The integration of artificial intelligence with computer vision has further advanced industrial quality control, employing deep learning techniques for high-precision fruit detection and classification (Javaid et al., 2022).

In smart agriculture, computer vision systems have optimized crop management, resource use, and yields (Sharma et al., 2022). Additionally, autonomous systems for fruit harvesting have shown remarkable advancements (Zhou et al., 2021). Computer vision techniques for

inspecting agricultural product quality are replacing manual inspections, reducing errors, and improving economic efficiency (Da Costa et al., 2020).

This project aims to identify the technical characteristics of a computer vision system for real-time image acquisition and electronic component evaluation, focusing on five types of fruits: watermelon, apple, pear, orange, and banana. The development will follow the Quality Function Deployment (QFD) methodology to prioritize technical characteristics and include designing printed circuits and arranging elements in the graphical interface (Ruiz García, 2020). Tests will be conducted to validate the system's accuracy and improve detection algorithms (Amaral et al., 2023).

The rest of this article is organized as follows. In Section 2, the Methods are described. In Section 3, the results and the limitations as well as the contributions of this investigation are analyzed. Finally, the conclusions are presented in Section 4.

Materials and Methods

Module Identification

To identify the design modules, the QFD (Quality Function Deployment) matrix was used, which determines

the most important technical characteristics of the project. Then, design modules were used for the selection of elements.

Table 1
List of elements

Design Module	Element
Detection Camera	ESP32CAM
Type of motors for blade movement	DC Motor
Type of mechanism for fruit cutting	Servomotor
Graphical interface for data visualization Matlab	Matlab
Control Board	Arduino UNO

System Design

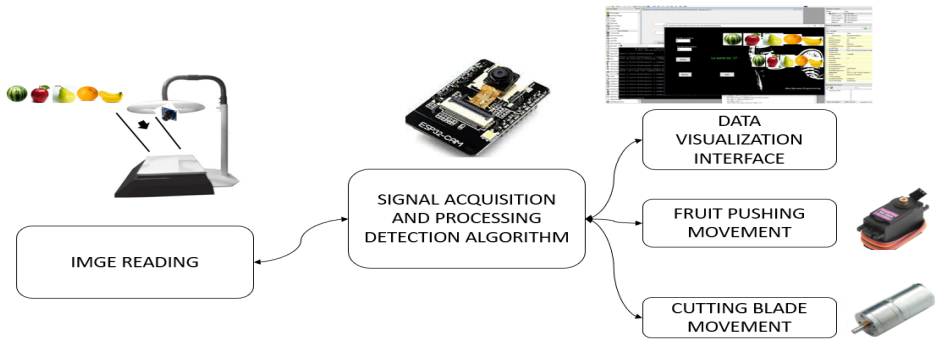The system design was carried out using 3D modeling software and electronic simulation tools to ensure the correct integration of all components. Figure 1 shows the 3D design of the complete system.

Figure 1
3D Design of the fruit detection and cutting system
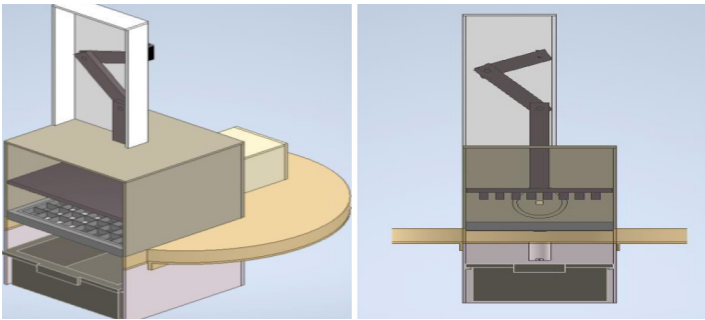
The Figure 2 shows the schematic diagram of the cutter.

Figure 2
Schematic Diagram

Detection Algorithm Programming

The detection algorithm was implemented using Python and programmed in the Matlab graphical interface. The flowchart of the detection algorithm is shown in Figures 3 and 4.

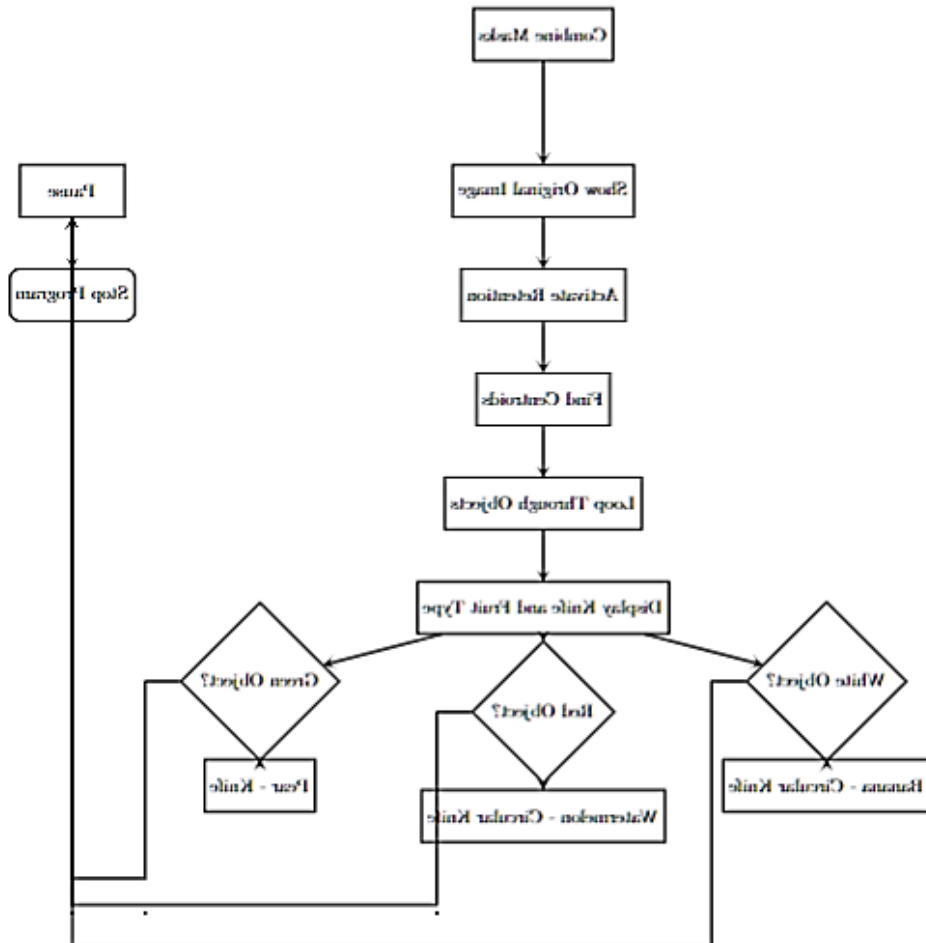**Figure 3**
Flowchart of the detection algorithm
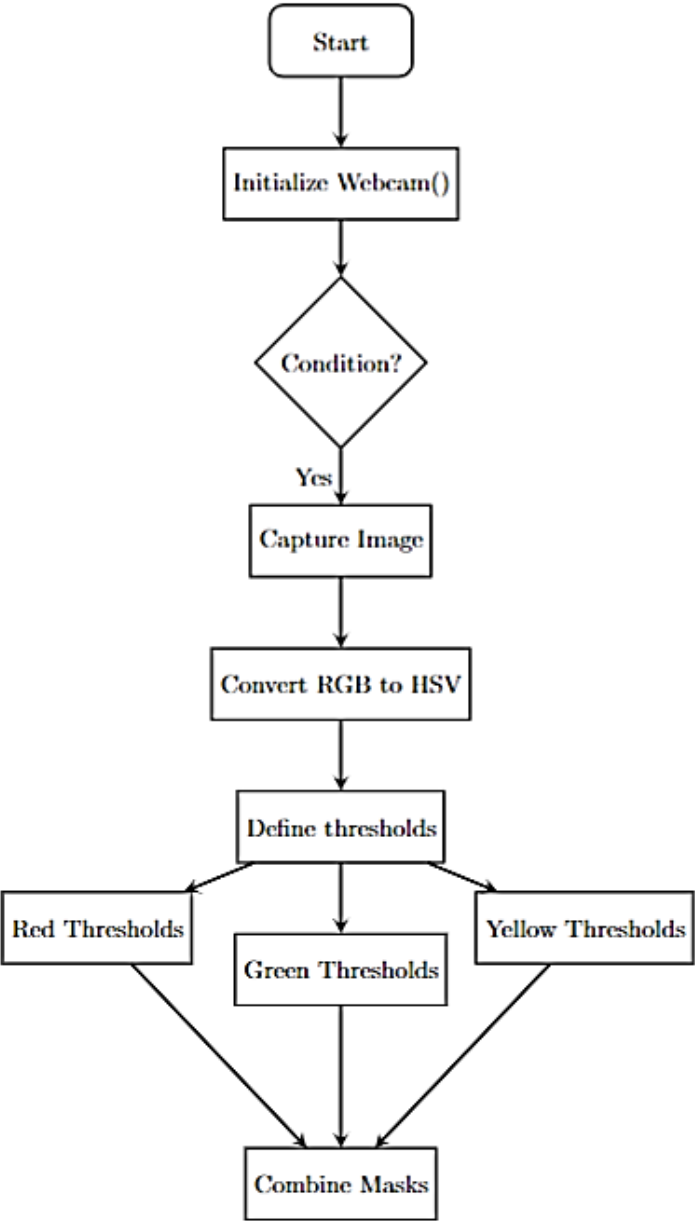
Figure 4

Flowchart of the detection algorithm

Combine Masks

Show Original Image

Activate Rotation

Find Centroids

Loop Through Objects

Display Knife and Fruit Type

Green Object?

Red Object?

White Object?

Pear - Knife

Watermelon - Circular Knife

Banana - Circular Knife

Stop Program

Pause

Results

This section presents the results obtained during the development and implementation of the fruit detection system. The tests conducted to verify the system's functionality and the analysis of the obtained results are described.

Development of the Hardware Construction Process

The construction process of the detection system was carried out by printing parts using a 3D printer. Figure 5 shows the assembly of the machine.

Figure 5
Machine assembly

Functionality Tests

Several tests were conducted to verify the functionality of the detection system. The tests included image acquisition, communication with the graphical interface, fruit detection, and the operation of the cutting mechanism.

Fruit Detection Test For fruit detection, the conditions of fruit type and blade assignment shown in Table 2 were considered.

Table 2
Conditions for Detection

Fruit	No. Color	Fruit Type	Assigned Blade
1	Intense Red	Watermelon	Grid - Circular
2	Green	Pear	Grid
3	Yellow-White	Banana	Grid - Circular
4	Yellowish Red	Apple	Grid
5	Orange	Papaya	Grid - Circular

Several fruit detection tests were conducted with different image acquisition backgrounds. Figure 6 shows the detection of the fruits.

Cutting Mechanism Functionality Tests of the downward movement of the axis mechanism and the cutting of the fruit were performed, as shown in Figure 7.
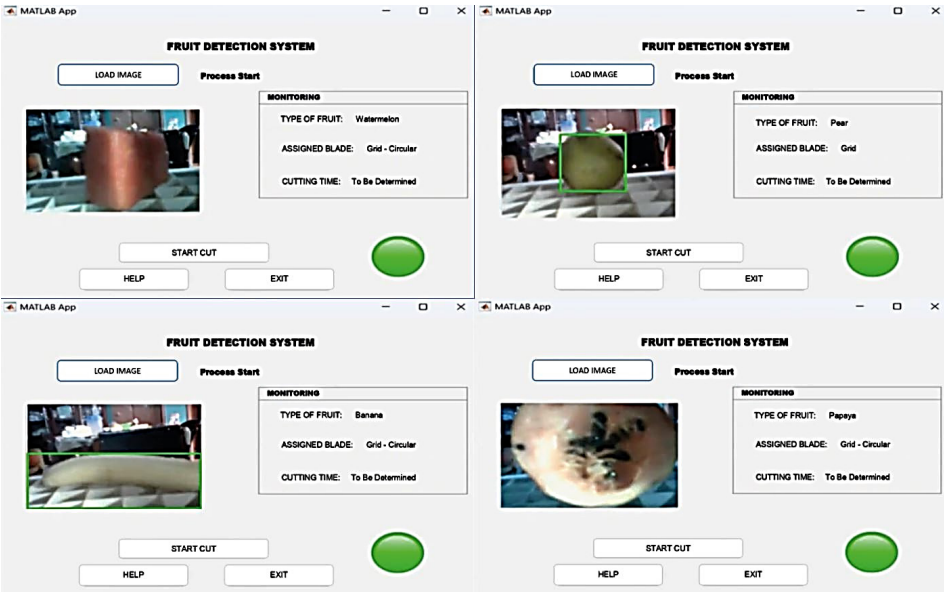
Figure 6
Fruit detection
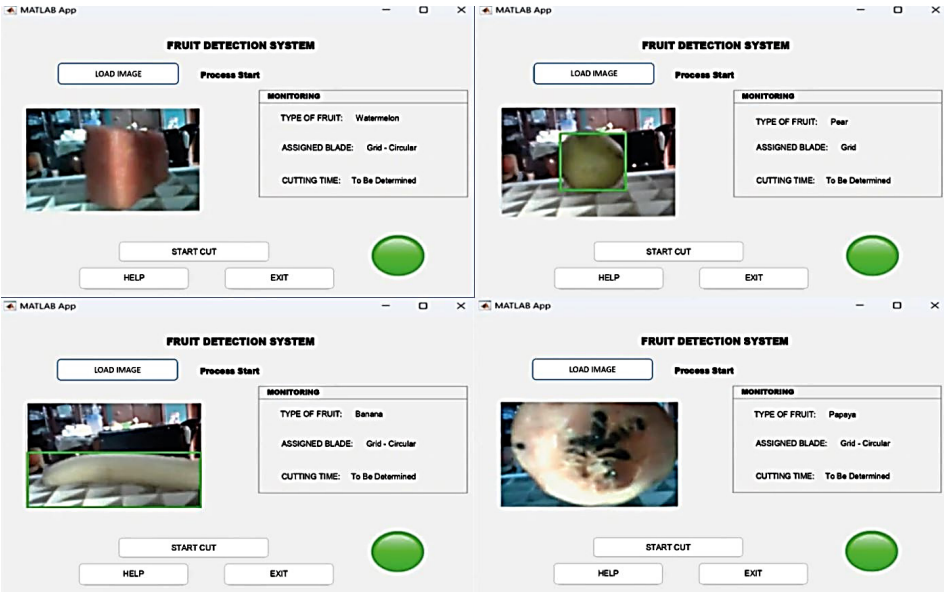
Figure. 7
*Movement of the axis mechanism - downward*

Analysis of the results

According to the main objective of this project, which is to detect five types of fruits using computer vision, the results obtained in the detection of each fruit are analyzed. Figure 8 shows the data of hits and misses in a set of 20 tests conducted for pear detection. It is observed that there are 18 hits and 2 misses in the case of pear detection.

Figure 8

Results of hits and misses for pear detection
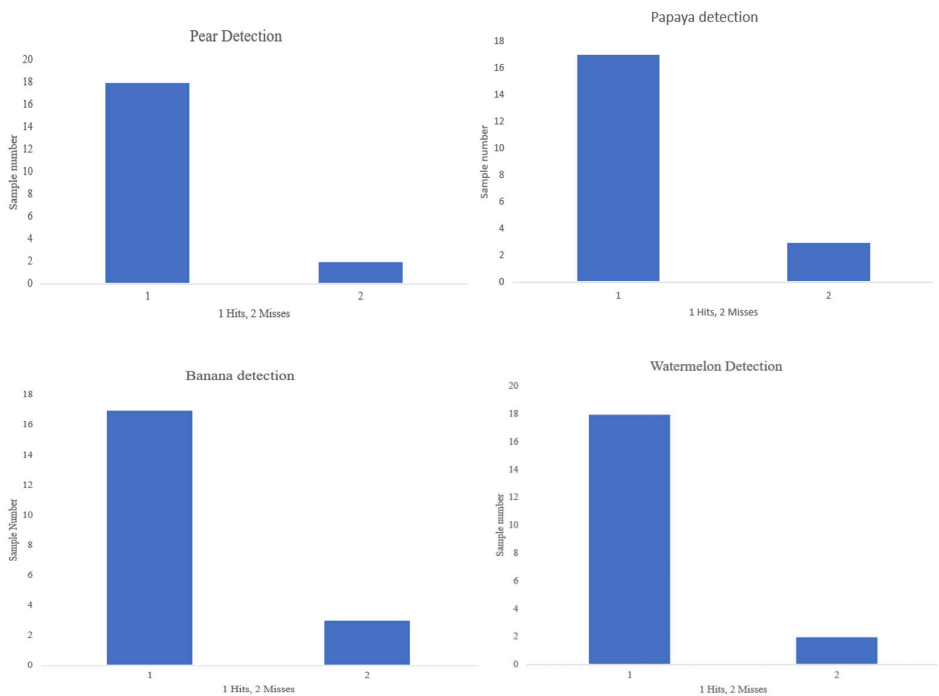
Similar tests were conducted for the detection of other types of fruits, obtaining the following results:

Banana: 17 hits and 3 misses
Papaya: 17 hits and 3 misses
Watermelon: 18 hits and 2 misses
Apple: 14 hits and 5 misses

Conclusions

The fruit detection system using computer vision has proven to be an effective and precise solution for improving efficiency in fruit salad preparation in a domestic environment. During the tests, the following results were obtai-

ned: banana with 17 hits and 3 misses, papaya with 17 hits and 3 misses, watermelon with 18 hits and 2 misses, apple with 14 hits and 5 misses, and pear with 18 hits and 2 misses.

These results indicate a high accuracy in fruit detection, with an average success rate of 88.8% in the tests conducted. The system not only correctly identified the fruits but also selected the appropriate blade for cutting, optimizing the preparation process. This has significant practical implications, as an automated system like this can significantly reduce the time and effort required in food preparation, improving productivity and efficiency in domestic settings and potentially in small businesses.

Areas for improvement were identified in the detection of certain types of fruits, such as apples, where the success rate was lower. It is recommended to optimize the detection algorithm to improve precision and robustness under variable lighting conditions. Additionally, the use of advanced machine learning techniques could further enhance detection accuracy, and the integration of additional sensors could allow for better fruit classification.

The implementation of this system in other similar businesses could significantly improve their productivity and competitiveness. Future improvements could also include the development of industrial versions of the system in the food industry, where efficiency and precision in food preparation and processing are critical.

References

Fan, Y., Cai, Y., & Yang, H. (2024). A detection algorithm based on improved YOLOv5 for coarse-fine variety fruits. Food Measure, 18, 1338-1354. https://doi.org/10.1007/s11694-023-02274-z

Patil, S. S., Patil, Y. M., & Patil, S. B. (2023). Review on automatic variable-rate spraying systems based on orchard canopy characterization. Informatics and Automation, 22(1), 57-86.

Del Castillo, B. A. L., Domingo, D. J. A., Herrera, G. G., & López, D. M. S. (2021). Sentidos y perspectivas de la investigación formativa en tiempos de pandemia: caso ingeniería. Universidad Libre.

Kang, H., & Chen, C. (2020). Fruit detection, segmentation and 3D visualisation of environments in apple orchards. Computers and Electronics in Agriculture, 171, 105302.

Sucari, L. R., Durán, Y. A., Yapo, E. Q., León, A. S., Quina, L. D. Q., & Torres, F. A. H. (2020). Visión artificial en reconocimiento de patrones para clasificación de frutas en agronegocios. Puriq, 2(2).

Fan, S., Li, J., Zhang, Y., Tian, X., Wang, Q., He, X & Huang, W. (2020). On line detection of defective apples using computer vision system combined with deep learning methods. Journal of Food Engineering, 286, 110102.

Javaid, M., Haleem, A., Singh, R. P., & Suman, R. (2022). Artificial intelligence applications for industry 4.0: A literature-based study. Journal of Industrial Integration and Management, 7(01), 83-111.

Sharma, A., Georgi, M., Tregubenko, M., Tselykh, A., & Tselykh, A. (2022). Enabling smart agriculture by implementing artificial intelligence and embedded sensing. Computers & Industrial Engineering, 165, 107936.

Zhou, H., Wang, X., Au, W., et al. (2021). Intelligent Robots for Fruit Harvesting: Recent Developments and Future Challenges. Preprint available at Research Square.

Da Costa, A. Z., Figueroa, H. E., & Fracarolli, J. A. (2020). Computer vision based detection of external defects on tomatoes using deep learning. Biosystems Engineering, 190, 131-144.

Ruiz García, P. (2020). Estudio y mejora del FabLab UValladolid desde una perspectiva Lean Manufacturing. Universidad de Valladolid.

Amaral, F., Matia, E., Oliveira Júnior, A., Zorawski, M., Queiroz, J., & Leitão, P. (2023). Módulo de aprendizaje para diseñar placas de circuito impreso para dispositivos basados en el IoT

Evaluation of the thermodynamic performance of R449A and R404A in a prototype of an ice rink

Isaac Simbaña

Grupo de Investigación en Ingeniería Mecánica y Pedagogía de la Carrera de Electromecánica (GIIMPCEM), Instituto Superior Universitario Sucre, Ecuador
Orcid: https://orcid.org/0000-0002-3324-3071

David Saquinga

Grupo de Investigación en Ingeniería Mecánica y Pedagogía de la Carrera de Electromecánica (GIIMPCEM), Instituto Superior Universitario Sucre, Ecuador
Orcid: https://orcid.org/0000-0001-8353-1621

Xavier Vaca

Grupo de Investigación en Ingeniería, Productividad y Simulación Industrial (GIIPSI), Universidad Politécnica Salesiana, Ecuador
Orcid: https://orcid.org/0000-0002-1231-5267

Introduction

The constant population growth significantly impacts energy demand, particularly in industrial refrigeration applications. As Dong et al. (2021) note, population increases lead to urbanization, with more people living and working in densely populated urban areas. This raises the demand for air conditioning systems in homes, commercial buildings, and industrial settings, thus increasing the load on energy systems. Additionally, there is a higher demand for industrial products, as many industries require refrigeration processes to maintain the quality and integrity of their products, further boosting energy demand. This heightened demand for energy in various industrial refrigeration applications puts pressure on energy resources and underscores the need for energy-efficient and sustainable solutions (Touaibi and Koten, 2021).

A refrigeration system with a chiller cools the working fluid, which is then used to cool a specific space or process. A chiller extracts heat from the working fluid using a vapor compression or absorption cycle and dissipates it into an external environment (Song et al., 2024). In ice rinks, a refrigeration system with a chiller is essential to maintain the rink in suitable condi-

tions for use. Ice rinks require specific temperatures to keep the water frozen appropriately for skating. According to Snyder et al. (2021), a well-designed refrigeration system can improve energy efficiency, lowering long-term operational costs. Additionally, it can be reliable and durable, reducing the likelihood of unplanned downtime. This reliability is crucial to avoid interruptions in the operation of the ice rink, which can negatively impact users and associated revenue (Taebnia et al., 2020).

Traditional refrigeration technologies often use refrigerants that are harmful to the ozone layer and contribute to global warming. According to a study by Anderson et al. (2021), new technologies, considering sustainable development, can opt for less harmful refrigerants or systems that use natural refrigerants, such as hydrocarbons, which have a lower environmental impact. This approach not only reduces operational costs for users but also decreases energy demand and the carbon footprint. These solutions can include designs that are more robust against extreme weather conditions or that utilize renewable energy sources, reducing dependence on fossil fuels and conventional energy supplies. With the growing number of regulations and standards related to refrigerant use and energy efficiency, industries adopting sustainable refrigeration technologies are better positioned to comply with these regulations (Hara-Chakravarty et al., 2022).

Heredia-Aricapa et al. (2020) reviewed the restrictions and environ-

mental impact of fluorinated refrigerants, highlighting the need to replace hydrochlorofluorocarbons (HCFCs) and hydrofluorocarbons (HFCs) with more sustainable alternatives, such as natural refrigerants or those with low global warming potential (GWP). The choice of refrigerant is crucial, and selecting refrigerants with a low GWP that does not contribute to ozone depletion is essential. It is anticipated that by 2024, HFC production will be reduced by approximately 40 %. Refrigeration system designs must adapt to the selected refrigerant, potentially requiring adjustments in compression capacity, performance, and refrigerant distribution within the system. Additionally, the thermodynamic and transport properties of the refrigerant must be considered to ensure proper performance. A design that facilitates proper maintenance allows easy access to key components for cleaning and inspection.

Chen et al. (2023) conducted a historical review of substances with high Global Warming Potential (GWP), noting that the development of refrigerants has been driven by the search for compounds that are safer for the environment and have less impact on climate change. R404A, a synthetic refrigerant, began to be widely used in the 1990s as an alternative to refrigerants banned due to their impact on the ozone layer, such as R502. R404A was noted for its high cooling capacity and chemical stability, making it a popular choice in commercial and transport refrigeration systems. However, with increasing awareness of global warming and the need to reduce

greenhouse gas emissions, more sustainable alternatives have been considered, as R404A has a GWP of 3922 CO_2e. One such alternative is R449A, a blend of hydrofluorocarbon (HFC) refrigerants proposed as a more environmentally friendly replacement for R404A.

Ghanbarpour et al. (2021) used neural network modeling to analyze the replacement of R404A with R449A. R449A has gained attention as a transitional option due to its lower GWP compared to R404A. While it offers similar performance in terms of cooling capacity, its GWP is significantly lower, with a value of 1397, making it more compatible with efforts to reduce greenhouse gas emissions. Therefore, R449A is considered a more sustainable replacement for R404A, aligning with global efforts to adopt refrigerants with a lower environmental impact. Reducing the environmental impact caused by the use of R404A in chiller refrigeration systems for ice rinks involves adopting several sustainable strategies. Alternatives like R449A, which has a lower GWP than R404A, can be an intermediate step towards refrigerants with an even lower environmental impact, close to zero. Improving system efficiency can reduce the total amount of refrigerant required and thus its environmental impact.

Lucchini et al. (2024) analyzed the thermodynamic properties of R449A as a replacement for HFC refrigerants like R404A and R507A. R449A is considered a viable replacement for R404A for several reasons, despite R404A potentially having slightly better performance in some applications. R449A has been designed to be compatible with existing equipment that uses refrigerants like R404A, facilitating the transition to a more sustainable alternative without significant changes to refrigeration infrastructure. As the demand for low GWP refrigerants increases, the availability and cost of R449A are likely to become more favorable compared to R404A in the future. Additionally, the cost of not complying with environmental regulations can be significant, making the use of more sustainable alternatives economically viable in the long term.

This research proposes a comparative analysis of the performance of a refrigeration system with a chiller using R404A and R449A as working fluids. A prototype ice rink was constructed to study the system thermodynamically until the rink surface crystallizes. This document is organized as follows: Materials and Methods describes the system's operation and presents the equations required for the thermodynamic analysis. Results showcase the equipment and temperature measurements, including comparative graphs of operational parameters with respective descriptions. In the Discussion, a relationship between the calculated results and existing literature is established to validate this work. Finally, the Conclusions summarize the most relevant information, emphasizing the comparative analysis of the system's thermodynamic performance using different working fluids.

Materials and Methods

System Description

A refrigeration system with a chiller is used to cool liquids and transfer heat from a space or process through a refrigeration cycle. Figure 1a presents the T-s diagram of the vapor compression refrigeration cycle. The process begins by compressing the refrigerant to increase its pressure and temperature. Next, the superheated vapor refrigerant passes through the condenser, where it travels through a series of tubes, cools, and condenses by releasing its heat to the surrounding medium. It is important to note that condensers can be air-cooled or water-cooled. The refrigerant exiting the condenser is in a subcooled liquid state but still at high pressure, so an expansion valve is used to regulate the refrigerant flow to the evaporator, reducing its pressure and temperature before entering this component. The analysis concludes with the evaporator, where heat transfer from the medium to be cooled (in this case, water) to the refrigerant occurs. The refrigerant evaporates, absorbing heat from the water and lowering the temperature of this medium [12]. Additionally, in a system with a chiller, a water pump is used to circulate water between the chiller and the point of use [13]. Figure 1b shows a schematic layout of the components for the prototype under analysis.

Figure 1
Refrigeration cycle a) T-s diagram, b) components
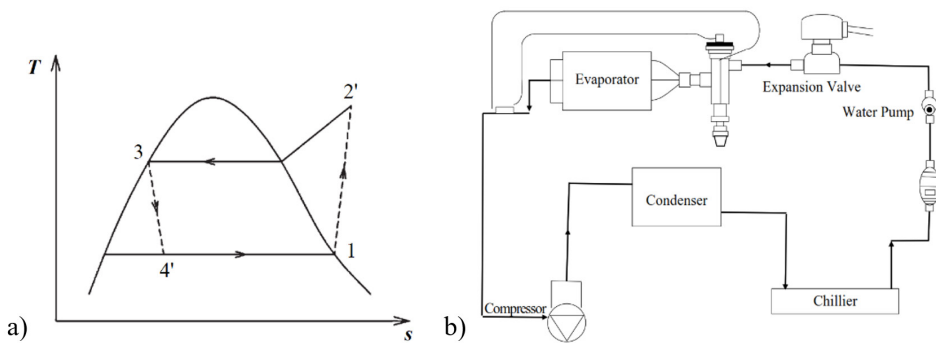
Thermodynamic analysis

The following is an analysis of a refrigeration system equipped with a chiller for water cooling, commonly used across various industrial, commercial, or comfort applications. An energy balance was conducted for each component of the system based on enthalpies. The energy balance equation for the system, as proposed by Gado et al. (2022), can be formulated as equation (1):

$$\dot{Q}_{evap} + \dot{W}_{comp} = \dot{Q}_{cond} \qquad (1)$$

Where $\dot{W}_{comp}$ represents the required power by the compressor, while $\dot{Q}_{cond}$ is the heat flow released in the condenser to the surroundings. In the evaporator, the refrigerant, operating at low pressure and temperature, absorbs heat from the water, thereby cooling it and transitioning back into a superheated vapor state. The heat absorbed by the evaporator $(\dot{Q}_{evap})$ is determined using equation (2), as provided by Nikhil-Babu et al. (2021):

$$\dot{Q}_{evap} = \dot{m} \cdot (h_{evap,o} - h_{evap,i}) \qquad (2)$$

Where $h_{evap,o}$ and $h_{evap,i}$ represent the enthalpies of the refrigerant at the outlet and inlet of the evaporator, respectively. The mass flow rate of the refrigerant $(\dot{m})$ is calculated by Simbaña et al. (2022) using equation (3):

$$\dot{m} = \frac{\eta \cdot N \cdot V_D}{v_{comp,i}} \qquad (3)$$

Where $v_{comp,i}$ denotes the specific volume of the refrigerant at the compressor inlet, η represents the volumetric efficiency, N signifies the rotational speed, and V_D is the displacement volume of the compressor. As the refrigerant transitions into the gaseous state, it is compressed, thereby increasing its pressure and temperature. The energy consumption of the compressor is determined through an energy balance, as outlined by Sabry and Ker (2020) with equation (4):

$$\dot{W}_{comp} = \dot{m} \cdot (h_{comp,o} - h_{comp,i}) \qquad (4)$$

The coefficient of performance (*COP*) serves as a metric for assessing the efficiency of a refrigeration system, defined as the ratio of the useful energy provided, for the ice rink, the heat extracted from the cooled water to the amount of electrical energy consumed. According to Pan et al. (2021), the *COP* of the refrigeration system is calculated using equation (5):

$$COP = \frac{\dot{Q}_{cond}}{\dot{W}_{comp}} = \frac{h_{comp,o} - h_{cond,o}}{h_{comp,o} - h_{comp,o}} \qquad (5)$$

The heat transfer from the water, where the evaporator is submerged, to the rear surface of the ice rink occurs via convection. The heat released by the water $(\dot{Q}_w)$ is determined by Qu et al. (2023) using equation (6):

$$\dot{Q}_w = \varphi \cdot A_{ir} \cdot \Delta°T \qquad (6)$$

Here, φ represents the convective heat transfer coefficient, A_{ir} denotes the surface area of the bottom of the ice rink, and $\Delta°T$ is the temperature differential. Additionally, the cooling transmitted to the ice rink must cool the water on its surface, thus it is transmitted via conduction. The heat conducted through the ice rink plate $(\dot{Q}_{ir})$, as proposed by Lee et al. (2020), is determined using equation (7):

$$\dot{Q}_{ir} = k \cdot \Delta°T \cdot \frac{A_t}{L} \qquad (7)$$

Where k is the conductive heat transfer coefficient, A_t is the cross-sectional area of the ice rink plate, and L represents the length.

Results

Figure 2 illustrates the prototype of the constructed ice rink, featuring a 1.5 HP compressor, model NJ9238GK, with a displacement of 26.11 cm³ and a rotation speed of 3500 rpm. Pressure measurements were taken using low and high analog gauges at the compressor's inlet and outlet, respectively, while temperature readings were obtained via thermocouples connected to a digital display. The water tank for cooling had dimensions of 450 x 450 x 600 mm, and copper pipes were employed for the heat exchangers.

Figure 2
Experimental prototype of ice rink with chiller

a)   b)

Given the presence of uninsulated components and areas susceptible to ambient temperature influence on thermocouple readings, a thermal imaging camera was utilized to capture these measurements. In Figure 3a, the compressor's operational temperatures are shown after 10 minutes of activity, with an average outlet temperature of 41.6 °C, closely aligning with the thermocouple measurement. Figure 3b displays the surface temperatures of the ice rink, where the crystallization of surface water was visually observed, with an average temperature of -1.4 °C. Notably, the expansion valve froze nearly instantly, reaching temperatures below -25 °C.
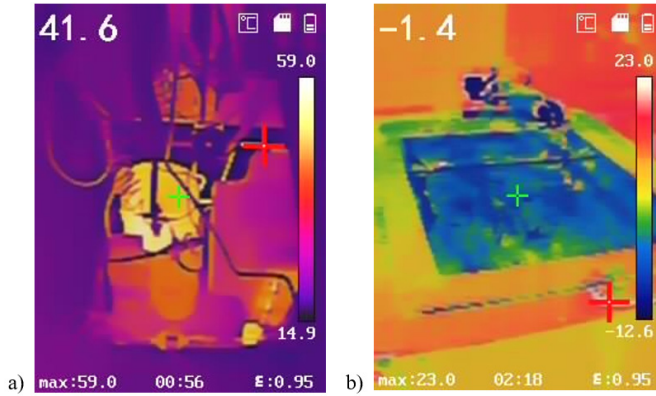
Figure 3

Thermography a) compressor, b) ice rink surface

a) max:59.0   00:56   ε:0.95   b) max:23.0   02:18   ε:0.95

Figure 4 displays the evaporation and condensation temperatures for the R404A and R449A refrigerants over the water-cooling duration. For R404A, the peak evaporation and condensation temperatures were -32.5 and 59.7 °C, respectively, whereas for R449A, these values stood at -27.3 and 58.6 °C. The heat extracted from the water for cooling varied as well; the ice rink surface began to crystallize after 212 and 226 minutes of operation with R404A and R449A, respectively. Figure 4b depicts the decline in the ice rink's surface temperature during operation. After 4 hours with R404A, the temperature reached -2.4 °C, whereas with R449A, it cooled to -1.6 °C.

Figure 4

Temperature concerning operating time a) evaporation and condensation of refrigerants, b) surface of the ice rink
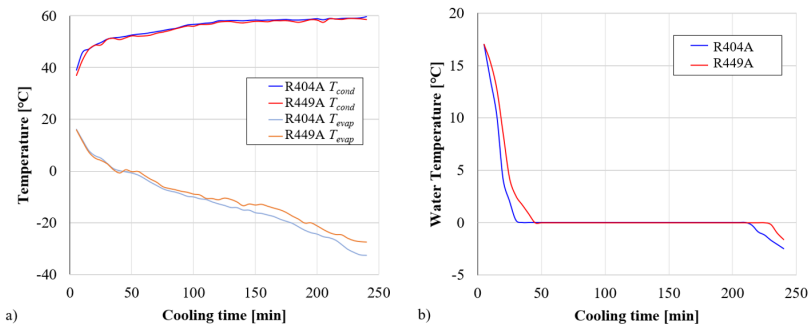
Figure 5 compares the cooling capacity in the evaporator relative to the evaporation temperature of the refrigerants under examination. R449A exhibited a higher maximum value than R404A, with 3.98 versus 3.68 kW, respectively, representing an average difference of 330 W during operation.

Figure 5

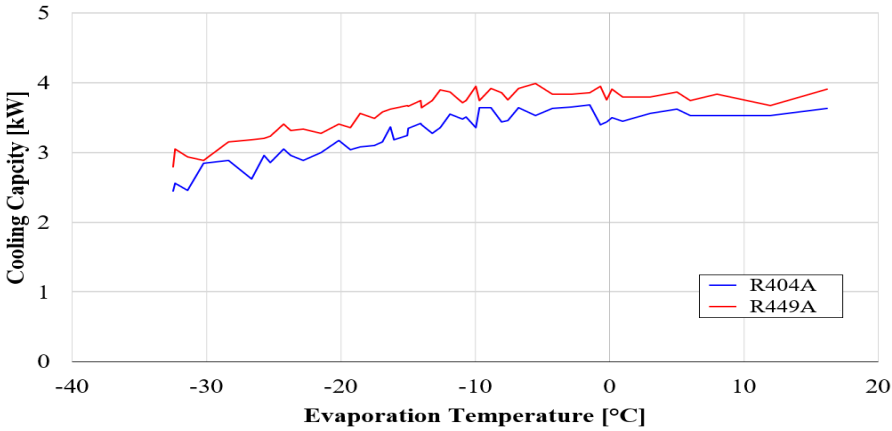*Cooling capacity vs. evaporation temperature*

Figure 6 illustrates the COP variation in the system with the refrigerants used, indicating a downward trend for this parameter over the operating period. The highest COP values were 4.65 and 4.32 for R449A and R404A, respectively, with an average difference of 3.08% during system operation with the refrigerants in use.

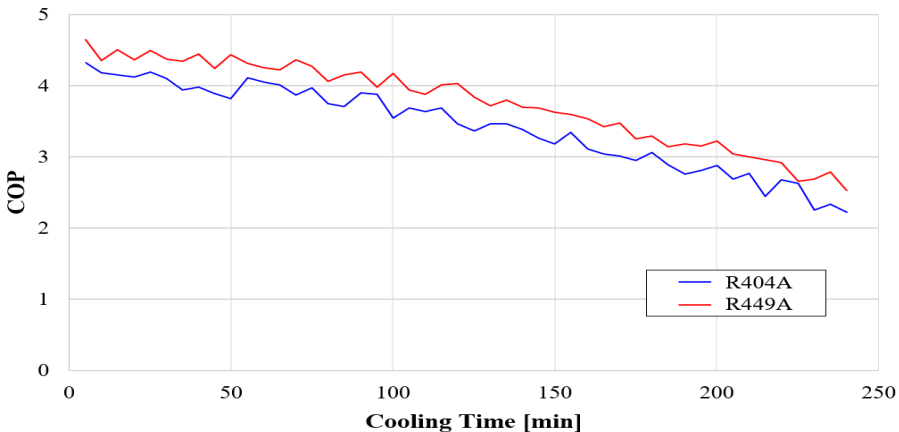**Figure 6**

Coefficient of performance of the system

Figure 7a shows the COP variation concerning the evaporation temperature using R404A and R449A in the refrigeration system. For R404A, achieving the lowest temperature of -32.5 °C resulted in a COP of 2.22, whereas with R449A, the lowest temperature of -27.3 °C corresponded to

a COP of 2.53. Figure 7b presents the COP values of the system relative to the condensation temperature of the refrigerants used. The maximum COP of the system with R404A was 4.32 at a temperature of 38.9 °C, decrea-

sing by 51.39% during operation until reaching 59.7 °C. Conversely, using R449A, the system's COP reached a maximum value of 4.65 at 37 °C, declining by 54.38% until the refrigerant reached 59.6 °C.

Figure 7

COP vs. temperatures a) evaporation, b) condensation
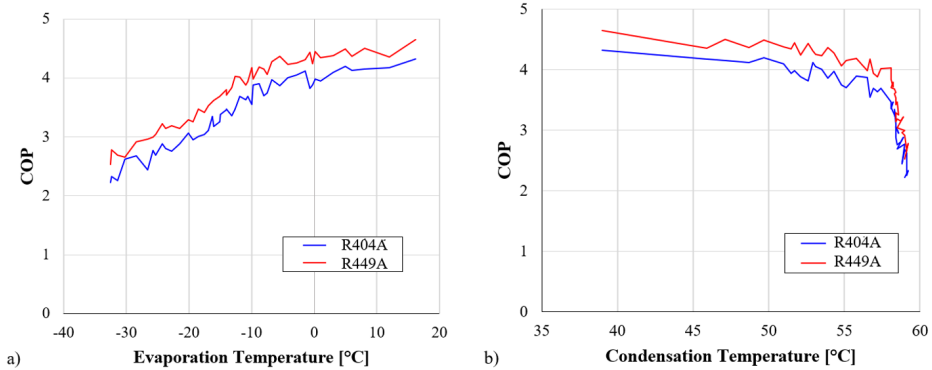
In this study, conducting experimental tests with the prototype revealed a maximum difference of 3.08 % in the Coefficient of Performance when comparing the use of R404A and R449A refrigerants during the cooling process. The *COP* is a measure of the energy efficiency of refrigeration systems, where a higher value indicates better performance, and the observed difference suggests that the prototype operates slightly better with R449A. In the research presented by Yildirim et al. (2023), a numerical analysis was performed to assess the feasibility of R449A as a sustainable alternative to R404A. In that study, it was determined that R449A offered approximately 5 % higher performance than R404A. This implies that, according to that analysis, refrigeration systems using R449A can ope-

rate with better performance and lower environmental impact than those using R404A. Comparing the experimental results obtained in this study with the numerical findings of that research shows consistency in the findings. Although the maximum calculated difference was 3.08 %, it is important to note that both studies suggest that R449A outperforms R404A. By experimentally obtaining a higher *COP* with R449A compared to R404A, and considering that this difference is similar to that found in the scientific literature, it can be affirmed that the prototype is functional. Furthermore, these results support the idea that R449A is a viable and more efficient alternative to replace R404A in refrigeration systems, aligning with efforts towards more sustainable solutions in the industry.

In the experimental tests conducted for this study, a *COP* of 4.32 was achieved for the R404A refrigerant. This value is consistent with the trends observed in the study conducted by Altinkaynak (2021), who also reported similar *COP* values when using R404A. This suggests that this prototype ice rink and the system analyzed in that research have comparable performance, thus validating the accuracy and effectiveness of the experimental tests conducted. On the other hand, when using the R449A refrigerant, a *COP* of 4.65 was obtained, which subsequently decreased to 2.52 during the cooling time. To better understand these results, the research by Alam and Jeong (2020), was analyzed, who calculated the thermodynamic properties of R449A using molecular dynamic simulation. Their studies also presented similar *COP* values, indicating that the experimental tests are aligned with theoretical models and simulations.

As indicated by Jeyakumar et al. (2022), a high *COP* indicates a more efficient refrigeration system. This means that the system requires less energy to perform the same amount of cooling work, which in turn reduces operating costs.

A higher *COP* implies lower electricity expenses and more economical operation of the refrigeration system, which is beneficial both economically and environmentally. Therefore, the *COP* has not only allowed the evaluation and comparison of the refrigeration system's performance in the prototype but has also been fundamental for selecting the most suitable refrigerant for our specific application. In this case, R449A, with a higher *COP* than R404A under the same conditions, emerges as a more viable alternative, reinforcing the idea that it may be a better option in terms of energy efficiency and operational cost reduction.

Conclusions

A comparative experimental analysis of a refrigeration system equipped with a chiller for cooling the surface of an ice rink prototype has been conducted. The prototype was built considering the vapor compression refrigeration cycle, utilizing a 1.5 HP electric compressor, and incorporating pressure gauges for measuring pressure at the inlet and outlet of this component. While thermocouples connected to a digital display were used for measuring the fluid's temperature, a thermal imaging camera was also employed to take measurements in areas exposed to ambient temperatures, such as the ice rink's surface. It was observed that R404 reached maximum evaporation and condensation temperatures of -32.5 and 59.7 °C, respectively, while for R449A, these temperatures were -27.3 and 58.6 °C. The crystallization of the ice rink's surface was observed after the system had been operating for 212 and 226 minutes with R404A and R449A, respectively.

In the thermodynamic analysis, it was determined that the maximum coo-

ling capacity was 3.68 kW using R449A as the working fluid, whereas with R404A, it was 3.63 kW. Consequently, it was established that the Coefficient of Performance (*COP*) for the system using R404A reached a maximum value of 4.32 when the refrigerant temperature was 38.9 °C and decreased by 51.39 %. Conversely, when using R449A as the working fluid, the system's maximum COP was 4.65 and decreased by 54.38 % during operation. Thus, an average difference of 3.08 % for the *COP* of the system between the refrigerants during the cooling time until the ice rink's surface completely crystallized after four hours was established.

R449A requires a slightly lower evaporation pressure than R404A to achieve the same evaporation temperature conditions, which influences the required amount of refrigerant. The system's performance using R449A is superior to that using R404A, as it necessitated lower refrigerant loads and, consequently, lower electricity consumption. From the literature review, it is evident that R404A has been widely utilized in the past due to its performance, but it is gradually being replaced by more sustainable alternatives owing to its high Global Warming Potential (GWP).

References

Alam, M. and Jeong, J. (2020). Calculation of the Thermodynamic Properties of R448A and R449A in a Saturation Temperature Range of 233.15 K to 343.15 K Using Molecular Dynamics Simulations. International Communications in Heat and Mass Transfer, 116, 104717. https://doi.org/10.1016/J.ICHEATMASSTRANSFER.2020.104717

Altinkaynak, M. (2021). Exergetic Performance Analysis of Low GWP Alternative Refrigerants for R404A in a Refrigeration System. International Journal of Low-Carbon Technologies, 16(3), 842-850. https://doi.org/10.1093/ijlct/ctaa104

Anderson, A., Rezaie, B. and Rosen, M. A. (2021). An Innovative Approach to Enhance Sustainability of a District Cooling System by Adjusting Cold Thermal Storage and Chiller Operation. Energy, 214, 118949. https://doi.org/10.1016/J.ENERGY.2020.118949

Chen, A., Chen, D., Hu, X., Harth, C., Young, D., Mühle, J., Krummel, P., O'Doherty, S., Weiss, R., Prinn, R. and Fang, X. (2023). Historical Trend of Ozone-depleting Substances and Hydrofluorocarbon Concentrations During 2004-2020 Derived from Satellite Observations and Estimates for Global Emissions. Environmental Pollution, 316, 120570. https://doi.org/10.1016/J.ENVPOL.2022.120570

Dong, Y., Coleman, M. and Miller, S. (2021). Greenhouse Gas Emissions from Air Conditioning and Refrigeration Service Expansion in Developing Countries. Annual Review of Environment and Resources, 46, 59-83. https://doi.org/10.1146/ANNUREV-ENVIRON-012220-034103/CITE/REFWORKS

Gado, M., Ookawara, S., Nada, S. and Hassan, H. (2022). Renewable Energy-based Cascade Adsorption-Compression Refrigeration System: Energy, Exergy, Exergoeconomic and Enviroeconomic Perspectives. Energy, 253, 124127. https://doi.org/10.1016/J.ENERGY.2022.124127

Ghanbarpour, M., Mota-Babiloni, A., Makhnatch, P., Badran, B., Rogstam, J. and Khodabandeh, R. (2021). ANN Modeling to Analyze the R404A Replacement with the Low GWP Alternative

R449A in an Indirect Supermarket Refrigeration System. Applied Sciences 2021, Vol. 11, Page 11333, 11(23), 11333. https://doi.org/10.3390/APP112311333

Hara-Chakravarty, K., Sadi, M., Chakravarty, H., Sulaiman-Alsagri, A., James-Howard, T. and Arabkoohsar, A. (2022). A Review on Integration of Renewable Energy Processes in Vapor Absorption Chiller for Sustainable Cooling. Sustainable Energy Technologies and Assessments, 50, 101822. https://doi.org/10.1016/J.SETA.2021.101822

Heredia-Aricapa, Y., Belman-Flores, J., Mota-Babiloni, A., Serrano-Arellano, J. and García-Pabón, J. (2020). Overview of Low GWP Mixtures for the Replacement of HFC Refrigerants: R134a, R404A and R410A. International Journal of Refrigeration, 111, 113-123. https://doi.org/10.1016/J.IJREFRIG.2019.11.012

Jeyakumar, N., Uthranarayan, C. and Narayanasamy, B. (2022). Energy Conservation in the Refrigeration System Through Improvement of Coefficient of Performance and Power Consumption Reduction Using Nanofluids. International Journal of Ambient Energy, 43(1), 1120-1126. https://doi.org/10.1080/01430750.2019.1687333

Lee, J., Seo, G., Mun, J., Park, M. and Kim, S. (2020). Thermal and Mechanical Design for Refrigeration System of 10 MW Class HTS Wind Power Generator. IEEE Transactions on Applied Superconductivity, 30(4). https://doi.org/10.1109/TASC.2020.2973117

Lucchini, A., Carraretto, I., Colombo, L., Mazzeo, D., Pittoni, P. and Lipori, G. (2024). Convective Condensation of R449a Inside a Smooth Tube. Journal of Physics: Conference Series, 2685(1), 012062. https://doi.org/10.1088/1742-6596/2685/1/012062

Nikhil-Babu, P., Mohankumar, D., Manoj-Kumar, P., Makeshkumar, M., Gokulnath, M., Gurubalaji, K., Harrish, G. and Ashok, M. (2021). Energy Efficient Refrigeration System with Simultaneous Heating and Cooling. Materials Today: Proceedings, 45, 8188-8194. https://doi.org/10.1016/J.MATPR.2021.03.072

Pan, X., Xing, Z., Tian, C., Wang, H. and Liu, H. (2021). A Method Based on GA-LSSVM for COP Prediction and Load Regulation in the Water Chiller System. Energy and Buildings, 230, 110604. https://doi.org/10.1016/J.ENBUILD.2020.110604

Qu, Y., Pan, E., Zhu, F., Jin, F. and Roy, A. (2023). Modeling Thermoelectric Effects in Piezoelectric Semiconductors: New Fully Coupled Mechanisms for Mechanically Manipulated Heat Flux and Refrigeration. International Journal of Engineering Science, 182, 103775. https://doi.org/10.1016/J.IJENGSCI.2022.103775

Sabry, A. and Ker, P. (2020). DC Environment for a Refrigerator with Variable Speed Compressor; Power Consumption Profile and Performance Comparison. IEEE Access, 8, 147973-147982. https://doi.org/10.1109/ACCESS.2020.3015579

Simbaña, I., Quitiaquez, W., Estupiñán, J., Toapanta-Ramos, F. and Ramírez, L. (2022). Performance Evaluation of a Direct Expansion Solar-assisted Heat Pump by Numerical Simulation of the Throttling Process in the Expansion Device. Revista Técnica "Energía" 19(1), 110-119. https://doi.org/10.37116/REVISTAENERGIA.V19.N1.2022.524

Snyder, D., Allgood, C. and McRae, T. (2021). Performance Evaluation of a Flooded Ice Rink Chiller Retrofit from R-22 to R-449A. International Refrigeration and Air Conditioning Conference. https://docs.lib.purdue.edu/iracc/2126

Song, J., Liu, G., Gong, J., Yang, Q., Zhao, Y. and Li, L. (2024). Simulation on Performance and Regulation Strategy of Centrifugal Refrigeration Compressor with Gas Bearings in Water Chiller. Applied Thermal Engineering, 236, 121650. https://doi.org/10.1016/J.APPLTHERMALENG.2023.121650

Taebnia, M., Toomla, S., Leppä, L. and Kurnitski, J. (2020). Developing Energy Calculation Methodology and Calculation Tool Validations: Application in Air-heated Ice Rink Arenas. Energy and Buildings, 226, 110389. https://doi.org/10.1016/J.ENBUILD.2020.110389

Touaibi, R. and Koten, H. (2021). Energy Analysis of Vapor Compression Refrigeration Cycle Using a New Generation Refrigerants with Low Global Warming Potential. Journal of Advanced Research in Fluid Mechanics and Thermal Sciences, 87(2), 106-117. https://doi.org/10.37934/arfmts.87.2.106117

Yildirim, R., Kumas, K., Akyuz, A. and Gungor, A. (2023). Numerical Analysis of Using R449A Refrigerant Alternative to R404A in Cooling Systems: 3E-Analysis (Energetic, Exergetic, and Environmental). Politeknik Dergisi, 26(4), 1319-1325. https://doi.org/10.2339/politeknik.1073335

Implementation of Kaizen Approach and Six Sigma Methodology to Improve Organic Eggs Productivity

Maribel Torres
Grupo de Investigación en Ingeniería, Productividad y Simulación Industrial (GIIPSI),
Universidad Politécnica Salesiana, Ecuador
Orcid: https://orcid.org/0009-0002-0457-6392

William Quitiaquez
Grupo de Investigación en Ingeniería, Productividad y Simulación Industrial (GIIPSI),
Universidad Politécnica Salesiana, Ecuador
Orcid: https://orcid.org/0000-0001-9430-2082

Isaac Simbaña
Grupo de Investigación en Ingeniería Mecánica y Pedagogía de la Carrera de Electromecánica
(GIIMPCEM), Instituto Superior Universitario Sucre, Ecuador
Orcid: https://orcid.org/ 0000-0002-3324-3071

Patricio Quitiaquez
Grupo de Investigación en Ingeniería, Productividad y Simulación Industrial (GIIPSI),
Universidad Politécnica Salesiana, Ecuador
Orcid: https://orcid.org/0000-0003-0472-7154

Introduction

The case study was carried out on a farm that has an ecological philosophy and its main income is the production of organic eggs. Those come from hens that are not exposed to stress or confinement and are fed with products without high percentages of hormones and chemicals (Sokołowicz et al., 2019). The monthly production of eggs on the farm is around 13 500 units distributed in Cotacachi, Imbabura. Due to the high production of eggs, it is necessary to implement a methodology that maintains the quality of the eggs. The main objective of *Six Sigma* is to improve production processes, reducing time and eliminating unnecessary processes (Smętkowska and Mrugalska, 2018). The phases during the application of this methodology are Define, Measure, Analyze, Improve, and Control (DMAIC) (De Mast and Lokkerbol, 2012). The methodological approach's importance is reducing operating costs and improving the company's organizational performance (Boon-Sin et al., 2015).

Deeb et al. (2018) implemented the *Six Sigma* methodology in small and medium-sized businesses (SMBs). This methodology was used to improve the performance of the company by reducing the variability of the results of the processes, which is formed by a meta-model, based on studies on *Six Sigma*, its phases, and tools. The main results define the requirements to reach in each of the phases of *Six Sigma* implementation. A list of requirements was created for assessing the obtained results, to validate the objectives and maintain the production improvement.

Ahmad (2011) developed several mathematical and artificial intelligence models to compare egg production forecasts. The study utilized a simple approach with one variable, egg production, thus simulating egg production through neural networks and genetic algorithms, by considering a sample of 240 hens and the daily information on egg production. Afterward, a comparison was developed between the models, obtaining that the general regression neural network provided the best fit of 0.71, determining that the neural models are more efficient in forecasting future egg production.

Valderrama-Mendoza et al. (2019) designed a SCADA-type software to measure, record, and control the involved variables to increase the productivity of poultry farms. For data collection, a sensor system in the sheds was installed, and a graphic description that represents the system code. The software was based on predicting the chicken weight, allowing poultry farmers to make the best decisions, hence, standardizing the parameters for production improvement.

Tirado and Abril (2020) analyzed the 5S methodology in companies in the poultry sector in the Province of Tungurahua. The profitability of a batch of traditionally raised hens was compared with one from organic breeding, applying the 5S method. The results showed activities of organization, cleaning, classification, standardization, and discipline, that reduced the cost of production and increased the profitability of the company. By the 5S methodology application, the company's profitability increased by 12.2 %, equivalent to USD 3 910.74, besides, a saving of 4 % in terms of total costs was confirmed.

Omomule et al. (2020) studied the various challenges on poultry farms that affect the quality of egg production. There was a requirement to establish an optimal fuzzy predictive model for poultry egg production, collected data on chick age, feed quantity, feed quality, and total egg production. To carry out the model, software SPSS and Matlab were used. The performance evaluation of the proposed design yielded a relative error of 0.1174 %. This method is profitable and correct for modeling egg production on a farm, with an increase of 10 % in egg production, according to the model results.

Hammershøj and Steenfeldt (2015) determined the manner in which nutrients and forage material affect the quality of organic eggs with two hen

genotypes, *Lohman Silver* and *New Hampshire*. Organic eggs are produced by chickens that have access to outdoor living and are fed traditionally. The applied methodology consisted of a sample of 1 200 hens, fed with three types of diets and an average amount of protein of 203, 199, and 182 g·kg^{-1} and two treatments of forage material in the different genotypes. The results indicated that the hen genotype influences all eggs' quality parameters, such as size, weight, yolk color, and shell hardness. Then, for the egg weight, the *Lohman* genotype's eggs were 2.8 g heavier than the *Hampshire* genotype.

Filipiak-Florkiewicz et al. (2017) carried out a comparative analysis between organic eggs and conventional eggs to determine their quality. The evaluation consisted of the basic chemical composition of the egg and the mineral content to determine the fatty acid profiles. Then, the eggs' ability to make mayonnaise was evaluated and the obtained results indicated that the conventional eggs contained the highest number of fatty acids, while the organic eggs contained the highest level of protein, 17.7 g per 100 g. For mayonnaise prepared with organic eggs, there was greater stability. There are significant differences between eggs from organic hens and conventional hens, organic eggs are characterized by a more beneficial chemical composition than conventional ones, including moisture, protein, fat, and ash.

Philippe et al. (2020) compared the performance of egg production associated with three types of housing, battery cages, enriched cages, and aviaries. The study considered 12 scale chambers that were equipped with each of three types of housing, with 30 laying hens in each chamber. The laying rate was significantly influenced by the type of housing. Alternative hen housing methods, such as enriched cages and aviaries, were the best option in egg production.

This investigation aims to improve the production of organic eggs on a farm, applying the *Six Sigma* methodology, with the objective of a continuous improvement of production processes, focused on customer satisfaction (Pérez-Vergara and Rojas-López, 2019). This document is distributed as follows, Methodology describes the steps to carry out this investigation, besides the required equations. Results present the obtained information from the software to analyze it and Conclusions summarize the document data, explaining the authors' perspective.

Materials and Methods

The *Six Sigma* methodology was utilized for the development of this study to improve productivity, reduce time, and eliminate unnecessary processes (Navarro-Albert et al., 2017). In the first instance, a statistical analysis of the production data from the previous semester when the investigation started was

carried out to obtain more information about the current situation of the farm. Then, a sequence of processes considered within the DMAIC methodological tool was applied, as shown in Figure 1.

The field where the method was applied and the improvement objectives were defined, according to the results of the statistical analysis. Data was measured to determine the behavior of the process, besides, the causes and effects of the detected problems in the production process were analyzed by using an Ishikawa diagram. Finally, improvements were imple-

mented throughout the production chain by integrating the *Kaizen* methodology, responsible for continuous improvement, and complementing it with a control phase to maintain the new performance.

The farm is dedicated to the production and marketing of organic eggs. The previous six months before the study had a total of 600 *Hy Line Brown* hens, the same breed that is specialized for laying hens. The average monthly production is 13 500 units and the production process is managed empirically, only based on the experience of the owners.

Figure 1
DMAIC process flow diagram
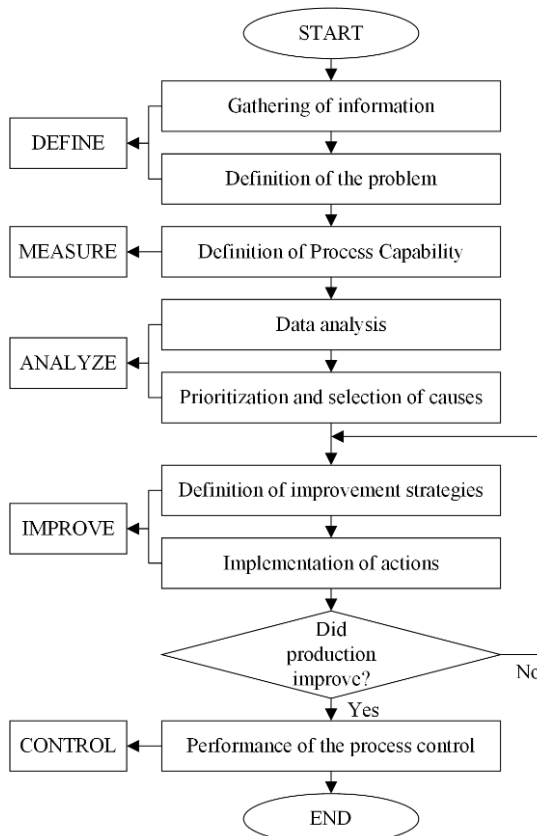
This business started in June 2020 as a response to the economic situation in the world due to the COVID-19 pandemic. In the beginning, a market survey was carried out superficially, because eggs are the cheapest protein source in the world and it is considered a food rich in essential amino acids, providing nutritional value to consumers (Lesnierowski and Stangierski, 2018). Therefore, a business of organic eggs started to produce them naturally by giving the chickens decent treatment, without confinement and stress (Dalle-Zotte et al., 2021). The quality of the eggs is measured by different parameters, such as chemical composition, resistance to breakage, or physical composition. Table 1 shows the comparison of the physical and chemical composition of conventional eggs and organic eggs, evidencing that organic eggs are larger and have a greater nutritional value.

Table 1

Comparative analysis for physical and chemical composition between traditional and organic eggs

Characteristics	Organic Eggs	Traditional Eggs
Weight [g]	60.7	60.7
Diameter [mm]	43.9	43.7
Width [mm]	56.9	56.7
Albumen Weight [g]	38.9	38.4
pH	8.80	9.15
Eggshell weight [g]	6.61	6.74
Thickness [mm]	0.35	0.36
Protein [g]	12.1	12.4
Lipids [g]	9.71	10.1
Cholesterol [g]	194	186

To apply the *Six Sigma* methodology, a dynamic analysis of the processes was carried out, through a graph of the process trend and the calculation of the process capacity. The capacity of the process (C_p) is obtained by relating the difference between the upper control limit (*LCS*) and the lower control limit (*LCI*) between six standard deviations of the process (σ) with eq. (1):

$$C_p = \frac{LCS - LCI}{6\sigma} \tag{1}$$

The upper process capability index (C_{pks}) is the quotient between, the difference between the upper control limit (*LCS*) and the average ($\bar{x}$) and three standard deviations of the process, obtained by eq. (2):

$$C_{pks} = \frac{LCS - \bar{x}}{3\sigma} \qquad (2)$$

The lower process capability index (C_{pki}) is calculated by applying eq. (3) as the quotient between, the difference between the average ($\bar{x}$) and the upper control limit (*LCI*) and three standard deviations of the process:

$$C_{pki} = \frac{\bar{x} - LCI}{3\sigma} \qquad (3)$$

The capacity of the process (C_p) is the extension of the natural variation, the optimum is that $C_p > 1$, therefore, it is considered that the process is prepared to comply with the parameters of *Six Sigma*. Therefore, C_{pks} and C_{pki}, if $C_{pks} > C_{pki}$, then there is a greater variation below the average, and if $C_{pks} < C_{pki}$, then there is a greater variation above the average (Ugr & Canatan, 2015). Then, by the C_p value, the *Sigma* level is observed. *Six Sigma* levels measure the number of times that an opportunity for error can be given. After the initial analysis, the DMAIC approach was applied in the Define phase (Kulkarni et al., 2021).

Results

The *Six Sigma* approach is used to improve company productivity by reducing variation in processes. This methodology develops continuous improvement in the production process. For this investigation, a descriptive statistical analysis was carried out on the production of organic eggs in the previous six months of the farm, obtaining the following results. There were 184 production data analyzed, which are equivalent to daily production for six months. The average daily production was 393 eggs, and the median and mode are 420 eggs, and the fact that they are the same indicates that there is no bias. The standard deviation of the process is 80.80, which shows the amplitude of the sample. During the study time, there was a minimum production of 120 eggs per day and a maximum of 510 eggs per day. Then, a dynamic analysis of the processes was carried out to know whether the process is stable. Figure 2 shows the trend of daily production, which has stabilized since March, as indicated by the red curve. However, it is necessary to calculate the capacity of the processes, to assure their stability. By carrying out the calculations, the values for C_p, C_{pks}, and C_{pki} were 0.92, 0,55, and 1.29, respectively.

The C_p value indicates that the process has a *Sigma* level of 2.75, consequently, it is equivalent to a 10 % probability of defects, compared to 100 % of production. By analyzing the values of C_{pks} and C_{pki}, it is defined that $C_{pki} > C_{pks}$, which indicates that there is greater variation above the average, consequently, the process is not symmetric. According to the process capacity data, the analyzed information is not stable.

These values must be greater than or equal to 1, therefore, it is necessary to stabilize the process. The DMAIC approach was used to reduce variation in the production process, through phases [20], Define, Measure, Analyze, Improve, and Control. For the Improve phase, the *Kaizen* approach was used, which is based on the application of a corrective action plan that continuously improves the process (Maarof & Mahmud, 2016).

Figure 2
Daily production trend for six months
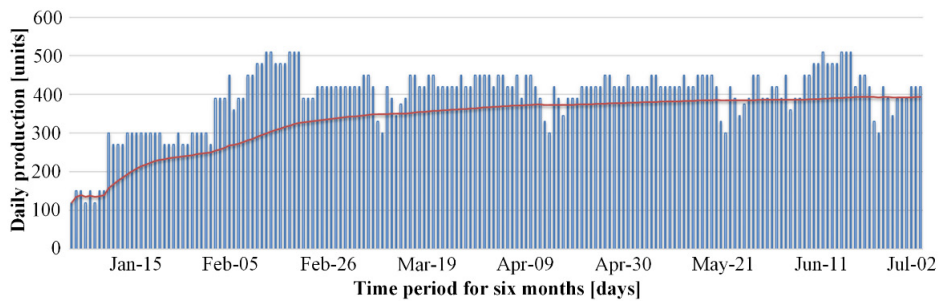
In the Define Phase, the current problem and the manner to address it are limited. According to the process capability analysis, the objective was to stabilize the process and for this purpose, it is necessary to know the process in detail. Table 2 shows the SIPOC diagram, through which the process is understood clearly (Nandakumar et al., 2020). Three processes that generate delays in egg production were identified, and these are Collection, egg classification by weight, and egg cleaning.

Table 2
SIPOC diagram

SUPPLIERS	INPUT	PROCESS	OUTPUT	CUSTOMERS
Agroscopio	*Hy Line Brown* laying hens		Eggs	Variable customers
agroscopio		1. Raise chicks 2. Eggs production 3. Recollection 4. Egg classification per weight 5. Eggs cleaning 6. Place eggs in trays 7. Commercialization		

For the Measure Phase, a total of 184 data were collected from January to June 2021. The variation of the process was studied, in this case, by the calcula-

tions. A C_p of 0.92 was obtained, which indicates 105 660 defects in 1 000 000 opportunities.

Figure 3 presents the histogram of all the data analyzed, that is, the frequency of the daily production presented in the six months. The graph is biased to the left, where the most repeated production was 420 eggs per day, with an average production of 393 units.

Figure 3
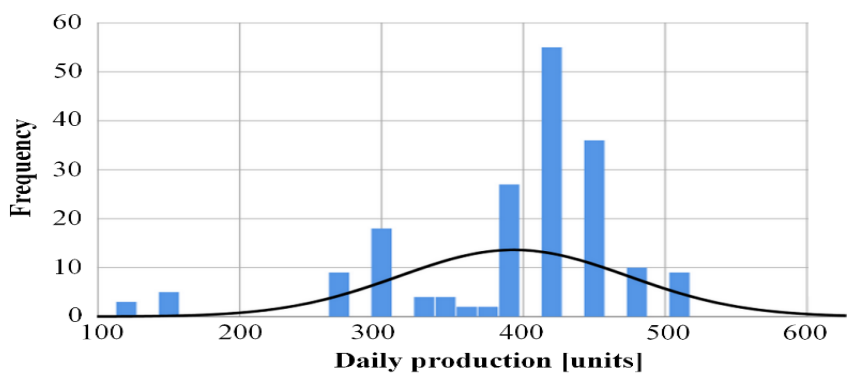*Histogram of the daily production of organic eggs*

Figure 4 presents the control of the process, indicating variability and several production peaks outside the limits, which confirms that the process is not stable and needs intervention to improve production processes and reduce failures. Besides, the upper (*LCS*) and lower (*LCI*) control limits can be identified, with values of 457.73 and 326.28, respectively.

Figure 4
Daily Production Control Chart
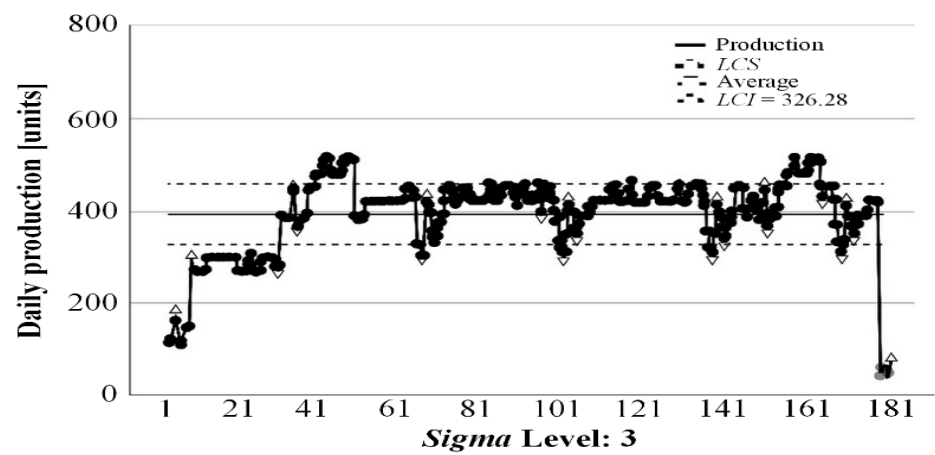
For the Analyze Phase, the root of the variation is studied and causes were selected to define the problem. The Ishikawa diagram was plotted, thus identifying some of the causes for the variability of the process. The factors considered to find the potential causes of the problem were labor, method, machine, material, and environment (Carvalho et al., 2021) as shown in Figure 5. The most important causes according to the analysis were labor and machine.
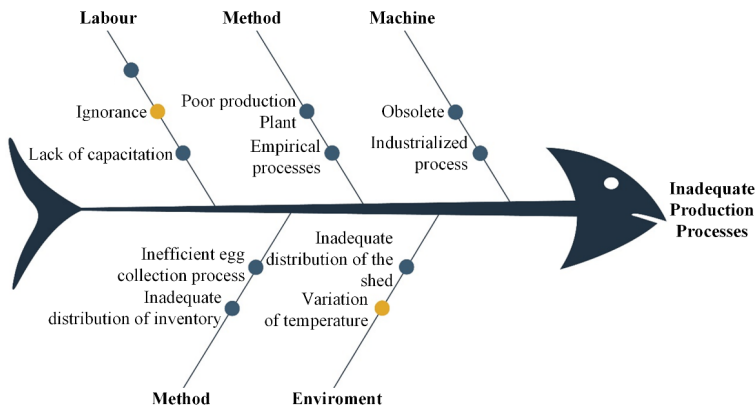
Figure 5
Ishikawa diagram

Figure 6 shows a simulation of the current situation of the shed, where the hens and nests are everywhere, slowing down the production process in the egg collection phase, because several hens lay eggs anywhere, losing several units per day.

Figure 6
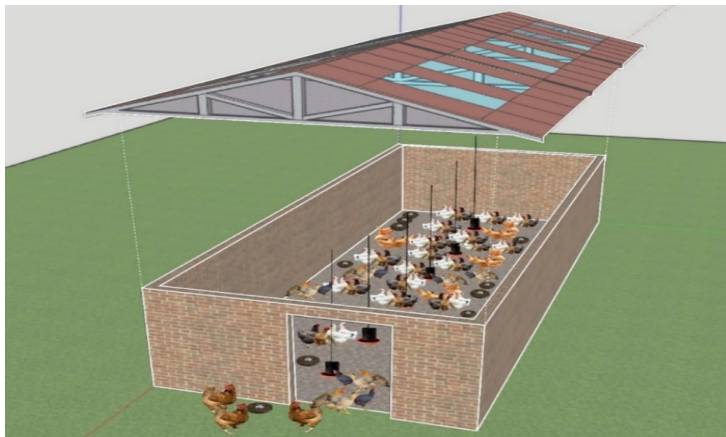*Current situation of the shed*

Figure 7 shows the box plot for the daily production of organic eggs, during the first half of the year. In January, the production is lower and there is a variation in the data. Meanwhile, from February to June the variation reduced and the production stabilized. In addition, in February there was atypical data, but the distribution of the data is skewed towards the production of 300 eggs.

Figure 7

Boxplot of the monthly production for organic eggs
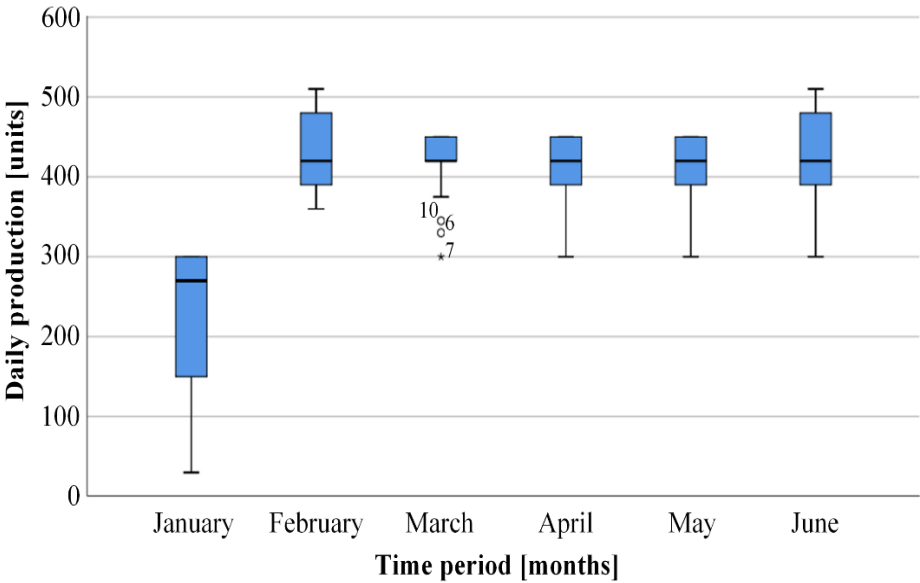
For the Improve Phase, improvement strategies were defined and the *Kaizen* methodology was applied, which focuses on continuous improvement. The first three steps of the methodology coincide with the DMAIC approach, therefore, only processes four and five were applied. According to the analysis of the causes of the problem, deficient planning in the production process of organic eggs and empirical management of production cause high variability in the process. Besides, the egg collection process and inadequate inventory control led to a loss of approximately 10 eggs per day. Poor house layout causes hens to lay their eggs in different places.

In the Control Phase, the processes were controlled by several tools. In this investigation, controls were carried out through the recording of daily production and by maintaining the upper control limit at 610 eggs and the lower control limit at 178 eggs per day, as seen in Figure 8. Also, sanitary control was necessary, placing lime at the entrance of the shed to protect the hens from various diseases. To control production planning, a checklist was carried out

where it was identified that more training is still needed for the people in charge of the farm and the production of organic eggs.

Figure 8

Process control chart after Six Sigma Implementation
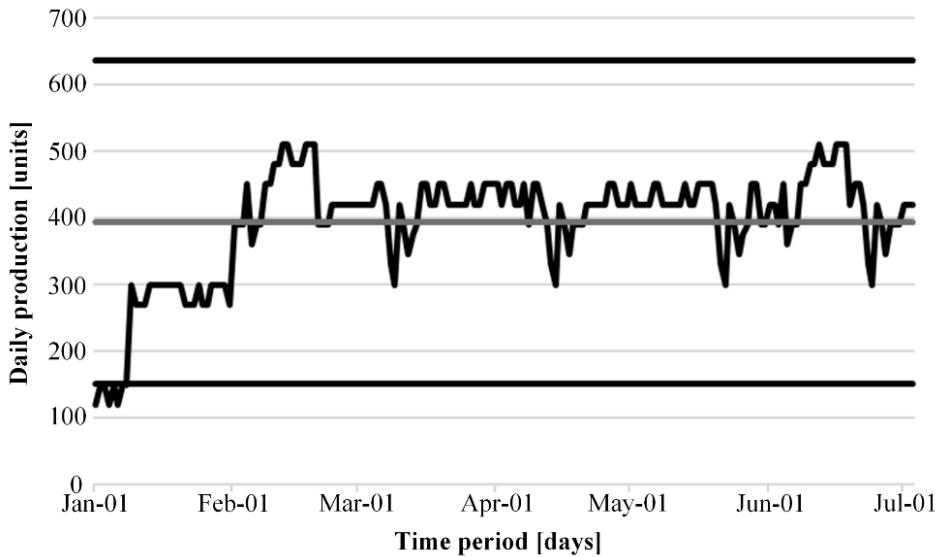
The corrective actions to solve each of the root causes are the Production Plan, increasing the batch of laying hens by implementing the process of rearing chicks. Besides, to stabilize the process, it is necessary to increase the control limits. Therefore, the new upper control limit will be 610 eggs per day, and the lower control limit 178 eggs per day. By increasing production, the obtained values of the statistical capacities of processes were 1.02, 1.01, and 1.00 for C_p, C_{pks}, and C_{pki}, respectively, which demonstrate that the process is stable. To solve the inefficient egg collection process and the inadequate inventory control, it was necessary to organize the processes and reduce the time. Figure 9 shows the optimized process of the production system of organic eggs, from the purchase of inputs for the shed to the transportation process. Then, the distribution of the shed was organized in a better manner, increasing the nests and spaces where the hens could remain after grazing.

Figure 9

Production process for organic eggs
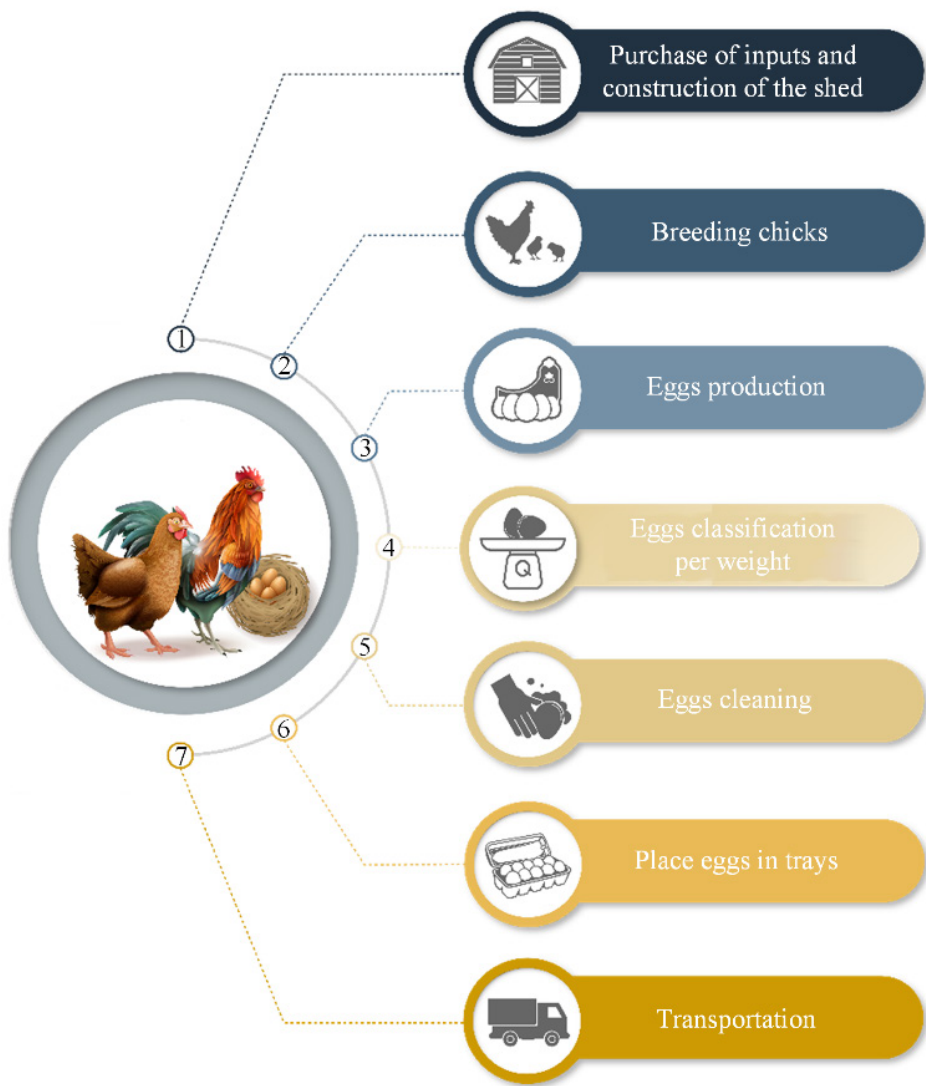
Conclusions

The application of the *Six Sigma* methodology, through the DMAIC approach, allowed to identify opportunities for improvement in the production process of organic eggs. It was determined that one of the processes with the greatest variability was egg collection and cleaning. Therefore, the process was

redesigned improving the collection process and the egg cleaning to maintain the quality and increase egg production.

In the Measurement phase, a statistical analysis of processes was carried out, obtaining as a result process capacity (C_p) of 0.92, upper process capacity (C_{pks}) of 0.55, and 1.29 for lower process capacity (C_{pki}). These results determined that the process presents a high variability. The DMAIC approach stabilized the process by increasing the values of the upper control limit with 610 eggs and the lower control limit with 178 eggs per day, thus obtaining values of 1.02, 1.01, and 1.00 for C_p, C_{pks}, and C_{pki}, respectively, which indi-cate stability in the process. Then, fulfilling the objective of the *Six Sigma* methodology is to reduce the variability of the production process.

An improved distribution of the shed was carried out, increasing 10 nests and 10 feeders to do the egg collection faster and more efficiently. The new distribution of the shed improved significantly the organic egg production process and reduced the mortality rates of the hens. It is necessary to change the mentality of the workers for the implementation of the methodology. Quality is a key indicator to position the business in the Ecuadorian organic egg market.

References

Ahmad, H. A. (2011). Egg production forecasting: Determining Efficient Modeling Approaches. Journal of Applied Poultry Research, 20(4), 463-473. https://doi.org/10.3382/japr.2010-00266

Boon Sin, A., Zailani, S., Iranmanesh, M. and Ramayah, T. (2015). Structural Equation Modelling on Knowledge Creation in Six Sigma DMAIC Project and its Impact on Organizational Performance. International Journal of Production Economics, 168, 105-117. https://doi.org/10.1016/j.ijpe.2015.06.007

Carvalho, R., Lobo, M., Oliveira, M., Raquel, A., Alonso, V., Lopes, F. and Souza, J. (2021). Analysis of Root Causes of Problems Affecting the Quality of Hospital Administrative Data: A Systematic Review and Ishikawa Diagram. International Journal of Medical Informatics. 156, 104584. https://doi.org/10.1016/j.ijmedinf.2021.104584

Dalle Zotte, A., Cullere, M., Pellattiero, E., Sartori, A., Marangon, A. and Bondesan, V. (2021). Is the Farming Method (cage, barn, organic) a Relevant Factor for Marketed Egg Quality Traits? Livestock Science, 246, 104453. https://doi.org/10.1016/j.livsci.2021.104453

De Mast, J. and Lokkerbol, J. (2012). An Analysis of the Six Sigma DMAIC Method From the Perspective of Problem Solving. International Journal of Production Economics, 139(2), 604-614. https://doi.org/10.1016/j.ijpe.2012.05.035

Deeb, S., Haouzi, H. B. El, Aubry, A. and Dassisti, M. (2018). A Generic Framework to Support the Implementation of Six Sigma Approach in SMEs. IFAC-PapersOnLine, 51(11), 921-926. https://doi.org/10.1016/j.ifacol.2018.08.490

Filipiak-Florkiewicz, A., Deren, K., Florkiewicz, A., Topolska, K., Juszczak, L. and Cieślik, E. (2017). The Quality of Eggs (organic and nutraceutical vs. conventional) and their Technological Properties. Poultry Science, 96(7), 2480-2490. https://doi.org/10.3382/ps/pew488

Hammershøj, M. and Steenfeldt, S. (2015). Organic Egg Production. II: The Quality of Organic Eggs is Influenced by Hen Genotype, Diet and Forage Material Analyzed by Physical Parameters,

Functional Properties and Sensory Evaluation. Animal Feed Science and Technology, 208, 182-197. https://doi.org/10.1016/j.anifeedsci.2015.07.012

Kulkarni, S., Prasanna, N., Mirunalini, S., Akshaya, C., Deekshitha, R., Kousalya, N. and Agalya, A. (2021). Enhancing the Process Capability of Machining Process of Boring Tool Holder by Application of Six Sigma Methodology. Materials Today: Proceedings, 52(3), 329-338. https://doi.org/10.1016/j.matpr.2021.09.043

Lesnierowski, G. and Stangierski, J. (2018). Trends in Food Science & Technology What's New in Chicken Egg Research and Technology for Human Health Promotion? - A Review. Trends in Food Science & Technology, 71, 46-51. https://doi.org/10.1016/j.tifs.2017.10.022

Maarof, M. G. and Mahmud, F. (2016). A Review of Contributing Factors and Challenges in Implementing Kaizen in Small and Medium Enterprises. Procedia Economics and Finance, 35, 522-531. https://doi.org/10.1016/S2212-5671(16)00065-4

Nandakumar, N., Saleeshya, P. G. and Harikumar, P. (2020). Bottleneck Identification and Process Improvement by Lean Six Sigma DMAIC Methodology. Materials Today: Proceedings, 24, 1217-1224. https://doi.org/10.1016/j.matpr.2020.04.436

Navarro Albert, E., Gisbert Soler, V. and Pérez Molina, A. (2017). Metodología e Implementación de Six Sigma. 3C Empresa: Investigación y Pensamiento Crítico, 6(5), 73-80. https://doi.org/10.17993/3cemp.2017.especial.73-80

Omomule, T., Ajayi, O. and Orogun, A. (2020). Fuzzy Prediction and Pattern Analysis of Poultry Egg Production. Computers and Electronics in Agriculture, 171, 105301. https://doi.org/10.1016/j.compag.2020.105301

Pérez-Vergara, I. and Rojas-López, J. (2019). Lean, Six Sigma and Quantitative Tools: A Real Experience in the Productive Improvement of Processes of the Graphic Industry in Colombia. Revista de Métodos Cuantitativos Para La Economáa y La Empresa, 27(27), 259-284. https://ideas.repec.org/a/pab/rmcpee/v27y2019i1p259-284.html

Philippe, F., Mahmoudi, Y., Cinq-Mars, D., Lefrançois, M., Moula, N., Palacios, J., Pelletier, F. and Godbout, S. (2020). Comparison of Egg Production, Quality and Composition in Three Production Systems for Laying Hens. Livestock Science, 232, 103917. https://doi.org/10.1016/j.livsci.2020.103917

Smętkowska, M. and Mrugalska, B. (2018). Using Six Sigma DMAIC to Improve the Quality of the Production Process: A Case Study. Procedia - Social and Behavioral Sciences, 238, 590-596. https://doi.org/10.1016/j.sbspro.2018.04.039

Sokołowicz, Z., Dykiel, M., Krawczyk, J. and Augustyńska-Prejsnar, A. (2019). Effect of Layer Genotype on Physical Characteristics and Nutritive Value of Organic Eggs. CYTA - Journal of Food, 17(1), 11-19. https://doi.org/10.1080/19476337.2018.1541480

Tirado, L. and Abril, J. (2020). Quality and Poultry Sector of the Province of Tungurahua. Revista de Investigación, Formación y Desarrollo: Generando Productividad In-stitucional, 8(2). 15-31.15-31. https://dialnet.unirioja.es/servlet/articulo?codigo=8273677

Ugr, O. L. and Canatan, H. (2015). Literature Search Consisting of the Areas of Six Sigma's Usage. 195(0212), 695-704. https://doi.org/10.1016/j.sbspro.2015.06.160

Valderrama-Mendoza, M., Rodríguez-Urrego, L., Cobo, L. and Martínez, G. (2019). Sistema de Análisis para el Incremento de la Producción de Granjas Avícolas en Colombia. Caso de estudio: Proyecto Proavícola. Avances: Investigación en Ingeniería, 16(1), 1-16. https://doi.org/10.18041/1794-4953/avances.1.5254

Ixora coccinea: A Phytochemical Treasure Trove - Unveiling Secondary Metabolites and Biological Activity for Ecuadorian Biotechnology

Jose Luis Ballesteros Lara
Universidad Politécnica Salesiana, (Ecuador)
Orcid: https://orcid.org/0000-0002-8426-3355

Kevin Gabriel Cedeño Vinces
Universidad Politécnica Salesiana, (Ecuador)
Orcid: https://orcid.org/0000-0001-6693-6141

Emily Carolina Chong Hermenegildo
Universidad Politécnica Salesiana, (Ecuador)

Nayeli Sofia Caraguay Carchi
Universidad Politécnica Salesiana, (Ecuador)

Introduction

The tropical dry forest is a biodiverse ecosystem characterized by a tropical climate, with prolonged periods of drought and shorter wet seasons that harbor many plant and animal species (Siyum, 2020). This unique ecosystem is home to numerous botanical families, among which Rubiaceae (Rosalba & Heidy Paola, 2020) stands out. Within this family, Ixora coccinea is a plant adapted to warm climates that flourishes under intense sun conditions, and its aesthetic value makes it frequent in gardens, nurseries, parks, and streets, where it is admired for its bright flowers (Mex et al., 2019).

In addition to being eye-catching, this species is also interesting to the scientific community for its biological diversity and impact on various industries. An article from the Federal Urdu University highlights the multiple medicinal effects of I. *coccinea*, including its ability to treat asthma, reduce lipid and glucose levels, prevent abnormal cell growth, and be effective against ulcers and parasites. It also possesses antioxidant activities and protective proper-

ties against liver and harmful chemicals (Muhammad et al., 2020).

Moreover, a study conducted at the Central Food Technology Research Institute in India found that I. *coccinea* fruits contain high levels of phenols, flavonoids, and anthocyanins, known for their beneficial health effects, thus proving their antioxidant activity and cytotoxicity against human prostate carcinoma cells, suggesting their potential for the development of new treatments for prostate cancer (Shreelakshmi et al., 2021).

Materials and Methods

This research uses the following experimental methodology to identify the plant's secondary metabolites and determine its antioxidant activity:

Figure 1

Phases for obtaining the extract, identifying secondary metabolites and evaluating antioxidant activity
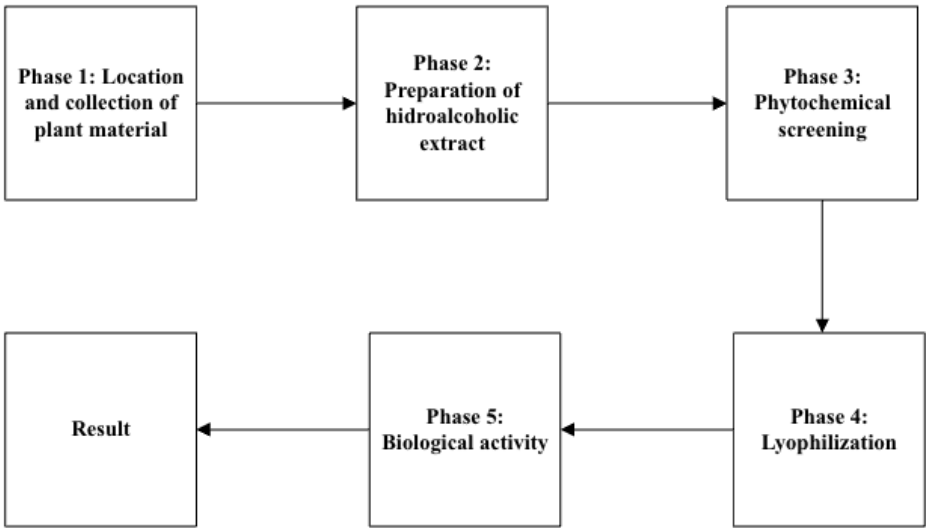
Phase 1: Location and collection of plant material

Ixora coccinea leaves were collected at the Maria Auxiliadora campus of the Salesian Polytechnic University, located at kilometer 19.5 of the Via a la Costa in Guayaquil, Ecuador. Samples of I. *coccinea* were collected, identified, and analyzed. These leaves were used to extract hydroalcoholic compounds, which will be subjected to phytochemical analysis and antioxidant activity tests.

Ixora coccinea: A Phytochemical Treasure Trove - Unveiling Secondary Metabolites and Biological Activity for Ecuadorian Biotechnology

101

Phase 2: Preparation of hydroalcoholic extract

The plant material was separated and cut, and then a washing process was carried out with distilled water to eliminate any impurities in the sample (Da Silva et al., 2018). Subsequently, the plant material was dried at room temperature for 1 hour to eliminate surface moisture and then transferred to a Binder oven, which was kept at 40 °C for 96 hours (Babu et al., 2018). This controlled drying process allowed the obtaining of completely dehydrated samples that were subsequently pulverized.

The Soxhlet method was employed to obtain the hydroalcoholic solution, using a mixture of 96% ethanol and distilled water in a 90:10 ratio (Al Jitan et al., 2018). Before phytochemical analysis, the hydroalcoholic extract was concentrated and purified using a rotary evaporator at 40 °C (Aronés Jara et al., 2022).

Phase 3: Phytochemical screening.

Different photochemical tests were performed to identify secondary metabolites in *I. coccinea* (see Table 1). These tests were based on the methodology of the National Polytechnic Institute of Mexico GSL Medical College and General Hospital of India (García-Granados et al., 2019; Kancherla et al., 2019).

Table 1

Assays performed for the identification of secondary metabolites

Test	Secondary metabolites
Mayer test	Alkaloids
Dragendorff test	
Hager test	
Wagner test	
Shinoda test	Flavonoids
Zinc test	
Sodium hydroxide test	Coumarins
Keller-Kilani test	Cardiotonic glycosides
Benedict test	Carbohydrates
Fehling test	
Terpenoid test	Proteins
Salkowski test	Triterpenes
Peroxide test	Saponins
Molish test	
Baljet test	Lactones sesquiterpenes

Phase 4: Lyophilization

A Christ Alpha 1-4 LSC freeze dryer was used, adjusting the conditions to a condenser freezing temperature of -50 °C and a vacuum pressure of 0.04 millibar. The process included a central drying for 4 hours and a final drying of 3 hours, after which the extracts were flash-frozen at -80 °C (Cheaib et al., 2018).

Phase 5: Biological activity.

The DPPH free radical technique was applied to perform the antioxidant activity assay, starting with preparing the leading solution composed of 5 milligrams of DPPH, gauged in 100 milliliters of 96% ethanol. In parallel, as a standard solution, 5 milligrams of ascorbic acid gauged in 50 milliliters of 96% ethanol was prepared (Castañeda et al., 2008). To prepare the sample solution, 5 milligrams of the hydroalcoholic extract was dissolved in 50 milliliters of 96% ethanol. For completing homogenization, the solution was agitated in an iSonic P4860 ultrasonic bath for 30 minutes (Das et al., 2014). Finally, to remove impurities or residues in the solution, the extract was filtered using 0.45-micrometer CHMLAB Group syringe filters (Ding & Scheer, 2004). To analyze the antioxidant activity of the hydroalcoholic extract of *I. coccinea* leaves, the amounts of extract, ethanol, and DPPH were specifically prepared (see Table 2).

After preparation, the vials were shaken at 300 rpm for 3-5 min at room temperature and were allowed to stand for 30 min before reading (La et al., 2011).

Table 2

Preparation of solutions for antioxidant activity testing

Flask	Amount of DPPH (milliliters)	Amount of ethanol 96 % (microliters)	Sample quantity (microliters)
White	2.9	100	0
1	2.9	95	5
2	2.9	90	10
3	2.9	80	20
4	2.9	50	50
5	2.9	20	80
6	2.9	0	100

Results

Healthy and mature leaves were selected, avoiding those affected by pests or physical damage (see Fig. 2). The samples were placed in sealed plastic bags and transferred to the Instrumental Laboratory of the Salesian Polytechnic University.

Figure 2
Collection of I. coccinea species

The morphological characteristics of the leaves of *I. coccinea* that were collected were verified (see Table 3). The hydroalcoholic extract was obtained with a final volume of 750 milliliters, presenting a dark green color and a pH of 5.40 (see Fig. 3). The green coloration of the hydroalcoholic extract is due to pigments such as chlorophyll and carotenoids; this tonality intensifies when exposed to air or light due to the oxidation of these pigments, which can affect the properties of the extract; this shows the importance of properly handling and storing the extract to maintain its quality (Tena & Asuero, 2020).

Table 3
General description of the morphological characteristics of I. coccinea leaves

Morphological characteristics of the leaves of I. coccinea						
Image	**Form**	**Size**	**Color**	**Odor**	**Texture**	**Consistency**
	Simple and lanceolate	Length: 4 centimeters Width: 2 centimeters	Dark green	No odor	Smooth	Rigid

Figure 3
Preparation of hydroalcoholic extract
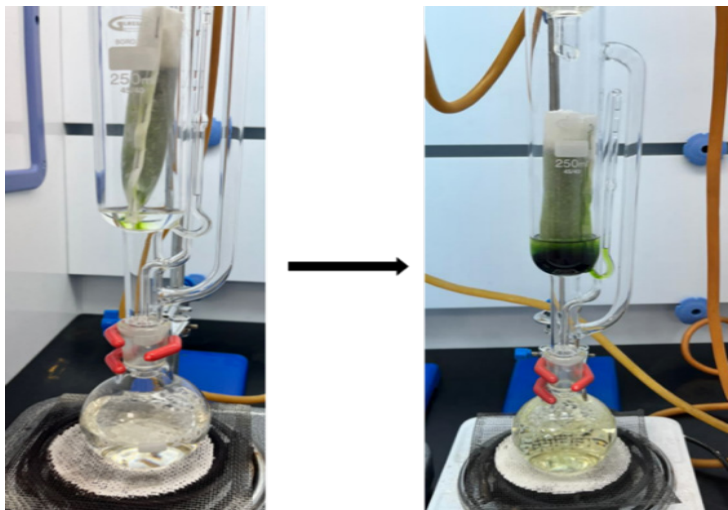
The secondary metabolites found in the hydroalcoholic extract of *I. coccinea* were qualitatively expressed with the following symbols: '+++' for abundant presence, '++' for moderate presence, '+' for low presence, and '-' for absence (see Table 4) [18]. (Loja et al., 2017).

Table 4
Phytochemical screening of the hydroalcoholic extract of I. coccinea leaves

| Secondary metabolites	Essay	Results
Alkaloids	Mayer	+++
	Dragendorff	+++
	Hager	+++
	Wagner	+++
Flavonoids	Shinoda	+
	Zinc	+++
Coumarins	NaOH	++
Cardiotonic glycosides	Keller-Kilani	-
Carbohydrates	Benedict	+++
	Fehling	+
Terpenoids	Terpenoids	+++
Triterpenes	Salkowski	++
Saponins	Peroxide	-
	Molish	-
Sesquiterpene Lactones	Baljet	+++

The DPPH technique indicates that the hydroalcoholic extract presents 1.79% inhibition with five microliters and 16.78% with 100 microliters, showing that the inhibition of free radicals increases with the concentration of the extract. In addition, it is demonstrated that *I. coccinea* has an IC50 of 10.65 micrograms over milliliters (see Table 5). The antioxidant activity of the hydroalcoholic extract was compared with that of ascorbic acid, a pure chemical reference with an antioxidant value of 5.38 micrograms per milliliter, demonstrating the strong antioxidant capacity of I. *coccinea* (see Fig. 4). This finding highlights the antioxidant capacity of I. *coccinea* in comparison with other species, such as *Cinchona pubescens Vahl*, belonging to the Rubiaceae family, which has an IC50 of 46.66 micrograms per milliliter, according to a study conducted at the Salesian Polytechnic University, Quito (Barukcic Revelo & Sola Montero, 2015).

Table 5

Results of the DPPH antioxidant test

Ixora coccinea (μl)	Concentration (μg/ml)	Absorbance at 517 nanometers		Average absorbance	Inhibition %
		Repetition 1	Repetition 2		
White	0	1.480	1.481	1.481	0
5	0.167	1.454	1.454	1.454	1.80
10	0.333	1.435	1.434	1.435	3.11
20	0.667	1.426	1.426	1.426	3.68
50	1.667	1.376	1.377	1.377	7.02
80	2.667	1.292	1.292	1.292	12.73
100	3.333	1.232	1.232	1.232	16.78
				IC50	10.65

Figure 4

Inhibition of the DPPH radical according to its concentration
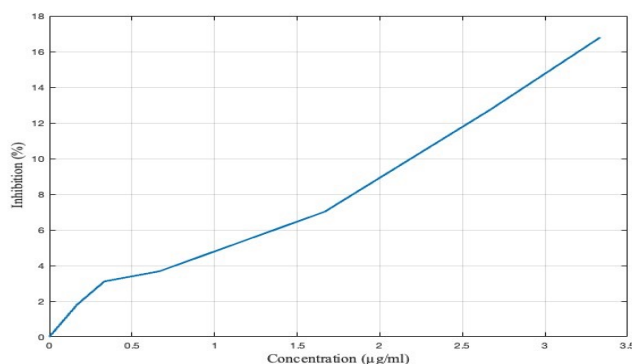
The hydroalcoholic extract of *I. coccinea*, rich in flavonoids, terpenoids, and triterpenoids, has a strong antioxidant potential, supportingsupports its application in medicine, agriculture, food, and the cosmetic industry, as well as in developing various sustainable products and practices (Castaño Amores & Hernández Benavides, 2018)

Conclusions

A diversity of secondary metabolites was determined through phytochemical screening, including alkaloids, flavonoids, coumarins, carbohydrates, terpenoids, and sesquiterpene lactones. These compounds were analyzed to explore their potential in biotechnological applications, such as developing drugs with therapeutic properties and formulating compounds for the food and cosmetic industries. The quantification of the antioxidant activity by DPPH obtained an IC50 of 10.65 micrograms over milliliters, indicating a significant antioxidant capacity. This result suggests a potential use of *I. coccinea* extracts in creating antioxidant products, which is interesting to the biotechnological industry, especially in health and cosmetics. Confirming the presence of secondary metabolites and quantifying antioxidant activity in *I. coccinea* promotes their study and sustainable use, benefiting society and the environment.

References

Al Jitan, S., Alkhoori, S. A., & Yousef, L. F. (2018). Phenolic Acids From Plants: Extraction and Application to Human Health. Studies in Natural Products Chemistry, 58, 389-417. https://doi.org/10.1016/B978-0-444-64056-7.00013-1

Amazônia, B., Carmosina, A., Queiroz, S., Marcia, A., Bizerra, C., & Lopes Machado, A. (n.d.). NOTA CIENTÍFICA Antioxidant and antimicrobial activities of organic extracts of Ixora coccínea L Atividades antioxidantes e antimicrobianas de extratos orgânicos de Ixora coccínea L 1* Esta obra estaíicenciada sob uma Licença Creative Commons Attribution. https://doi.org/10.18561/2179-5746/biotaamazonia.v8n4p49-53

Aronés Jara, M. R., Cárdenas Landeo, E., Luna Molero, H. R., Barbarán Vilcatoma, S. M., & Gómez Quispe, M. (2022). TAMIZAJE FITOQUÍMICO, CONTENIDO DE COMPUESTOS FENÓLICOS Y POTENCIAL ANTIOXIDANTE DE TRECE PLANTAS MEDICINALES DE LOS AFLORAMIENTOS ROCOSOS DEL BOSQUE DE PIEDRAS DE HUARACA EN PERÚ. Revista de La Sociedad Química Del Perú, 88(2). https://doi.org/10.37761/rsqp.v88i2.388

Babu, A. K., Kumaresan, G., Raj, V. A. A., & Velraj, R. (2018). Review of leaf drying: Mechanism and influencing parameters, drying methods, nutrient preservation, and mathematical models. In Renewable and Sustainable Energy Reviews (Vol. 90, pp. 536-556). Pergamon. https://doi.org/10.1016/j.rser.2018.04.002

Barukcic Revelo, A. M., & Sola Montero, M. J. (2015). Desarrollo de formulaciones fito - cosméticas antioxidantes empleando como sustancia activa el extracto seco de Cinchona pubescens Vahl, Rubiaceae (Cascarilla). http://dspace.ups.edu.ec/handle/123456789/9377

Castañeda Castañeda, B., Ramos Llica, E., & Ibáñez Vasquez, L. (2008). Evaluación de la capacidad antioxidante de siete plantas medicinales peruanas. Horizonte Médico (Lima), 8(1), 56-72. https://doi.org/10.24265/horizmed.2008.v8n1.04

Castaño Amores, C., & Hernández Benavides, P. J. (2018). Activos antioxidantes en la formulación de productos cosméticos antienvejecimiento. Ars Pharmaceutica (Internet), 59(2), 77-84. https://doi.org/10.30827/ars.v59i2.7218

Cheaib, D., El Darra, N., Rajha, H. N., El-Ghazzawi, I., Maroun, R. G., & Louka, N. (2018). Effect of the extraction process on the biological activity of lyophilized apricot extracts recovered from apricot pomace. Antioxidants, 7(1), 11. https://doi.org/10.3390/antiox7010011

Das, N., Islam, M. E., Jahan, N., Islam, M. S., Khan, A., Islam, M. R., & Parvin, M. S. (2014). Antioxidant activities of ethanol extracts and fractions of Crescentia cujete leaves and stem bark and the involvement of phenolic compounds. BMC Complementary and Alternative Medicine, 14(1), 1-9. https://doi.org/10.1186/1472-6882-14-45

Ding, W., & Scheer, L. (2004). Syringe filter efficiency and the effect of filtration on HPLC column life. EBR - European Biopharmaceutical Review, AUTUMN, 60-63. www.pall.com/contact

García-Granados, R. U., Cruz-Sosa, F., Alarcón-Aguilar, F. J., Nieto-Trujillo, A., & Gallegos-Martínez., M. E. (2019). ANÁLISIS FITOQUÍMICO CUALITATIVO DE LOS EXTRACTOS ACUOSOS DE Thalassia testudinum BANKS EX KÖNING ET SIMS DE LA LOCALIDAD DE CHAMPOTÓN, CAMPECHE, MÉXICO, DURANTE EL CICLO ANUAL 2016-2017. Polibotánica, 48. https://doi.org/10.18387/polibotanica.48.12

Kancherla, N., Dhakshinamoothi, A., Chitra, K., & Komaram, R. B. (2019). Maedica-a Journal of Clinical Medicine Preliminary Analysis of Phytoconstituents and Evaluation of Anthelminthic Property of Cayratia auriculata (In Vitro) Preliminary analysis of Phytoconstituents and evaluation of anthelminthic ProPerty of cayratia auri. Maedica A Journal of Clinical Medicine, 14(4), 350-356. https://doi.org/10.26574/maedica.2019.14.4.350

La, A., Toro, R., Fredy, G., López, V., & Taipe, M. (2011). Evaluación De La Actividad Antioxidante Del Pisco Peruano Mediante Voltametría Cíclica. Rev Soc Quím Perú, 77(2), 127-134. http://www.scielo.org.pe/scielo.php?script=sci_arttext&pid=S1810-634X2011000200005&lng=es&nrm=iso&tlng=es

Mex, R., Garma, P., Blanco, P., Robaldino, D., Campos-Marques, A., & Acal-Interián, D. (2019). Actividad Antioxidante de Ixora coccinea. Revista Iberoamericana de Ciencias, 6(3), 2-9. www.reibci.org

Muhammad, H., Qasim, M., Ikram, A., Versiani, M. A., Tahiri, I. A., Yasmeen, K., Abbasi, M. W., Azeem, M., Ali, S. T., & Gul, B. (2020). Antioxidant and antimicrobial activities of Ixora coccinea root and quantification of phenolic compounds using HPLC. South African Journal of Botany, 135, 71-79. https://doi.org/10.1016/J.SAJB.2020.08.012

Rosalba, R. V., & Heidy Paola, S. R. (2020). Floristic diversity of the tropical dry forest in the lower and middle sinú subregion, córdoba, colombia. Revista de Biologia Tropical, 68(1), 167-179. https://doi.org/10.15517/rbt.v68i1.38286

Shreelakshmi, S. V., Chaitrashree, N., Kumar, S. S., Shetty, N. P., & Giridhar, P. (2021). Fruits of Ixora coccinea are a rich source of phytoconstituents, bioactives, exhibit antioxidant activity and cytotoxicity against human prostate carcinoma cells and development of RTS beverage. Journal of Food Processing and Preservation, 45(7), e15656. https://doi.org/10.1111/JFPP.15656

Siyum, Z. G. (2020). Tropical dry forest dynamics in the context of climate change: syntheses of drivers, gaps, and management perspectives. In Ecological Processes (Vol. 9, Issue 1, pp. 1-16). Springer. https://doi.org/10.1186/s13717-020-00229-6

Tena, N., & Asuero, A. G. (2020). Antioxidant capacity of anthocyanins and other vegetal pigments. In Antioxidants (Vol. 9, Issue 8, pp. 1-3). https://doi.org/10.3390/antiox9080665

Lean Manufacturing Implementation in a Protective Mask Production Process: A Case of Study in Quito

Ricardo Salazar

Grupo de Investigación en Ingeniería, Productividad y Simulación Industrial (GIIPSI), Universidad Politécnica Salesiana, Ecuador
Orcid: https://orcid.org/0009-0002-5111-7279

William Quitiaquez

Grupo de Investigación en Ingeniería, Productividad y Simulación Industrial (GIIPSI), Universidad Politécnica Salesiana, Ecuador
Orcid: https://orcid.org/0000-0001-9430-2082

Isaac Simbaña

Grupo de Investigación en Ingeniería Mecánica y Pedagogía de la Carrera de Electromecánica (GIIMPCEM), Instituto Superior Universitario Sucre, Ecuador
Orcid: https://orcid.org/ 0000-0002-3324-3071

Patricio Quitiaquez

Grupo de Investigación en Ingeniería, Productividad y Simulación Industrial (GIIPSI), Universidad Politécnica Salesiana, Ecuador
Orcid: https://orcid.org/0000-0003-0472-7154

Introduction

Face masks have been important to the personal protection against the COVID-19 pandemic, in different fields such as academic, industrial, and others., The dominant factors in mask performance are currently being investigated, including the thickness and filling rate of melt-blown fibers for a filtering layer (Shi et al., 2021). Masks are manufactured with nonwoven materials, such as spunbond (S) and melt-blown (M), which are most often utilized in composite form, in spunbond - melt-blown - spunbond type structures designated as SMS fabric (Hutten, 2015).

The fast spread of COVID-19 is driven by a major route of person-to-person transmission via viral saliva droplets (> 10 μm) and aerosols (<10 μm), which infected people release into the air when they breathe, talk, cough, or sneeze. Viral aerosols less than 5 μm in diameter are critically dangerous, as they remain suspended in the air for long periods and can reach the lower

respiratory tract of a susceptible host (Kutter et al., 2018). Wearing a protective mask is fundamental to avoid propagation of the virus, as Leung et al. (2020) demonstrated when stating protective mask use reduced viral transmission from 30 % of positive cases to 0 %, at droplet diameters less than 5 μm and from 40 % of positive cases to 0 % in aerosols with droplet diameters above 5 μm. Drewnick et al. (2021) indicated that surgical masks and KN95 have a higher than 80 % for small particles, between 30 to 250 nm, compared to handcrafted masks, which only efficiently filter large particles from 0.5 to 10 μm.

The efficiency of the masks is due to the unique, single-step melt-blown process to obtain fibrous nonwoven membranes from polymeric resins, with an average fiber diameter from 1 to 10 μm (Hassan et al., 2013). However, by modifying the processing parameters, it has been possible to obtain fibers up to 36 nm (Soltani and Macosko, 2018). Masks are already part of people's daily, but by reusing them after 3 days, their filtration efficiency decreases rapidly, approximately 12%, and by continuing to reuse them for another four days, the mask filtration efficiency drops drastically to 55% (Wu et al., 2021).

Sterilization as a method of mask reuse is carried out with vaporized hydrogen peroxide (VHP) and it is the only method currently approved by the U.S.A. Food and Drug Administration (FDA). By applying VHP, the level of hydrogen peroxide decreased to 0.6 ppm, below the safe limit of 1 ppm for 2 hours after treatment, and became undetectable after 3 hours. Nevertheless, the VHP treatment has several limitations, including the cost of the technology, degradation of the elastic bands, and organic waste deactivation of the hydrogen peroxide. Due to the decrease in filtration efficiency over time and the challenge of reuse, it is necessary to change the mask at least in 3 days and at most in 7 days (Ju et al., 2021).

The World Health Organization (OMS) recommends the use of masks in public and private spaces, leading to an increase in demand and greater production by specialized companies in mask manufacturing. The case study is a company in the city of Quito, where the production of surgical masks tripled. Before the pandemic, the annual production was 9'000 000 units and now the annual production is 27'000 000 units. KN95 masks were recently introduced with an annual production of 2'880 000 units. This information coincides with Ardusso et al. (2021), indicating that the monthly mask production in the Colombian plastic industry increased from 2 to 10 million surgical masks and 60,000 to 100,000 units for N95 masks, affirming the trend in South America to increase mask production. Considering the current demand as well as the production, it is necessary to implement the Lean Manufacturing (LM) methodology in the company that manufactures the masks. Bhadu et al. (2022) state that the main objective of LM is to implement a philosophy of continuous improvement that allows companies to

reduce costs, improve processes, and eliminate waste to achieve customer satisfaction and maintain profit margins.

There are direct benefits of lean tools in the textile industry, as Demirci and Gündüz (2020) demonstrated, by combining the techniques of value stream mapping (VSM) with the time measurement method for universal system analysis. By eliminating non-value-added activities and standardizing the movements, it was observed that the production time reduced at a rate of 56 %, and also the duration of non-value-added activities improved by 57 %. By applying the VSM tool in a Peruvian textile company, it managed to reduce the rework by a defect from 13.12 to 4.23 %, decreased the processes that were delayed from 18.49 to 9.61 %, and increased the productivity index of the cutting area from 0.38 to 1.16 (Alanya et al., 2020). Guleria et al. (2021) applied LM to the production of filter media and obtained a reduction in the rejection of the final product from 12 to 4%. Likewise, in the finishing and dyeing of textiles, a reduction of up to 8.14% in reprocesses has also been achieved (Romero-Sánchez et al., 2019).

The objective of the present study is to improve the melt-blown area of a company dedicated to protective mask manufacturing by implementing the Lean Manufacturing methodology. It is important to mention that this area started operations in October-November 2020 and the line is not adequately balanced to work with synergy with the subsequent areas. The document is divided as follows: Methodology describes the activities in the field data collection process. The Results present the calculated values and the presentation of comparative Figures. Finally, Conclusions synthesize the information in an objective way for the evaluation of the fulfillment of the proposed objective.

Materials and Methods

The methods to be used are mainly exploratory and descriptive, based on the collection and analysis of data from the melt-blown area, through written and/or digital documents containing specialized bibliography, and interviews with people involved in the production process of the masks. It also includes applied research, understood as an efficient alternative response to the current pandemic need and the industrial situation of health and biosafety.

Approach and Variables

In an approach based on the lean manufacturing philosophy, any use of resources or actions that do not generate value for the customer is considered waste and should be eliminated. This means that with Lean, only what the customer asks for is produced (Tissir et al., 2020). Therefore, the variables considered are two, production and enterprise. The indicators for production are Operating times and the reduction of

waste. For the company variable, they are Quality and competitiveness. The results of the documentary and bibliographic research will contribute to the necessary data for the thematic development and its consequent theoretical-practical inferences that allow obtaining the necessary conclusions.

Collection of information

For health research, it is common to use the Odds Ratio (OR) as a way of expressing the possibility of the occurrence of an event of interest or the presence of exposure (Cerda et al., 2013). A systematic review and meta-analysis of a total of 5178 eligible articles in databases and references from different countries showed that the use of a facemask is associated with a significant reduction in the risk of COVID-19 infection (OR = 0.38; 95 % CI: 0.21-0.69) (Li et al., 2021). This means that the chance of occurrence of infection is 38 % with a confidence interval of 95 %. The results show a concordance with the previous findings of Leung et al. (2020) on the reduction of infection when wearing a facemask. The different types of masks and their effectiveness in protection against the SARS-CoV-2 virus vary depending on the material, although fabric masks are more comfortable and economical in the long term, the person who wears them ends up being just as exposed, since their filtration efficiency for particles smaller than 0.3 µm is 0%. Nonwoven fiber masks have a higher filtration efficiency, ranging from 60 to 95%, with KN95 having the highest efficiency; a more detailed summary is presented in Table 1.

Table 1

Comparison between the different masks (Das et al., 2021)

Type of mask	Material	Efficiency	Purpose	Reusable
Fabric	Common textiles, generally cotton, and polyester	0 % on particles smaller than 0.3 µm	Dust particles, viruses, and bacteria.	Yes
Surgical	Nonwoven fabric	60 to 80 % on particles smaller than 0.3 µm	Dust particles, pollen, viruses, and bacteria.	No
KN95	Non-woven polypropylene fabric	80 to 95 % on particles smaller than 0.3 µm	Dust particles, pollen, virus, and bacteria aerosols	No

Melt-blown fusion is a simple, one-step process from a polymer resin. The melt-blown configuration generally consists of an extruder, metering pump, melt-blown die assembly, and drum manifold (Sarbatly et al., 2021), as shown in Fig 1.

Figure. 1
Melt-blown fiber production process
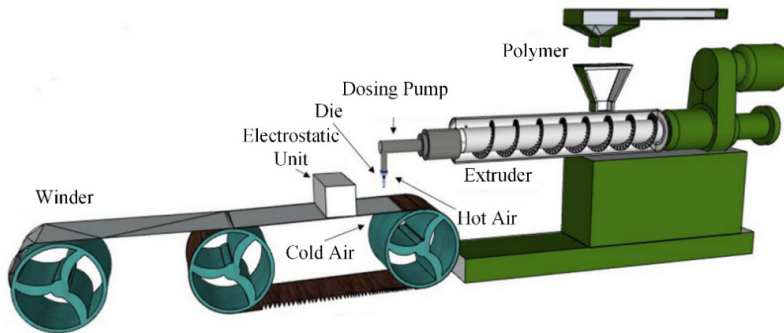
Current situation

The company's production is 27'360 000 surgical masks and 2'880 000 KN95, resulting in a total of 30'240 000 units produced. For this production volume,

Table 2 summarizes the operating conditions of the melt-blown area, which are: two 12-hour shifts, approximately 44 rolls per week, with a 14 % waste rate, and 2-day cleaning of the equipment.

Table 2
Melt-blown Production Summary

Parameter	Operation
Working Day	Double shift from Monday to Friday from 7:30 a.m. to 7:30 p.m. and from 7:30 p.m. to 7:30 a.m.
Quantity	0.5 rolls per hour of melt-blown fiber
Weight	31.3 kg per roll
Waste	4.5 kg per roll
Cleaning	Friday in the first shift 7:30 am to 7:30 pm

In the production process, the characterization of the raw material is carried out in an accredited laboratory to know the state of the raw material and the local environmental conditions. The production process starts with the mixing of polypropylene pellets with a fluidity index of 1500 (PP HSD 1500) and electret masterbatch pellets (PP ZJ101) in a proportion of

97 and 3 %, respectively. The mixing takes approximately 15 minutes and the start-up process takes 2 hours, because of the heating of the zones until they reach 270 ˚C; from then on, the machinery works until the last day. At the end of the process, we wait for the parts to lower their temperature to 65 ˚C for their disassembly and transfer to the washing area.

The cleaning is done in 2 stages, the first stage is physical and starts with the disassembly of the mold when it has cooled down and a manual cleaning of the mold orifices. The chemical stage consists of placing the mold in an oven at 480 ˚C for calcination of the polypropylene (PP) and subsequently washing it with a sodium hydroxide solution for 4 hours in an ultrasound. Finally, the residues are marketed to plastic industries. The storage of both raw materials and the final product is at room temperature, however, this environment is not controlled, since it depends on the environmental conditions of the surroundings, which change throughout the day, varying the temperature and relative humidity.

Operating Conditions

A batch statistical hypothesis test is performed to know if the densities obtained experimentally contain the true value of the population mean, and if they are within or outside a confidence interval; the proposed interval is 90 %. The free software *R Studio* is used for statistical analysis. The significance level is 0.1, since the sample is less than 30, the *t student* statistical test is used and the decision rule is: if the calculated *t* is less than the critical *t*, the null hypothesis is accepted. Hence, the null hypothesis states $H0 = \mu$, while the alternative hypothesis is $H1 \neq \mu$. The equation (1) utilized for the *t*-student statistic is presented below:

$$t = \frac{\bar{x}\text{-}\mu}{s/\sqrt{n}} \qquad (1)$$

Where $\bar{x}$ is the average of the obtained data, μ is the population, s is the standard deviation, and n is the total amount of data. To control the output quality of the product, it should be understood that the phenomenon that governs the production process is the melting of polypropylene. Therefore, operating pressure and temperature ranges should be established as a function of the initial density and environmental conditions, and with the Spencer-Gilmore equation, it is possible to approximate the operating conditions based on pressure and temperature. The general equation (2) is then presented:

$$(P + \pi)(V\text{-}W) = R'T \qquad (2)$$

Where π, W, and R' are constants, in the case of PP the values are 3080 atm, 0.70 cm/g, and 2, respectively. Then, the modified equation would be the following (Foster et al., 1966):

$$(P + 3080)(V\text{-}0.7) = 2T \qquad (3)$$

Equation 2 describes the behavior of polypropylene in the liquid state, whose means is above the melting temperature of the polymer. The pressure (P) is the ratio of the operating pressure to the atmospheric pressure, the units required are atmospheres. The specific volume (V) is an intensive property necessary in order not to depend on the amount of raw material to be used in the process, and the temperature (T) is absolute. For a better prediction of the behavior of the material, it will be operated under the same conditions of the flow index, which are a temperature of 230 ˚C and an operating pressure of 0.34 bar (5 psi), then the absolute pressure is

1.34 atm. With these conditions the specific volume of the molten polypropylene is calculated, clearing from equation (3) resulting in equation (4):

$$V = \frac{2T}{P + 3080} + 0.7 \qquad (4)$$

The result of the specific volume is 1.0265 cm³/g, this value is the one to be obtained in the production process. Now, the suggested operating pressure is 5 psi based on 1 atm of atmospheric pressure. In Quito, the atmospheric pressure is lower, it is 0.71 atm, therefore, a new operating pressure must be found with the new conditions. The absolute pressure (P_{abs}) is obtained by adding the atmospheric pressure (P_{atm}) to the gauge pressure (P_{gauge}), as shown in equation (5):

$$P_{abs} = P_{atm} + P_{gauge} \qquad (5)$$

The absolute pressure is 1.34 atm and the atmospheric pressure in Quito is 0.71 atm, clearing the gauge pressure gives 0.63 atm, for instance, 9.26 psi, then the gauge pressure in the process must be increased to 9 psi. The operating temperature must be changed to obtain the flow rate condition. Currently it is 225 ± 5 ˚C, when the operating temperature must be increased to 230 ± 5 ˚C. The variation of ± 5 ˚C is based on

the pro-average temperature changes recorded in Quito. In addition, the process during the transformation of the raw material is subject to high temperatures and the presence of oxygen, it is there where damage occurs at the molecular level that degrades the material, thus causing non-uniformity in the grammage of the fabric, from here derives the presence of crystals, brittle fabric and low tensile strength of the fabric.

Problems can occur if the material is kept at the processing temperature for an excessive amount of time, for instance, during a machine stop. These problems reduce when using thermoplastic solid binding resins, polyamides, polyethylene, EVA, PVC, and thermosets, such as phenolic resins (Pintea and Manea, 2019), since they favor the bonding, transformation, and finishing of the melt-blown fabric. The international standard for nonwovens is ISO 9073 with its 18 sections, in Ecuadorian legislation, is INEN NTE-ISO 9073. However, this standard is an identical translation of the same international standard with its 18 sections. The quality control in the fabric is the grammage that must be in a range of 20 to 30 g/m³ (gsm) for use in masks. Currently, this range is met, ensuring air filtration and retention of external agents within the fiber mesh of the melt blown.

Results

Quality Control of Raw Materials

One of the initial findings in the raw material was that the physical charac-

teristics of virgin polypropylene and electret masterbatch are not constant, so currently the physical characteriza-

tion of the flow index is performed in specialized laboratories. In addition, at the time of receipt of the raw material, there is no documented support for the specific conditions of the received batch of PP. The proposal to improve the reception of raw materials is to have parameters and acceptance ranges. Table 3 shows the polypropylene parameters, in addition to requesting the Certificate of Analysis (COA) from the supplier.

Table 3
PP quality parameters

Property	Test	Conditions	Units	Values
Density	ISO 1183	23 °C	g/cm³	0.9125 ± 0.0018
Flow Index	ISO 1183	230 °C / 2.16 kg	g per 10 min	1500 ± 100
Melting Point	DSC	---	°C	155 - 175
Ash Content	ISO 3451	850 °C / 60 min	%	≤ 0.03
Volatile Components	ISO 787	105 °C	%	≤ 0.03
Water Amount	---	105 °C / 2 hours	%	≤ 0.05

Note: DSC is Differential Scanning Calorimetry

At the beginning of the process, it is important to know the value of the density of the polypropylene to adjust the melting temperature ranges. The density measurement does not require specialized equipment so it was possible to do it *in situ*. The density of the 4 different batches of raw material that were acquired together with the melt-blown machinery in October 2020 was characterized. The procedure to obtain this measurement is described in the ISO-1183 tests (ISO, 2019), and the results are presented in Table 4.

Table 4
The density of the raw material

Description	Batch 01 [g/mL]	Batch 02 [g/mL]	Batch 03 [g/mL]	Batch 04 [g/mL]
Virgin polypropylene	0.9106	0.9122	0.9142	0.9127
	0.9104	0.9127	0.9144	0.9132
	0.9101	0.9121	0.9147	0.9124
Partial Average	0.9104	0.9123	0.9144	0.9128
Global Average	0.9124			

For the critical t is necessary the degrees of freedom (d_f), which is calculated as $n - 1$. The results for each of the batches are presented in Table

5. Batches 01 and 03 do not enter the confidence interval, Batch 01 for being below, and Batch 03 for being above the confidence interval. Now with the quality control chart made in IBM SPSS, the average and distribution of the values obtained for the densities are presented, as well as the upper control limit (*UCL*) and lower control limit (*LCL*).
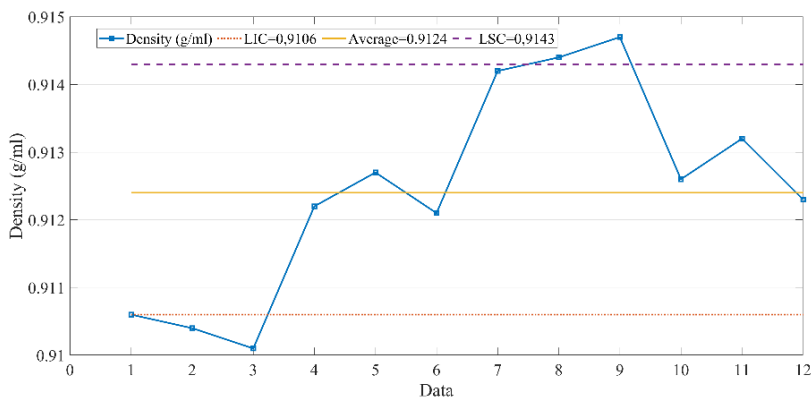
Table 5
Results of hypothesis testing by batch

Parameters	Batch 01	Batch 02	Batch 03	Batch 04
$\bar{x}$	0.9125	0.9125	0.9125	0.9125
μ	0.9104	0.9123	0.9144	0.9128
s	0.002517	0.000321	0.000252	0.000404
n	3	3	3	3
t-calculated	-14.6826	-0.8980	13.3061	1.1429
df	2	2	2	2
t-critical	± 2.91999	± 2.91999	± 2.91999	± 2.91999
Decision	H_0 Rejected	H_0 Accepted	H_0 Rejected	H_0 Accepted

Figure 2 shows values outside the upper and lower control limits, of which points 1, 2, and 3 belong to Batch 01 and points 8 and 9 belong to Batch 03. With these two statistical and graphical evidences, there could be no production of the melt-blown fabric with these batches.

Figure 2
Distribution of raw data

However, it is not economically feasible to discard two lots of purchased raw material, so by mixing the four lots in equal proportions the result is already within the proposed confidence interval of 0.1, as presented in Table 6.

Table 6
Results of global hypothesis tests

Parameters	Results
μ	0.9125
$\bar{x}$	0.9124
s	0.00165
n	4
t-calculated	-0.0303
d_f	3
t-critical	± 2.3534
Decision	H_0 accepted

With these results, the new range of acceptance of the product is defined as the upper control limit (UCL) a maximum density of 0.9144 g/ml, and the lower control limit (LCL) a minimum density of 0.9104 g/ml. It can be seen in Figure 3 that there is still a tendency for two Batches to be at the extremes of the required density. However, they enter the confidence interval since the average value is close to the mean of the density required for operation.

Figure 3
Distribution of new data
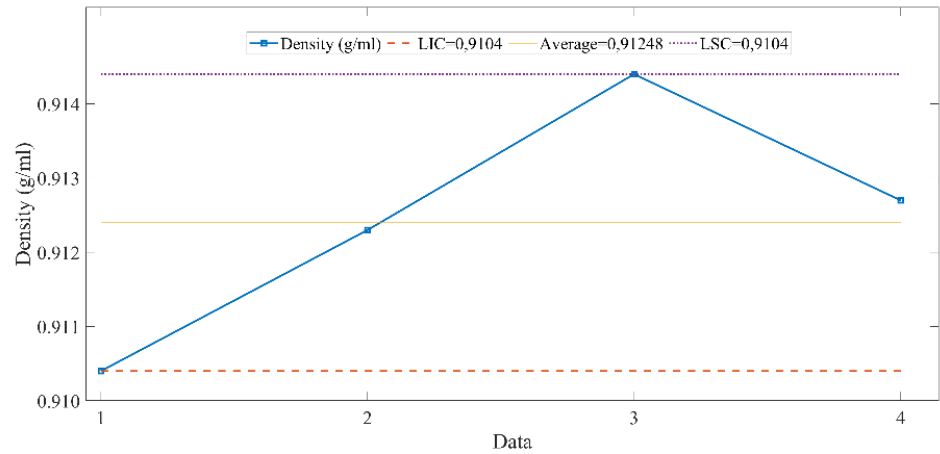
The density of each Batch of raw material to be used must be within the significance level of 0.1 since the melting temperature implies providing enough energy for the chains to move as a whole. Polypropylene, being a semi-crystalline material, is composed of both amorphous zones, branched structures, and crystalline or compact zones linear structures. Consequently, the energy to break the bonds in the compact zones is higher (Kar'kova et al., 2019), with this in mind the proportionality between density and melting temperature can be established, as directly proportional to the linear crystallinity and inversely proportional to branched structures.

Another finding in the raw material was the storage conditions of the polypropylene, currently, the bags are covered inside the facilities. Nevertheless, they still do not have control over environmental variations such as light, humidity, and temperature. The raw material is susceptible to degradation when exposed to heat and UV radiation, causing a network of fine cracks and the longer the exposure time the more severe the internal damage of the raw material (Pathak et al., 2021), this damage at the molecular level causes non-uniformity in the weight of the fabric. The proposal for improvement is to adapt a space to control the storage conditions, in which there are temperature and humidity records; the use of a thermo-hygrometer can help for this purpose. Concerning exposure to UV radiation, simply providing physical protection from sunlight and artificial light is sufficient to ensure the quality of the raw material.

The cleaning of the molds of the current 2-stage procedure should be maintained but the change should be made in the washing solution, from sodium hydroxide to decalin, decahydronaphthalene, which is a bicyclic hydrocarbon and is used as an organic solvent (Troughton, 2008). The amount of dissolved polypropylene, as a solute, in the final washing solution differs between sodium hydroxide and decalin, where each week the parts to be washed were separated between decalin and sodium hydroxide, obtaining an average percentage by weight of solute in sodium hydroxide of 1.15 %, while in decalin it is 4.18 % as shown in Figure 4. The percentage of solute in decalin is four times higher than that contained in sodium hydroxide, therefore, it turns out that the solute is completely dissolved in decalin and partially in sodium hydroxide. Hence. the utilization of the organic solvent causes an improvement in the washing stage with a decrease in the working time.

Figure 4
Percentage of solute
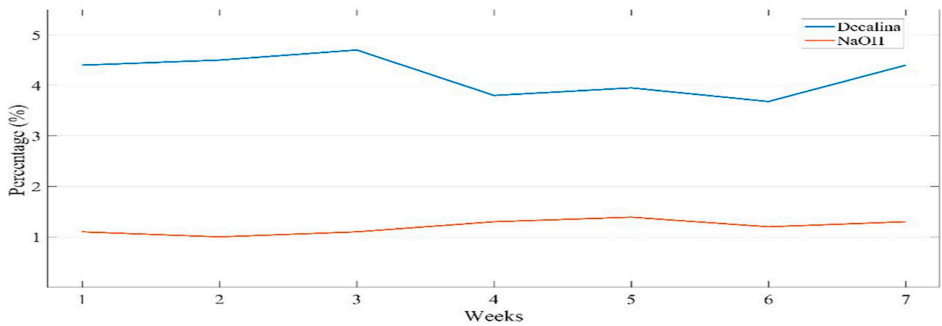
Final indicators

The stages that give the production rate are the conditions of the raw material, as well as the control in the process, besides the cleaning of the equipment should be as short and effective as possible. With these results, the following improvements in production time are obtained. The start of production is given by the preparation of the raw material and the heating of the melting and blowing zones. Table 7 presents the optimizations, showing that the start of the process is reduced by 55.56 % since with the initial characterization the machinery is programed and the trial-and-error process is eliminated. Now, with the range of temperatures and operating pressure, unexpected or unscheduled downtime is reduced by 62.50%.

Table 7
Optimization of production times

Process	Then [hours]	Now [hours]	Optimized [%]
Process Startup	2.25	1	55.56
Daily Contingencies	2	0.75	62.50
Weekly Cleaning	8	5	37.50

Scheduled downtime for cleaning is reduced by 3 hours, being 37.50 %, this is due to the change from an aqueous cleaning solution to an organic solvent exclusive for polypropylene. With the change from sodium hydroxide solution to decalin, only one hour would be needed for the dismountable parts to be immersed in the ultrasound. The solid waste of finished product decreases due to the optimization of both the daily contingencies, less raw material expense at the start of the process and stabilization. The reduction was 1.42 kg/roll, representinga 31.56 % for the initial waste of 4.50 kg/roll. Each roll weighs an average of 31.30 kg, as presented in Table 2, and with the present optimization,

the waste was reduced from 14.38 to 9.84 %. The optimizations are summarized in Figure 5, wherein in each process there is an improvement in both, time and amount of waste.
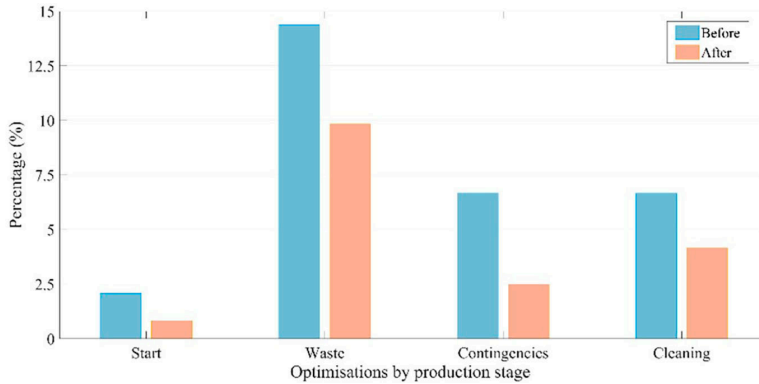
Figure 5
Overall results

Figure 6 presents the values in hours of normal production and the new production applying Lean Manufacturing. With the reduction of 50.68 % of the times in the different production stages, there was a reduction from 18.25 to 9 hours, which caused the net production of melt-blown rolls to increase from 101.75 to 111 hours, representing an increase of 9.09 % concerning the normal production hours. The implications for the organization of these improvements range from increased stock for sales to supply the demand for masks and/or a reduction in working hours to optimize resources.

Figure 6
Melt-blown production
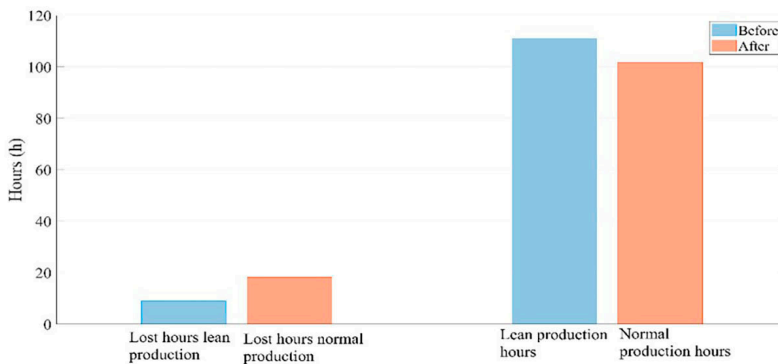
Currently, in the melt-blown area, there are two technical operators and due to the unforeseen events of the machinery, it is necessary to be aware of the production. By the standardization of the process, it is possible to train an operator, and thus optimize the human and economic resources of the company.

Table 8 shows the economic optimization focused on human resources salaries. The net saving is USD. 400 per month, i.e., a savings of 33.33 %. This saving, together with compliance with international standards, not only guarantees the quality of filtration but also improves competitiveness by presenting better masks to the market, as well as the possibility of exporting and being a local supplier of raw material with melt-blown fabric.

Table 8
Economic optimization

Status	People	Position	Salary [USD]	Total Monthly Cost [USD]	Optimization [%]
Then	2	Technical	600	1200	33.33
Now	2	Operator	400	800	

Conclusions

Regarding the concept of Lean manufacturing, which is the identification of waste and its elimination or reduction through the continuous improvement of the process, wastes of time, resources, and products were determined. The reason is the lack of acceptance parameters of raw materials and standardized parameters of finished products. Therefore, by identifying waste, the melt-blown area for the production of face masks was improved by characterizing raw materials, technical controls, and specification of operating conditions.

The production depends on the raw material and the working conditions, especially in the area of raw materials; the physical characteristics of polypropylene are not constant between batches., For this reason, only 2 Batches of the 4 existing ones could be used for the production of the melt-blown fabric, however, a combination between the four Batches was achieved, guaranteeing the adequate characteristics for the production. The data presented show the relationship between the working conditions and the environmental conditions. In Quito, with an atmospheric pressure of 0.71 atm, the working pressure increases from 5 psi to 9.26 psi, an equivalent total pressure of 1.34 atm. With this new working condition, the flow rate necessary to obtain a melt-blown fabric with constant characteristics is ensured.

With the described changes, process start-up times improved by 55.56

%, unexpected events were reduced by 62.50 %, and cleaning was optimized by 37.50 % of the total washing time. In addition, product waste is reduced by 4.54 % and the savings in economic resources is USD 400 per month.

The optimization of economic resources should be the subject of further investigations, focusing on the cost of raw materials, production, and finished product, based on current and future market demand.

References

Alanya, B., Dextre, K., Nunez, V., Marcelo, G., and Alvarez, J. Improving the cutting process through lean manufacturing in a peruvian textile SME, In: *IEEE International Conference on Industrial Engineering and Engineering Management,* 1117-1121. IEEM, Singapore (2020). https://doi.org/10.1021/acs.iecr.0c06232

Ardusso, M., Forero-López, A., Buzzi, N., Spetter, C., and Fernández-Severini, M. (2021). COVID-19 pandemic repercussions on plastic and antiviral polymeric textile causing pollution on beaches and coasts of South America. *Science of The Total Environment, 763.* 144365. https://doi.org/10.1016/j.scitotenv.2020.144365

Bhadu, J., Kumar, P., Bhamu, J. et al. (2022). Lean production performance indicators for medium and small manufacturing enterprises: modelling through analytical hierarchy process. *International Journal of System Assurance Engineering and Management, 13.* 978-997. https://doi.org/10.1007/s13198-021-01375-6

Cerda, J., Vera, C., and Rada, G. (2013). Odds ratio: aspectos teóricos y prácticos. *Revista médica de Chile, 141*(10). 1329-1335. https://doi.org/10.4067/S0034-98872013001000014

Das, S., Sarkar, S., Das, A., Das, S., Chakraborty, P., and Sarkar, J. (2021). A comprehensive review of various categories of face masks resistant to Covid-19. *Clinical Epidemiology and Global Health, 12.* 100835. https://doi.org/10.1016/j.cegh.2021.100835

Demirci, O., and Gunduz, T. (2020. Combined application proposal of value stream mapping (VSM) and methods time measurement universal analysis system (MTM-UAS) methods in textile industry. *Journal of Industrial Engineering, 31*(2). 234-250. https://doi.org/10.46465/endustrimuhendisligi.728061

Drewnick, F., Pikmann, J., Fachinger, F., Moormann, L., Sprang, F., and Borrmann, S. (2021). Aerosol filtration efficiency of household materials for homemade face masks: Influence of material properties, particle size, particle electrical charge, face velocity, and leaks. *Aerosol Science and Technology, 55*(1). 63-79. https://doi.org/10.1080/02786826.2020.1817846

Foster, G., Waldman, N., and Griskey, R. (1966). Pressure-volume-temperature behavior of polypropylene. *Polymer Engineering and Science, 6*(2). 131-134.

Guleria, P., Pathania, A., Bhatti, H., Rojhe, K., and Mahto, D. (2021). Leveraging Lean Six Sigma: Reducing defects and rejections in filter manufacturing industry. *Materials Today: Proceedings, 46*(17). 8532-8539. https://doi.org/10.1002/pen.760060208

Hassan, M., Yeom, B., Wilkie, A., Pourdeyhimi, B., and Khan, S. (2013). Fabrication of nanofiber melt-blown membranes and their filtration properties. *Journal of Membrane Science, 427.* 336-344. https://doi.org/10.1016/j.memsci.2012.09.050

Hutten, I. Handbook of Nonwoven Filter Media, Oxford: Elsevier Science & Technology (2015).

ISO 1183-1: 2019: Plastics - Methods for determining the density of non-cellular plastics. Part 1: Immersion method, liquid pycnometer method, and titration method. https://www.iso.org/standard/74990.html

Ju, J., Boisvert, J., and Zuo, Y. (2021). Face masks against COVID-19: Standards, efficacy, testing and decontamination methods. *Advances in Colloid and Interface Science, 292*. 102435. https://doi.org/10.1016/j.cis.2021.102435

Khar'kova, E., Mendeleev, D., Guseva, M. et al. (2019). Structure and Properties of Polymer-Polymer Composites Based on Biopolymers and Ultra-High Molecular Weight Polyethylene. *Journal of Polymers and the Environment, 27*. 165-175. https://doi.org/10.1007/s10924-018-1326-0

Kutter, S., Spronken, M., Fraaij, P., Fouchier, R., and Herfst, S. (2018). Transmission routes of respiratory viruses among humans. *Current Opinion in Virology*, *28*. 142-151. https://doi.org/10.1016/j.coviro.2018.01.001

Leung, N., Chu, D., Shiu, E. et al. (2020). Respiratory virus shedding in exhaled breath and efficacy of face masks. *Nature Medicine, 26*(5), 676-680. https://doi.org/10.1038/s41591-020-0843-2

Li, Y., Liang, M., Gao, L., Ayaz-Ahmed, M., Uy, J., Cheng, C., Zhou, Q., and Sun, C. (2021). Face masks to prevent transmission of COVID-19: A systematic review and meta-analysis. *American Journal of Infection Control, 49*(7). 900-906. https://doi.org/10.1016/j.ajic.2020.12.007

Pathak, A, Zhou, Y., Lecointre, L. et al. (2021). Polypropylene nanocomposites with high-loading conductive carbon nano-reinforcements for multifunctional applications. *Applied Nanoscience, 11*. 493-503. https://doi.org/10.1007/s13204-020-01594-6

Pintea, A., and Manea, D. (2019). New types of mortars obtained by aditiving traditional mortars with natural polymers to increase physico-mechanical performances. *Procedia Manufacturing, 32*. 201-207. https://doi.org/10.1016/j.promfg.2019.02.203

Romero-Sanchez, J., Martinez-Vilchez, R., Galvez-Zarate, C., and Raymundo-Ibanez, C. (2019). Process management model in dry cleaning and fabric finishes applying Lean Manufacturing and Kaizen matrix for the textile sector. In: *39th Central America and Panama Convention*, 1-6. IEEE, Guatemala (2019). https://doi.org/10.1109/CONCAPANXXXIX47272.2019.8976988

Sarbatly, R., Sariau, J., and Alam, M. (2021). Advances in nanofiber membrane. *Materials Today: Proceedings*, *46*. 2118-2121. https://doi.org/10.1016/j.matpr.2021.05.483

Shi, J., Zou, Y., Wang, J., Zeng, X., Chu, G., Sun, B., Wang, Dan., and Chen. J. (2021). Investigation on Designing Meltblown Fibers for the Filtering Layer of a Mask by Cross-Scale Simulations. *Industrial & Engineering Chemistry Research, 60*(4). 1962-1971. https://doi.org/10.1021/acs.iecr.0c06232

Soltani, I., and Macosko, C. (2018). Influence of rheology and surface properties on morphology of nanofibers derived from islands-in-the-sea meltblown nonwovens. *Polymer, 145*. 21-30. https://doi.org/10.1016/j.polymer.2018.04.051

Tissir, S., El Fezazi, S., and Cherrafi, A. (2020). Industry 4.0 impact on Lean Manufacturing: Literature Review. In: *13th International Colloquium of Logistics and Supply Chain Management*, 1-5. IEEE, Marruecos (2020). https://doi.org/10.1109/LOGISTIQUA49782.2020.9353889

Troughton, M. Handbook of Plastics Joining, 2nd ed., vol. 1. NY: Elsevier Science & Technology Books (2008).

Wu, J., Zhou, H., Zhou, J., Zhu, X., Zhang, B., Feng, S., Zhong, Z., Kong, L., Xing. W. (2021). Meltblown fabric vs nanofiber membrane, which is better for fabricating personal protective equipments. *Chinese Journal of Chemical Engineering, 36*. 1-9. https://doi.org/10.1016/j.cjche.2020.10.022

Mitigation of Cadmium Uptake in Cocoa Seedlings (Theobroma cacao L.) Through Arbuscular Mycorrhizal Symbiosis of Contaminated Soils

Jairo Jaime-Carvajal
Universidad Politécnica Salesiana, (Ecuador)
Orcid: https://orcid.org/ 0000-0002-8728-8195

Jaime Naranjo-Moran
Universidad Politécnica Salesiana, (Ecuador)
Orcid: https://orcid.org/0000-0002-4410-9337

Angela Pacheco
Universidad Politécnica Salesiana, (Ecuador)
Orcid: https://orcid.org/0000-0002-7417-7218

Introduction

In Ecuador, cocoa is a very important crop, both economically and culturally. However, the presence of heavy metals such as cadmium (Cd) in the soil and in cocoa plants raises significant concerns. Studies have shown that Ecuadorian agricultural soils are contaminated by cadmium, with concentrations that can affect cocoa quality (Pernía et al., 2021).

Cadmium uptake in cocoa is influenced by the diversity of arbuscular mycorrhizal fungi present in the soil, which in turn affects plant growth (Vallejos-Torres et al., 2021). The high concentration of Cd in cocoa beans has raised concerns among Ecuadorian producers who export to international markets (Unda et al., 2021).

It is crucial to understand how Cd affects cocoa quality and safety, considering that Ecuador is recognized for its fine aroma cocoa worldwide (Villacis et al., 2022). The genetic diversity of cocoa in Ecuador, especially the "Nacional" or "Arriba" variety, is an important asset in the cocoa value chain in the country (Villacis et al., 2022).

The sustainability of cocoa agroforestry systems in Ecuador is also influenced by factors such as management intensity and the diversity of non-vascular epiphytes in cocoa plantations

(Andersson & Gradstein, 2005; Neira, 2016). The genetic variability of cacao populations in Ecuador has been studied using genetic markers, which has revealed interesting patterns of genetic diversity (Nieves-Orduña et al., 2021). The genetic diversity of cocoa in Ecuador, including ancestral varieties such as Criollo, is favored by the presence of mycorrhizae, which helps to conserve valuable genetic material and improve cocoa quality in new varieties (Solorzano et al., 2009).

Mycorrhizae are key to cocoa crops in Ecuador by improving nutrient and water uptake by cocoa plants. These symbiotic associations between plant roots and arbuscular mycorrhizal fungi are essential for the optimal development of cocoa plants, especially in soils degraded or contaminated by heavy metals such as Cd (Tezara et al., 2016).

The presence of a high diversity of arbuscular mycorrhizal fungi in the soil can positively influence Cd uptake and plant growth of cocoa, which contributes to mitigate the negative effects of heavy metal contamination (Zug et al., 2019).

The quality of cocoa cultivation in Ecuador benefits from the presence of mycorrhizae, as these associations improve plant resistance to diseases and environmental stresses, which in turn contributes to the production of high-quality cocoa appreciated worldwide for its distinctive organoleptic characteristics. In a context where Cd contamination in cocoa crops is a growing concern, mycorrhizae play a crucial role in influencing the uptake and mobilization of this heavy metal in cocoa plants. Studies have shown that the presence of mycorrhizae can re-duce cadmium accumulation in cocoa beans, which is critical to ensure food safety and quality of cocoa produced in Ecuador (Zug et al., 2019).

Therefore, the objective of this research is to evaluate the impact of arbuscular mycorrhizal symbiosis on the attenuation of Cd uptake in T. cacao L. seedlings grown under greenhouse conditions.

Materials and Methods

Plant material: Grafted seedlings of national cocoa from the National Institute of Agricultural Research (INIAP) located at Km. 26 Vía Duran -Tambo, Virgen de Fátima parish, Yaguachi canton in the province of Guayas were used.

Experimental design: A completely randomized experimental design with interaction was implemented to evaluate the effect of Cd on the growth and physiology of plants of T. cacao L. The design included four levels of Cd (0, 2, 4 and 6 mg/kg) with six replicates per level. The response variables evaluated were: plant height, number of leaves, aerial biomass, root biomass, soil pH, soil electrical conductivity and quantification of Cd uptake.

$$DCA = \gamma = \mu + \delta + \varepsilon$$

Mitigation of Cadmium Uptake in Cocoa Seedlings (Theobroma cacao L.) Through Arbuscular Mycorrhizal Symbiosis of Contaminated Soils

127

Sample Preparation & Analysis

Seedlings were transplanted into a substrate composed of chaff and sand in a 1:1 (v/v) ratio, which had an electrical conductivity of 0.561 dS m-1 and a pH of 6.90. After the establishment of the trials, the plants were irrigated for two weeks with a modified Steiner's nutrient solution and water, which contained 0, 2, 4 and 6 ppm of cadmium nitrate (Cd($NO_3)_2$). The substrate was maintained at field capacity by applying 70 ml of the above solutions three times per week.

Evaluation of agronomic parameters

To evaluate both root and aerial biomass, roots are washed with distilled water and dried in an oven at 80 °C for 24 hours or until constant weight, recording the dry weight as root biomass (g/plant). In the case of aerial biomass, stem and leaves are separated, weighed on an analytical balance (wet weight) and dried in an oven at 80 °C for 24 hours or until constant weight, recording the dry weight as aerial biomass (g/plant).

Biomass (g/plant) = Initial humid weight (g/plant) - Final dry weight (g/plant)

Separation of spores and identification of abuscular mycorrhizae

To separate arbuscular mycorrhizal spores according to the methodology of wet sieving and decantation of spores by their density (Furlán et al., 1980), the sediment from the 45 um sieve is dissolved in water with tween 20 and 50% sucrose for 5 minutes at 3000 rpm in a centrifuge, 1980), the sieve sediment 45 um dissolved in water with tween 20 and 50% sucrose for 5 minutes at 3000 rpm in a centrifuge, collected in a 50 ml falcon tube, and then characterized the spores at the taxonomic level using morphological catalogs of spores obtained from INVAM, according to the morphological attributes of the spores present, such as color, shape, texture, size, mucilage, walls, presence of ornamentation.

Root staining: At the end of the experiment, roots were extracted from seedlings to analyze the presence of fungal structures (hyphae, vesicles or arbuscules), a method modified by Phillips and Hayman (1970). Secondary roots were immersed in 10% potassium hydroxide for the first decolorization, then the second decolorization with 3-4% hydrogen peroxide for 24 hours, followed by washing and immersion with 1% hydrochloric acid and staining with trypan blue in 0.02% lactic acid. Finally, they were observed under the microscope (40x objective) to evaluate the percentage of mycorrhizal colonization, using 10 rootlets per object-to plate and fixed with lactoglycerol (lactic acid, glycerol, distilled water in a 1:1:1 ratio), to demonstrate mycorrhizal colonization.

Determination of cadmium: For quantifying Cd concentrations, approximately 0.25 g of soil, 0.5 g of roots and 1 g of leaves were weighed, 7 ml of nitric acid and 3 ml of hydrogen peroxide were added, and the samples were placed in Milleston Connect microwave beakers. Ramp heating was performed to 180 °C for 10 min, the temperature was held constant for 15 min, and finally the

samples were allowed to cool for an additional 15 min. Samples were transferred to 25-ml volumetric flasks, volumetrically diluted with HPLC water, and filtered with 22 μm syringes and microfilters prior to analysis by graphite furnace atomic absorption spectrophotometry (Table 1). A total of 96 samples were analyzed

Table 1

Instrumental conditions of Graphite Furnace Atomic Absorption Spectrometry (GFAAS)

Wavelength	228.80 nm
Calibration curve	0.25 ug/L
	0.50 ug/L
	1.0 ug/L
	2.0 ug/L
	5.0 ug/L
Fuel	Argon
Matrix Modifier	0.015 mg Pd + 0.01 mg Mg (NO3)2
Background Corrector	On

In this study, the limit of detection (LOD) of 0.006 mg/kg was established based on the variability of the blank samples, calculated as three times the standard deviation of the average blank concentration value. To determine the limit of detection (LOQ), samples with known low concentrations of cadmium were analyzed in triplicate, resulting in 0.1 mg/kg. Finally, the coefficient of correlation ($R2$) was established with a value of 0.998811 following the methodology established by the EPA-3051A method.

Data analysis

Data processing and analysis were performed using RStudio software version 4.3.2 (2023-10-31 ucrt). Means and standard deviations were calculated for all measured variables, including cadmium solution in soil, cadmium concentration in roots and leaves of seedlings, bioconcentration factor (BCF), translocation factor (TF), soil pH, electrical conductivity, aerial and root biomass, number of leaves and height of seedlings. Scatterplot matrices with least squares lines were constructed to visualize the relationship between the different variables measured. The least squares lines allowed identifying linear patterns and estimating the slope of the relationship between the variables. Concentration ellipsoids were generated with a 90% confidence level for each variable, which made it possible to identify the regions of greatest data concentration.

Results

Figure 1 explores the relationship between cadmium (Cd) concentration in the soil and several growth variables in cocoa seedlings inoculated with arbuscular mycorrhizal fungi. The data presented are from measurements taken

at different Cd concentrations, represented by the dots in the graph. The distribution of the data for each growth variable at each Cd concentration is visualized by box plots, while the concentration ellipsoids represent the joint variability of the growth variables at each Cd level. The results reveal a positive correlation between Cd concentrations and the growth variables analyzed. This correlation is evident in seedling height, where the 6 mg/kg Cd concentration induces a maximum growth of 9.50 cm, significantly higher than that of the control group. In addition, this Cd concentration generates a considerable increase in the number of leaves. These findings suggest that, within the range of Cd concentrations used in this study, no adverse effects on the growth variables evaluated are observed. In this range, aerial and root biomass reached values of 13.91 g and 6.91 g, respectively, showing a tendency to gradually increase as Cd concentration increases.

Figure 1

Effect of Cd concentration on seedling height, aerial biomass, root biomass and number of leaves of cocoa seedlings with arbuscular mycorrhizae. Scatter plots show the relationship between the response variable
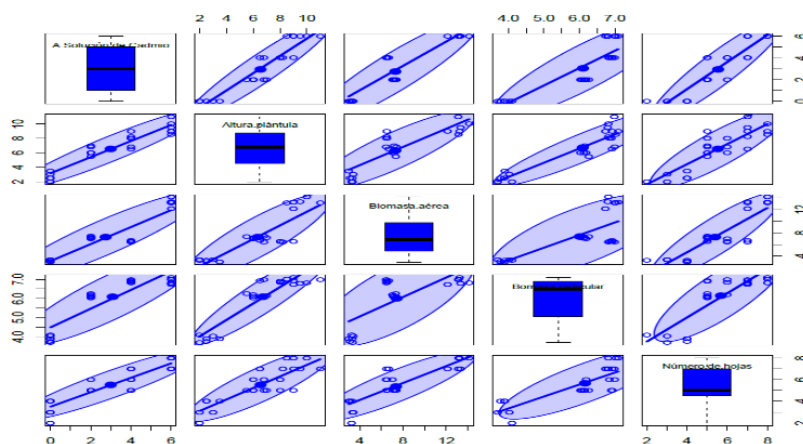

Figure 2 presents a scatterplot matrix with box plots and concentration ellipsoids to examine the relationship between cadmium (Cd) concentration in soil and its content in different plant parts (root, leaves), as well as BCF, TF, pH and electrical conductivity in cocoa seedlings inoculated with arbuscular mycorrhizal fungi. The results reveal a positive relationship between Cd concentrations in the soil and its content in different parts of the plant (root, leaves), BCF and electrical conductivity. This correlation is evidenced by a gradual increase in these variables as soil Cd concentration increases. The BCF of 2.67 ± 0.10 indicates a high potential of the plant to accumulate Cd in its leaves and roots, which is corroborated by the strong correlations observed be-

tween Cd in the soil and its content in the aerial parts. However, an inverse relationship was observed between Cd concentrations and TF, which means that the higher the concentration of Cd in the soil, roots and leaves, the less Cd is transferred to the aerial parts. The FT in this study was 0.7 ± 0.01. It is important to highlight the strong correlation between electrical conductivity and the presence of Cd in the soil, roots and leaves, with a maximum electrical conductivity value of 94.11 µS/cm. For the pH range studied, a significant correlation was observed with the Cd content. However, it is suggested to widen the pH range in future research, since cocoa growing soils tend to be more acidic.

Figure 2

Effect of cadmium application at different concentrations (0, 2, 4 and 6 mg/kg) on cadmium content in soil, root, leaves, FBC, FT, pH and electrical conductivity in cocoa seedlings with
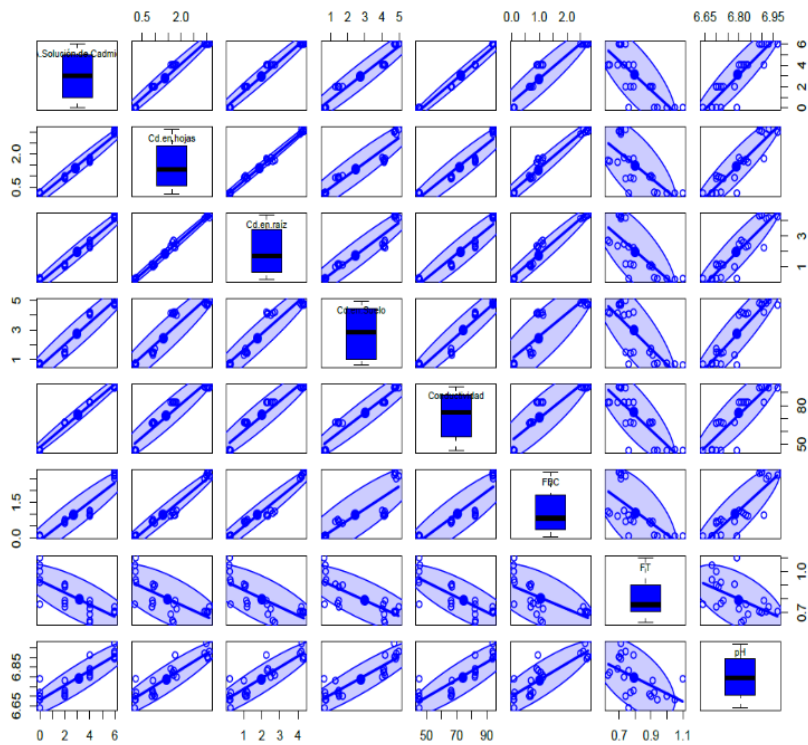

As a result of spore identification, ten genera were obtained in all the evaluated samples of arbuscular mycorrhizae in symbiosis with cocoa seedlings; the most representative genera were *Acaulospora* and *Entrosphospora* as shown in Fig. 3. The morphological observation of spores shows that they benefit plant growth and production, especially its ability to absorb soil nutrients, phosphorus and water.

Mitigation of Cadmium Uptake in Cocoa Seedlings (Theobroma cacao L.) Through Arbuscular Mycorrhizal Symbiosis of Contaminated Soils

131

Figure 3

Arbuscular mycorrhizal spores present in cocoa seedlings; A-d) Diversispore, B-E-O) Pa-cispora, C-J-W) Ambispora, F-Q-T-X) Acaulospora, G-U-V) Scutellospora, h) Racocetra, K-I-L-M) Entrosphospora, P-R-S) Gigaspora, y) Glomus.
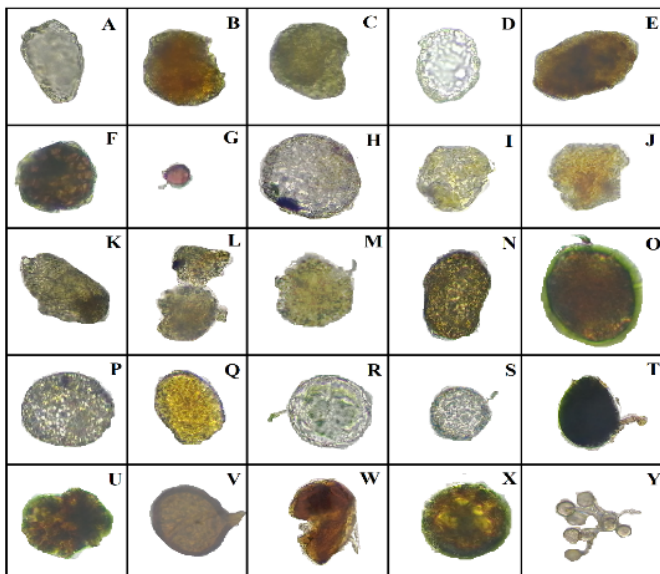

It was found that cocoa seedlings were 100% colonized in all treatments and typical fungal structures of arbuscular mycorrhizae such as intra and extra-radices hyphae, vesicles and arbuscules were observed (Fig. 4). This shows that mycorrhizae have a significant contribution in the phytostabilization of Cd in the rhizosphere of cocoa plants.

Figure 4

Mycorrhizal colonization of the roots of cocoa seedlings (Theobroma cacao L.)
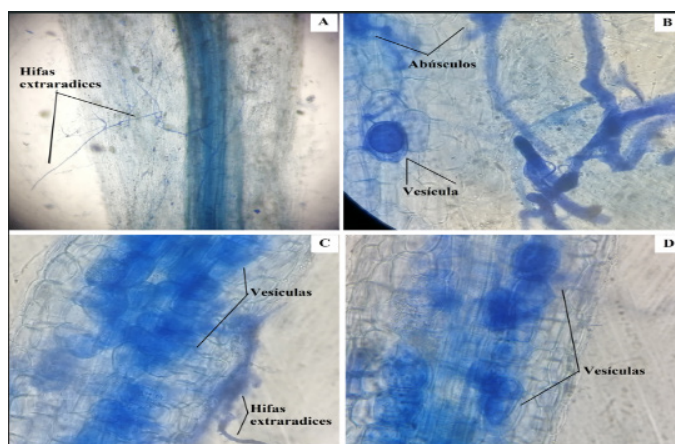
Discussions

The results presented in Figure 1 provide valuable information on the tolerance of cocoa seedlings inoculated with arbuscular mycorrhizae to Cd exposure in soil. The absence of negative effects on growth variables, and even the observation of enhanced growth at some Cd concentrations, suggests that arbuscular mycorrhizal symbiosis could play a protective role in the response of cocoa seedlings to Cd stress. This hypothesis is based on the ability of arbuscular mycorrhizae to enhance nutrient and water uptake by plants, which could compensate for the adverse effects of Cd and, in some cases, even stimulate growth (Tezara et al., 2016). The findings presented in Figure 2 provide information on the distribution and behavior of Cd in cocoa seedlings inoculated with arbuscular mycorrhizal fungi. The gradual accumulation of Cd in the plant parts as its concentration in the soil increases suggests that Cd uptake and retention mechanisms are not significantly affected by arbuscular mycorrhizal symbiosis. The high BCF indicates that cocoa has a high capacity to concentrate Cd, which could pose a risk to human health if this metal is transferred to the edible parts of the plant. However, the relatively low TF suggests that the arbuscular mycorrhizal symbiosis could limit the transfer of Cd to the aerial parts, which could reduce the risk of contamination in the cocoa bean. The strong correlation between electrical conductivity and the presence of Cd in soil, root and leaves suggests

that soil salinity could be influencing Cd availability and uptake by the plant. The significant relationship between pH and Cd content within the range studied indicates that soil acidity could affect Cd bioavailability. However, further studies are needed to explore this phenomenon in a wider pH range, representative of cocoa growing conditions.

Similar results have further explored the mechanisms of metal transfer from soil to grain, which is crucial for understanding bioaccumulation (Galvis, 2023). It also explores the potential of cadmium-tolerant rootstocks to reduce cadmium uptake, suggesting an effective tool to reduce levels in grain (Luis-Alaya et al.,2023).

The presence of arbuscule mycorrhizal symbioses that could play a role in the phytostabilization of cadmium in the soil, with the GRSP protein contributing to its immobilization and reduced availability to plants, is also discovered (Bisht et al., 2024), by selecting the most efficient AMF species that provide functional complementarity to the symbiosomes to induce Cd tolerance in pigeon pea plants (Blommaert et al., 2022). Inoculation of cocoa seedlings with arbuscular mycorrhizal fungi has been shown to result in increased plant growth, increased fruit production, and increased disease resistance. An example of these studies is the one conducted in 2021 in Ivory Coast (Rincón et al., 2021), where it was found that the arbuscular mycorrhizal fungi community contributes to

Mitigation of Cadmium Uptake in Cocoa Seedlings (Theobroma cacao L.) Through Arbuscular Mycorrhizal Symbiosis of Contaminated Soils

133

the establishment of seedlings and allows the development of sustainable systems in tropical environments similar to that of Ecuador. Another study, conducted in Ponce Erriquez, a mining area of Ecuador where cocoa crops have a dangerous exposure to heavy metals, is is interesting because of the level of exposure Ramos et al., 2022). Also, it was found in Colombian cocoa crops that mycorrhizal species can vary with respect to the concentration of Cd present in the soil, where *Diversispora spurca, Rhizoglomus spp*. and *Claroideoglomus etunicatum* stand out (Pineda et al., 2020). Our results coincide with research reported with inoculations of cocoa seedlings in the greenhouse phase, where their nutritional level has been increased (Ricárdez-Pérez et al., 2020).

Conclusions

The cadmium concentrations evaluated in this study did not negatively affect the growth of cocoa seedlings. In this context, arbuscular mycorrhizae are chosen as key allies to mitigate this risk. By colonizing 100% of the seedling roots, these fungi promote the phytostabilization of cadmium in the rhizosphere. This plant-mycorrhizal fungus symbiosis is presented as a promising strategy to reduce soil contamination by this heavy metal, thus protecting human health and the environment.

References

Andersson, M. and Gradstein, S. (2005). Impact of management intensity on non-vascular epiphyte diversity in cacao plantations in western ecuador. Biodiversity and Conservation, 14(5), 1101-1120. https://doi.org/10.1007/s10531-004-7840-5

Bisht, A., & Garg, N. (2024). Harnessing the role of arbuscular mycorrhizae in arresting nodular senescence by modulating osmolyte synthesis and ascorbate-glutathione pool in cadmium stressed pigeon pea. Plant Growth Regulation, 102(2), 409-427.

Blommaert, H., Aucour, A., Wiggenhauser, M., Moens, C., Télouk, P., Campillo, S., … & Sarret, G. (2022). From soil to cacao bean: unravelling the pathways of cadmium translocation in a high cd accumulating cultivar of theobroma cacao l. Frontiers in Plant Science, 13. https://doi.org/10.3389/fpls.2022.1055912

EPA Method 3051A: Microwave Assisted Acid Digestion of Sediments, Sludges, and Oils | US EPA. (2023, 31 julio). US EPA. https://www.epa.gov/esam/us-epa-method-3051a-microwave-assisted-acid-digestion-sediments-sludges-and-oils

Galvis, D. A., Jaimes-Suárez, Y. Y., Rojas Molina, J., Ruiz, R., León-Moreno, C. E., & Carvalho, F. E. L. (2023). Unveiling cacao rootstock-genotypes with potential use in the mitigation of cadmium bioaccumulation. Plants, 12(16), 2941. https://doi.org/10.3390/plants12162941

Luis-Alaya, B., Toro, M., Calsina, R., Ogata-Gutiérrez, K., Gil-Polo, A., Ormeño-Orrillo, E., … & Zúñiga-Dávila, D. (2023). Evaluation of the presence of arbuscular mycorrhizae and cadmium content in the plants and soils of cocoa plantations in san martin, peru. Diversity, 15(2), 246. https://doi.org/10.3390/d15020246

Mejoramiento de la calidad del cultivo de cacao en ecuador. (2020). Revista Venezolana De Gerencia. https://doi.org/10.37960/rvg.v25i3.33375

Neira, D. (2016). Energy efficiency of cacao agroforestry under traditional and organic management. Agronomy for Sustainable Development, 36(3). https://doi.org/10.1007/s13593-016-0386-6

Nieves-Orduña, H., Müller, M., Krutovsky, K., & Gailing, O. (2021). Geographic patterns of genetic variation among cacao (theobroma cacao l.) populations based on chloroplast markers. Diversity, 13(6), 249. https://doi.org/10.3390/d13060249

Pérez-Díaz, A., Aranda-Azaharez, R., Rivera-Espinosa, R. A., Bustamante-González, C. A., & Pérez-Suarez, Y. (2023). Indicadores de calidad para posturas microinjertadas de Theobroma cacao inoculadas con hongos micorrízicos arbusculares. Agronomía Mesoamericana, 51102-51102.

Pernía, B., Añazco, K., Mero, M., Mayía, Y., & Cobos, P. (2021). Efectos del cadmio sobre la germinación y crecimiento inicial de cinco variedades de oryza sativa l. cultivadas en ecuador. Acta Agronómica, 70(1), 82-92. https://doi.org/10.15446/acag.v70n1.87636

Pineda, J. F. S., Pérez, U. A., Rodriguez, A., & Rojas, E. T. (2020). Alta presencia de cadmio resulta en baja diversidad de hongos formadores de micorrizas arbusculares asociados a cacao (Theobroma cacao L.). Acta Biológica Colombiana/Acta BiolóGica Colombiana, 25(3), 333-344. https://doi.org/10.15446/abc.v25n3.78746

Ramos, C., Ruales, J., Rivera-Parra, J. L., Sakakibara, M., & Díaz, X. (2022). Sustainability of Cocoa (Theobroma cacao) Cultivation in the Mining District of Ponce Enríquez: A Trace Metal Approach. International journal of environmental research and public health, 19(21), 14369. https://doi.org/10.3390/ijerph192114369

Ricárdez-Pérez, J. D., Gómez-Álvarez, R., Álvarez-Solís, J. D., Pat-Fernández, J. M., Jarquín-Sánchez, A., & Ramos-Reyes, R. (2020). Vermicomposta y micorriza arbuscular, su efecto en la nutrición del cacao en fase de invernadero. Ecosistemas y recursos agropecuarios, 7(3).

Rincón, C., Droh, G., Villard, L., Masclaux, F. G., N'guetta, A., Zeze, A., & Sanders, I. R. (2021). Hierarchical spatial sampling reveals factors influencing arbuscular mycorrhizal fungus diversity in Côte d'Ivoire cocoa plantations. Mycorrhiza, 31(3), 289-300. https://doi.org/10.1007/s00572-020-01019-w

Solorzano, R., Risterucci, A., Courtois, B., Fouet, O., Jeanneau, M., Rosenquist, E., & Lanaud, C. (2009). Tracing the native ancestors of the modern theobroma cacao l. population in ecuador. Tree Genetics & Genomes, 5(3), 421-433. https://doi.org/10.1007/s11295-008-0196-3

Tezara, W., Urich, R., Jaimez, R., Coronel, I., Araque, O., Azócar, C., & Chacón, I. (2016). Does criollo cocoa have the same ecophysiological characteristics than forastero?. Botanical Sciences, 94(3), 563-574. https://doi.org/10.17129/botsci.552

Unda, S., Galarza, I., & Mora, E. (2021). Comparación de niveles de cadmio en hojas, testa y almendra en cultivares de theobroma cacao. Ciencia Unemi, 14(37), 73-80. https://doi.org/10.29076/issn.2528-7737vol14iss37.2021pp73-80p

Vallejos-Torres, G., Ruíz-Valles, R., María, C., Gaona-Jimenez, N., & Marín, C. (2021). Una alta diversidad de hongos micorrízicos arbusculares influye en la absorción de cadmio y crecimiento vegetal del cacao. Bioagro, 34(1), 75-84. https://doi.org/10.51372/bioagro341.7

Villacis, A., Alwang, J., Barrera, V., & Domínguez, J. (2022). Prices, specialty varieties, and postharvest practices: insights from cacao value chains in ecuador. Agribusiness, 38(2), 426-458. https://doi.org/10.1002/agr.21730

Villacis, A., Barrera, V., Alwang, J., Caicedo, C., & Quiroz, J. (2022). Strategies to strengthen ecuador's high-value cacao value chain.. https://doi.org/10.18235/0003960

Zug, K., Yupanqui, H., Meyberg, F., Cierjacks, J., & Cierjacks, A. (2019). Cadmium accumulation in peruvian cacao (theobroma cacao l.) and opportunities for mitigation. Water Air & Soil Pollution, 230(3). https://doi.org/10.1007/s11270-019-4109-x

Validation of the Tensile Test of A36 Steel Through Finite Element Method and Experimental Data

Isaac Simbaña

Grupo de Investigación en Ingeniería Mecánica y Pedagogía de la Carrera de Electromecánica (GIIMPCEM), Instituto Superior Universitario Sucre, Ecuador
Orcid: https://orcid.org/0000-0002-3324-3071

David Saquinga

Grupo de Investigación en Ingeniería Mecánica y Pedagogía de la Carrera de Electromecánica (GIIMPCEM), Instituto Superior Universitario Sucre, Ecuador
Orcid: https://orcid.org/0000-0001-8353-1621

Marco Macías

Grupo de Investigación en Ingeniería Mecánica y Pedagogía de la Carrera de Electromecánica (GIIMPCEM), Instituto Superior Universitario Sucre, Ecuador
Orcid: https://orcid.org/0009-0004-5386-4790

Leonidas Ramírez

Grupo de Investigación en Ingeniería, Productividad y Simulación Industrial (GIIPSI), Universidad Politécnica Salesiana, Ecuador
Orcid: https://orcid.org/0000-0003-2569-2974

Introduction

Structural steel, manufactured under the standards set by the American Society for Testing and Materials (ASTM) A36, finds widespread use in construction and structural engineering. Its versatility stems from its availability in various profiles and sheets, making it essential in the construction of buildings, industrial facilities, suspension bridge cables, and reinforcements (ASTM International, 2019). A36 structural steel is the primary material choice for building and bridge construction due to its ubiquity and reliability. Its low carbon content and absence of alloying elements are often linked to AISI 1018 steel due to its similar chemical composition (Márquez-Herrera et al., 2022). Moreover, its use facilitates compatibility with complementary materials at a reduced cost for finishing. However, drawbacks include the need for costly maintenance, as the material is susceptible to corrosion and necessitates periodic painting. Exposure to high temperatures can compromise its

structural integrity, while its profiles are prone to deformation with any torsion or movement (Rahangmetan et al., 2020).

The mechanical properties of a material encompass its inherent strength and resilience when subjected to external forces. In essence, they define a material's capacity to transmit and endure forces or deformations (Rodríguez et al., 2022). These properties are essential during the designing phase, as materials intended for engineering applications must exhibit sufficient mechanical strength to withstand various loads. This strength is quantified as stress, representing the relationship between the applied force and the cross-sectional area (Fajardo et al., 2019). Stress manifests as tension, compression, or stretching within a body subjected to an axial load, serving as a key indicator of how materials respond to external forces, potentially leading to deformation or fracture (Ramos-Quintero et al., 2022).

To ascertain the characteristics and properties of materials, researchers conduct experiments commonly referred to as material tests.

Gunter et al. (2021) describe these tests as laboratory experiments aimed at determining attributes such as stiffness, wear resistance, thermal or electrical conductivity, acidity, corrosion resistance, density, sound transmission, ductility, and impact resistance. A prevalent approach involves destructive testing, where methods are used to induce damage or breakage to the sample under analysis. This helps in comprehending and forecasting how the material will

respond to various physical stresses, essentially assessing its capacity to withstand such pressures (Prakash-Pasupulla et al., 2022). In destructive tests, the material cannot be reused, as these procedures often push the material's physical properties to their limits, sometimes surpassing them until failure occurs. This process aids in identifying the material's behavior in extreme conditions.

Material tests serve various purposes such as material testing and enhancement, defect detection and evaluation in the metal industry, failure analysis, and fundamental research on material strength. Tensile testing stands as a key mechanical method used to determine the characteristic values of materials. Throughout the tensile test, the force and elongation of the specimen are measured (Liao et al., 2020). The applied tensile force tends to stretch the material from both ends, allowing for the determination of its strength, until failure occurs. As the load reaches its maximum, a concentration of deformations occurs in the central zone, leading to necking and a reduction in cross-sectional area. As noted by Dhoska (2019), the test becomes unstable, and the resisted load gradually decreases over time.

Calderón et al. (2021) scrutinized the experimental outcomes concerning the tensile strength and hardness of A36 structural steel. Their experimental framework encompassed accounting for temperature fluctuations during the welding process, which triggers alterations in the steel's internal structure, thereby delineating a correlation between stren-

gth and hardness. The specimens exhibited an augmentation in their maximum stress tolerance, reaching up to 440 MPa. Additionally, it was affirmed that the surface hardness diminishes in the fusion zone owing to temperature variations, which affect these properties. In contrast, Serrano and Albán (2022) assessed the mechanical properties of welded joints employing A36 structural steel. The study was conducted experimentally and also using ANSYS software for simulations, with a relative error of less than 10 % between both analyses. They determined that the maximum stress attained was 468.68 MPa in flat specimens with an 8 mm thickness. These values are significantly influenced by the welding process used to obtain the specimens, indicating that thicker welds will increase the cross-sectional area, enabling them to support a greater load and resulting in higher stress.

The finite element method (FEM) is a numerical technique used to approximate the deformation of mechanical elements by defining various boundary and initial conditions, including movement constraints and the application of external forces, along with their directions (Vantyghem et al., 2020). This method entails breaking down the geometry of an element into small finite-sized elements with simple geometries and finite dimensions. Within each of these small elements, simple interpolation functions are established to correlate the displacements of individual points, known as nodes, within the finite element to the displacement of a series of characteris-

tic points within it. This process simplifies differential equations into algebraic equations that establish the relationship between the forces at the nodes and their displacements within each finite element (Arroba et al., 2021). By solving these algebraic equations for the finite elements composing the element and combining them, a system of equations is formulated for the original element. This approach provides an approximate solution for the displacement of each node in the problem, and subsequently for any point, utilizing the defined interpolation functions (González et al., 2020).

Larsen and Thorstensen (2020) highlight that this method originated in the 1 950s and has since found widespread use in both industry and research, enabling the analysis of an object's behavior without necessitating its physical construction. García-Garrino et al. (2021) conducted studies on processing challenges in Solid Mechanics, particularly focusing on large elastoplastic deformations using computational numerical simulation. The dominant tetrahedral technique has been deemed the most effective for mesh generation due to its versatility in adapting to various geometries. Moreover, adhering to the dimensions specified for specimens in different standards, simulation results have yielded the desired values for mechanical properties. It is advisable to gradually update work methodologies, such as integrating virtual machines (VMs) to allow the modification of one or more variables to obtain results for the dependent variables.

Computer-aided design (CAD) leverages computer systems as supportive tools across all processes involved in designing and manufacturing diverse products. Rigorous quality tests have been conducted, validating that the implemented components function correctly and meet specified requirements across various applications (Falivene et al., 2019). The primary utility entails utilizing computers to facilitate the creation, modification, analysis, or optimization of designs. In 3D modeling, it is notably straightforward to analyze surfaces and solidsBarenghi et al. (2019) suggest that CAD expedites task completion. CAD software is geared towards streamlining mechanical modeling in both 2D and 3D, offering diverse options for generating precise extractions, plans, and exchange files (Zhou et al., 2020).

On the other hand, computer-aided engineering (CAE), has evolved in response to the demands imposed by ongoing technological progress. Through CAE, a wide array of analyses can be performed, extending beyond structures or fluids to encompass thermodynamic processes, and acoustic and electromagnetic phenomena, among others. CAE software stands as a cornerstone tool in engineering, particularly in stress simulation and safety factor analysis. Wei et al. (2021) point out the availability of various CAE software applications for designing, analyzing, and simulating parts using finite element methods. These applications offer options for 3D modeling or importing geometries from CAD software, facilitating the transition to the preparation stage by generating a mesh and ensuring the discretized element is ready for FEM analysis. The outcomes of these simulations are instrumental in assessing the potential failure of specific components under defined load conditions and determining the requisite safety factors to be integrated into the design. This ensures stability during operation, mitigating the risk of mechanical failures induced by excessive loading forces beyond the parameters expected in typical usage scenarios (Al-shoaibi and Ali-Fageehi, 2022).

Research conducted by Erazo-Arteaga (2022) delved into the design, manufacturing, and computer-aided engineering (CAD/CAM/CAE) of product development in Latin America. Over the past decade, there has been significant evolution, particularly evident in the enhancements in vehicle, machinery, and general industrial supplies design and production. Notable progress has also been made in the development of prosthetics and medical equipment. There is a growing trend towards digital manufacturing development, which integrates these tools into automated facilities, adhering to the philosophy of global thinking and local manufacturing. One of the primary advantages of employing these computer-assisted techniques is cost reduction, starting with reduced time dedicated to the design, optimization, and manufacturing of various elements. Furthermore, the elimination of the need to construct prototypes for performance evaluation conserves essential resour-

ces, as this type of software enables the prediction of object behavior under specified conditions. Berselli et al. (2020) introduced CAD/CAE-based learning tools for use in higher education, particularly in engineering disciplines. Software optimization has led to improved result accuracy and a more user-friendly interface, contributing to the increasing application of these technologies across diverse industries.

Li et al. (2020) conducted experimental and numerical studies on the tensile strength of concrete specimens reinforced with structural steel fibers. The steel improved tensile deformation, mitigating the brittleness of structural elements. The relative error between the experimental procedure and numerical results was below 15 %. However, mathematical modeling enables the approximation of responses under various conditions, including impact and fatigue. Serrano-Aguiar et al. (2021) investigated the effect of cracks in welded joints of A36 structural steel under tension through computational numerical simulation. A qualitative analysis was performed using SolidWorks and ANSYS software, considering round A36 structural steel pipes ranging from 100 to 500 mm in diameter, available in the market. Upon applying an axial stress of 250 MPa to prevent permanent deformation of the pipes, it was

found that cracks acted as stress concentrators, with a relative error of 1.46 % between the experimental process and simulations for equivalent stress, reaching 648.5 MPa before fracture. Therefore, the authors concluded that the safety factor should be increased by 0.35 units to meet the requirements.

This study aims to validate obtained stress results through computational numerical analysis using CAD and CAE software by comparing them with values obtained from experimental tensile destructive testing. This necessity arises from the absence of a universal testing machine in several educational centers unable to afford its acquisition cost, though they have access to such software. This approach aims to enhance the explanation of mechanical properties and improve the learning and understanding of students in technical fields. The document is structured as follows: Materials and Methods used, explaining the experimental test and the process to carry out the simulations. The results present the figures and values obtained for their respective analysis. The Discussion section compares the scope of the results with the information found in the literature, along with the authors' perspective. Finally, the Conclusions section synthesizes the most relevant information and presents the assertions derived from this research.

Materials and Methods

The shapes of tensile specimens can vary significantly, prompting the ASTM

E8 standard (ASTM International, 2024) to define standard specimens for sheets,

thin sheets, tubes, jaws, and special specimen holders, along with standard round specimens for other metallic products. This standard specifies the initial lengths corresponding to all deformation values. Specimens must be manufactured without altering the material properties. The preferred specimen shapes, according to the ASTM E8 standard, are flat and round specimens, illustrated in Figure 1. This standard aims to outline the fundamental components of a tensile test and offers an overview of materials testing equipment, software, and necessary tensile samples. The dimensions provided by this standard have been consideredfor fabricating specimens in A36 structural steel.

Figure 1

Geometry of the specimen for the tensile test (ASTM International, 2024)
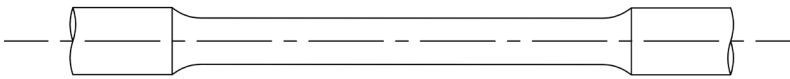
For the experimental tensile test, we utilized a Test Resources model 1608018 universal testing machine (Test Resources, 2024), which has a load capacity ranging from 15 to 150 kN. According to the manufacturer, it may have a minimum error of 0.2 % and a maximum value of 5 %, depending on the loads and clamping elements. A 12.7 mm diameter A36 structural steel shaft was machined following the dimensions specified in the ASTM E8 standard, as depicted in Figure 2a. Figure 2b illustrates the outcome of the tensile destructive test, where the specimen, as it undergoes permanent elongation, reduces its area until reaching the point of fracture. The maximum applied load was 34.53 kN, thus a value of 35 kN was designated for the application of the axial load in the simulations.

Figure 2

Specimen a) machined, b) after tensile test

a)

b)

In Figure 3a, the 3D modeling of the specimen conducted in CAD software, specifically SolidWorks, is depicted. This design was deemed essential to advance with the simulations. The process started with a structural static study within the CAD software. For the Finite Element Method (FEM) analysis, 10 861 elements and 47 060 nodes were generated for mesh creation, as illustrated in Figure 3b.

Figure 3
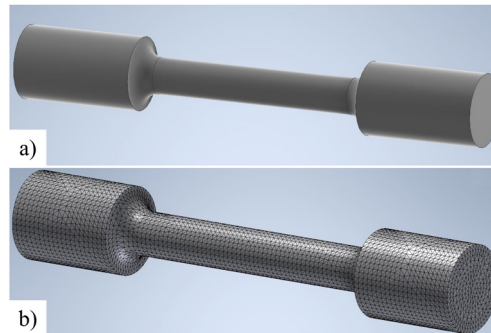
Specimen drawn in CAD software a) 3D modeling, b) meshing


a)

b)

Figure 4a shows how a fixed support was placed on the cylindrical surface on the left side, where the specimen is attached to the base of the universal testing machine. Figure 4b illustrates the application of the axial load outward to the cross-sectional area of the specimen, which was defined as 35 kN, considering the maximum load value applied in the experimental test.
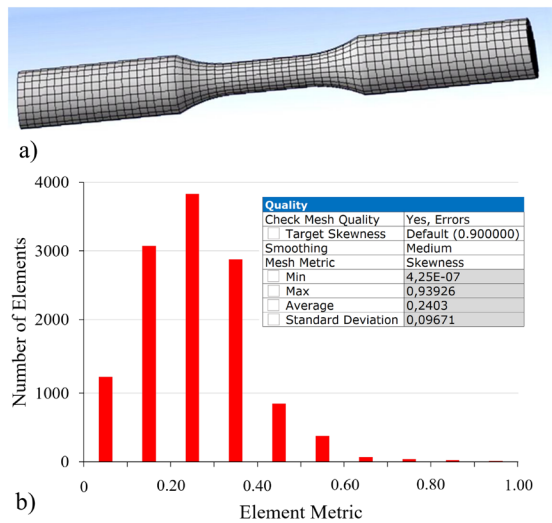
Figure 4

Initial conditions for the simulation a) fixed support, b) axial load

a)

b)
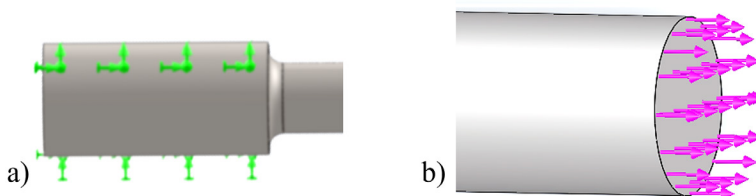
For the CAE analysis, we utilized the ANSYS software, equipped with various modules in the Workbench interface for conducting diverse studies. In Fig. 5a, it was noted that the mesh generation in the CAE software selected the default hexahedral option, resulting in 3 829 elements and 7 480 nodes. This meshing technique was continued due to its lower computational resource requirements, validated by the skewness metric, with an average value of 0.2403, considered excellent mesh quality as it falls below 0.25 (Simbaña et al., 2022). Fig. 5b provides an overview of the values achieved for discretizing the specimen in the mesh.

Figure 5

CAE Meshing: a) 3D Modeling, b) Metrics

a)

b)

Results

Figure 6 illustrates the stress-strain curve derived from the specimens employed in the experimental tests. Specimen 1 attained the highest ultimate strength value at 434.8 MPa, while specimen 3 exhibited the lowest value for this stress at 415.8 MPa. The average ultimate strength obtained from these experimental tests was 422.45 MPa, accompanied by a mean deformation of 4.2 mm.

Figure 6

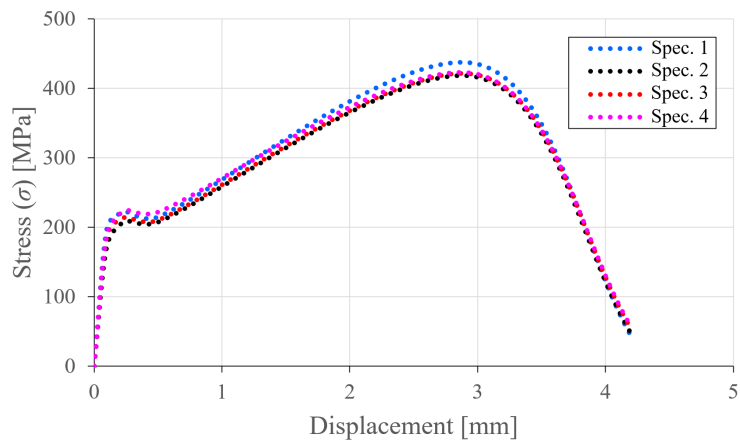*Stress-strain diagram of the specimens in the experimental process*

Figure 7 presents the outcomes of the computational numerical analysis for the tension test conducted in CAD software. It is noticeable that the most significant stress concentration appears in the regions where section changes occur, with the maximum stress recorded at 217.28 MPa. Although the color scale aids in comprehending the test results, the actual outcome, where the maximum stress ideally should be at the center of the specimen, is not distinctly evident. However, considering the dimensions recommended by the ASTM E8 standard and the application of the axial load obtained experimentally, the maximum stress closely aligns with the manufacturer's specified value of 420 MPa (American Metals Co., 2024).

Figure 7
CAD simulation for tensile stress

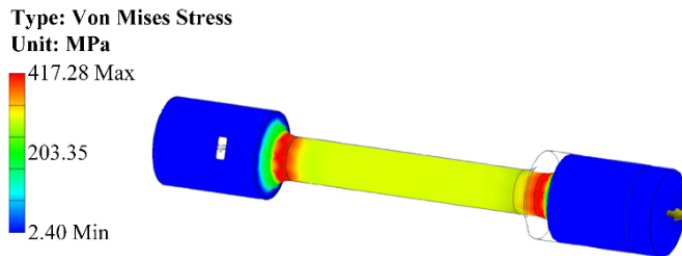Figure 8 displays the outcomes of the simulation conducted with CAE, employing the Explicit Dynamics module of ANSYS software. The maximum stress achieved until the specimen ruptured was 426.59 MPa, under identical geometric conditions, constraints, and applied axial load.
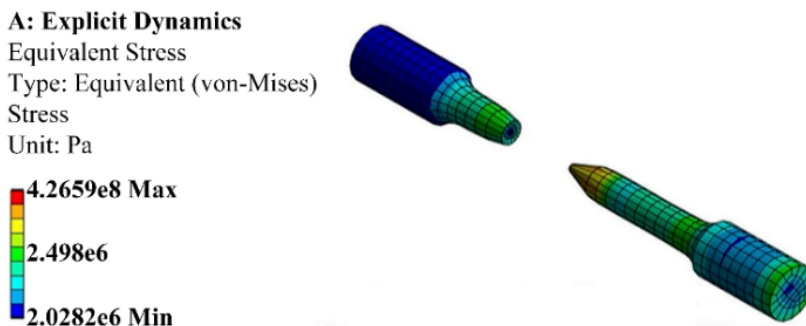
Figure 8
CAE Simulation for Tensile Stress

Figure 9 illustrates the stages obtained when conducting the simulation in specialized CAE software. This visually enhances the understanding of the process being conducted through the destructive tensile test, where the

application of axial load results in permanent elongation, leading to a reduction in the cross-sectional area until reaching the point where it cannot withstand the stress, ultimately leading to fracture.

Figure 9
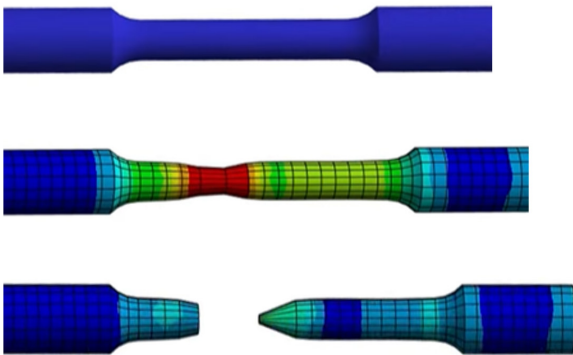*Stages of CAE simulation for the tensile test*

Figure 10 comparatively presents the stress values obtained for each procedure conducted in this research work, also indicating the stress value provided by the manufacturer of 420 MPa (American Metals Co., 2024). During the experimental destructive test, four specimens were used, and the average recorded stress was 422.45 MPa. On the other hand, through simulation in CAD and CAE software, the maximum stress was 417.2 and 426.59 MPa, respectively.

Figure 10
Comparative analysis of maximum stress results
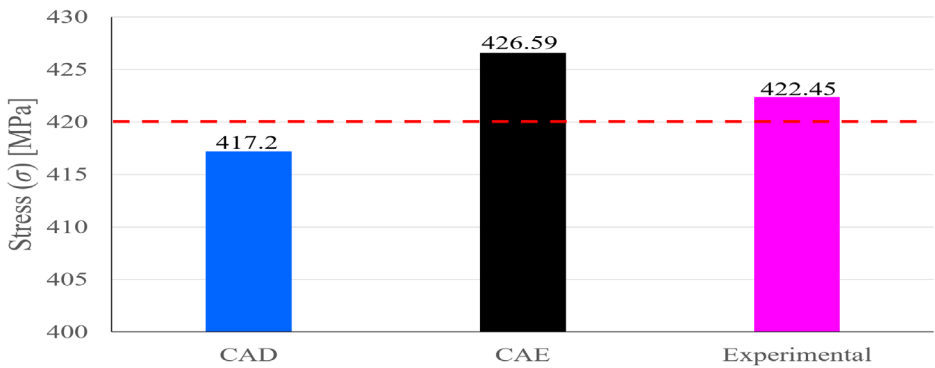
The accuracy of results produced by finite element methods relies on several factors, including the size of finite elements and the type of interpolation

functions employed. FEM models integrate mathematical equations with physical principles such as Newton's laws or Hooke's law, elucidating how forces interact with objects like polymer samples in test scenarios like compression or tension tests (Juárez-Luna and Ortiz Gálvez, 2021). Mesh generation procedures in software typically involve automatic meshing, which can be adjusted by concerning elements such as size, tolerance, and local control specifications. CAD or CAE software conceptualizes the model as a network of interconnected discrete elements. Meshing creates solid elements for individual analysis through discretization, with tetrahedra in 3D demonstrating the most reliable convergence (Ramírez et al., 2020). In the case of the tensile test, it starts with a theoretical phase, followed by sample preparation adhering to ASTM E8 standards [3], where cylindrical specimens with diameters of up to 12.7 mm are employed.

It is noteworthy that the manufacturer of A36 structural steel specifies in the datasheet that the maximum stress this material can withstand is 420 MPa.

However, external factors exert an influence on this value, such as exposure to environmental conditions with abrupt temperature changes, rainfall leading to corrosion, and even mishandling, which may induce internal cracks, thus compromising the steel's quality. These factors contribute to the observed variability in the experimental maximum stress values, resulting in an average exceeding the manufacturer's specified value. Consequently, a relative error was calculated concerning the manufacturer's provided value for the three cases analyzed, amounting to 0.67, 1.56, and 0.56 % for the maximum stress obtained in CAD software, CAE, and experimental testing, respectively. In literature reviews, researchers like Serrano and Albán, (2022) have validated both experimental and numerical results when they fall within a 10 % difference. Therefore, it can be asserted that utilizing technological tools such as SolidWorks and ANSYS software is valid for conducting this tensile test via computational numerical analysis in scenarios where the necessary equipment is unavailable.

Conclusions

A comparative analysis was performed on the maximum stress values obtained in the tensile testing of A36 structural steel specimens, conducted through experimental destructive testing and utilizing CAD and CAE software. The literature review indicates that studies on the tensile properties of A36 structural steel primarily emphasize the welding process, predominantly comprising experimental studies. While studies employing FEM often focus on material composition enhancement, the objective of this research was to validate the simulation process in CAD and CAE software for the tensile test

as an alternative to the experimental approach, thereby contributing to the scientific domain.

In the destructive tensile test, we adhered to the ASTM E8 standard, employing a universal testing machine and four specimens. These specimens endured a maximum axial load of 34.53 kN, resulting in an average maximum stress of 422.45 MPa. SolidWorks as CAD software and ANSYS Explicit Dynamics module as CAE software were employed for physical discretization and subsequent computational FEM. The maximum stress values recorded were 417.2 and 426.59 MPa using CAD and CAE software, respectively. Comparing these with the manufacturer's specified maximum stress of 420 MPa for A36 structural steel, a relative error of 0.67 % was observed for CAD software and 1.56 % for CAE software, whereas for the experimental test, this error was 0.56 %. Hence, considering the dimensions outlined in the ASTM E8 standard and the configuration of the maximum axial load derived from experimental results, the maximum stress outcomes obtained through CAD and CAE software are deemed valid, contingent upon the proficiency and skills of individual users.

References

Alshoaibi, A. and Ali-Fageehi, Y. (2022). 3D modelling of fatigue crack growth and life predictions using ANSYS. Ain Shams Engineering Journal, 13(4), 101636. https://doi.org/10.1016/J.ASEJ.2021.11.005

American Metals Co. (2024). A36 Steel Technical Datasheet. https://www.metalshims.com/t-A36-Steel-Technical-Datasheet.aspx

Arroba, C., Flores, M.., Salinas, J., Ortega, S. and Ortega, H. (2021). Experimental Tests and Numerical Analysis of the Structure of the Alternative Composite Material for the Repair of Flight Surfaces in Aircraft. Enfoque UTE, 12(2), 37-51. https://doi.org/10.29019/ENFOQUEUTE.723

ASTM International. (2019). A36/A36M Standard Specification for Carbon Structural Steel. https://www.astm.org/a0036_a0036m-14.html

ASTM International. (2024). E8/E8M Standard Test Methods for Tension Testing of Metallic Materials. https://www.astm.org/e0008_e0008m-22.html

Barenghi, L., Barenghi, A., Cadeo, C. and Di Blasio, A. (2019). Innovation by Computer-Aided Design/Computer-Aided Manufacturing Technology: A Look at Infection Prevention in Dental Settings. BioMed Research International, 2019. https://doi.org/10.1155/2019/6092018

Berselli, G., Bilancia, P. and Luzi, L. (2020). Project-based Learning of Advanced CAD/CAE Tools in Engineering Education. International Journal on Interactive Design and Manufacturing, 14(3), 1071-1083. https://doi.org/10.1007/s12008-020-00687-4

Calderón, L., Bohórquez, O., Rojas, M. and Pertuz, A. (2021). Experimental Relationship of Tensile Strength and Hardness of Welded Structural Steel. Journal of Physics: Conference Series, 2046(1), 012065. https://doi.org/10.1088/1742-6596/2046/1/012065

Dhoska, K. (2019). Tensile Testing Analysis of the HRB400 Steel Reinforcement Bar. International Journal of Innovative Technology and Interdisciplinary Sciences, 2(3), 253-258. https://doi.org/10.15157/IJITIS.2019.2.3.253-258

Erazo-Arteaga, V. (2022). El diseño, la Manufactura y Análisis Asistido por Computadora (CAD/CAM/CAE) y Otras Técnicas de Fabricación Digital en el Desarrollo de Productos en América Latina. Información Tecnológica, 33(2), 297-308. https://doi.org/10.4067/S0718-07642022000200297

Fajardo, J., Villa, M., Pozo, J. and Urgilés, D. (2019). Characterization of the Tensile Properties of an Epoxy-Carbon Laminated Composite Used in the Development of a Single-seater Formula SAE Type. Enfoque UTE, 10(3), 1-12. https://doi.org/10.29019/ENFOQUE.V10N3.381

Falivene, L., Cao, Z., Petta, A., Serra, L., Poater, A., Oliva, R., Scarano, V. and Cavallo, L. (2019). Towards the Online Computer-aided Design of Catalytic Pockets. Nature Chemistry 2019 11:10, 11(10), 872-879. https://doi.org/10.1038/s41557-019-0319-5

García-Garrino, C., Careglio, C., Pacini, E., Miraso, A., Papeleux, L. and Ponthot, J. (2021). Procesamiento de Problemas de Mecánica de Sólidos en Entornos de Cloud Computing. XXIII Workshop de Investigadores En Ciencias de La Computación (WICC 2021, Chilecito, La Rioja), August 2021, 963-968. http://sedici.unlp.edu.ar/handle/10915/120382

González, O., Martínez, G. and Graciano, C. (2020). Evaluación Paramétrica de las Principales Variables Geométricas en el Diseño de un Tren de Aterrizaje para un Avión Notripulado Utilizando el Método de los Elementos Finitos. Revista UIS Ingenierías, 19(2), 149-160. https://doi.org/10.18273/REVUIN.V19N2-2020017

Gunter, S., Marchenko, E., Yasenchuk, Y., Baigonakova, G. and Volinsky, A. (2021). Portable Universal Tensile Testing Machine for Studying Mechanical Properties of Superelastic Biomaterials. Engineering Research Express, 3(4), 045055. https://doi.org/10.1088/2631-8695/AC41B4

Juárez-Luna, G. and Ortiz-Gálvez, P. (2021). Importancia del Mallado de Elementos Finitos de Muros de Mampostería Confinada en el Análisis Sísmico de Edificios. Revista Internacional de Ingeniería de Estructuras, 26(4), 712-745. https://doi.org/10.24133/RIIE.V26I4.2640

Larsen, I. L. and Thorstensen, R. T. (2020). The Influence of Steel Fibres on Compressive and Tensile Strength of Ultra High Performance Concrete: A Review. Construction and Building Materials, 256, 119459. https://doi.org/10.1016/J.CONBUILDMAT.2020.119459

Li, X., Zhang, Y., Shi, C. and Chen, X. (2020). Experimental and Numerical Study on Tensile Strength and Failure Pattern of High Performance Steel Fiber Reinforced Concrete Under Dynamic Splitting Tension. Construction and Building Materials, 259, 119796. https://doi.org/10.1016/J.CONBUILDMAT.2020.119796

Liao, W., Chen, P., Hung, C. and Wagh, S. (2020). An Innovative Test Method for Tensile Strength of Concrete by Applying the Strut-and-Tie Methodology. Materials 2020, Vol. 13, Page 2776, 13(12), 2776. https://doi.org/10.3390/MA13122776

Márquez-Herrera, A., Saldaña-Robles, A., Zapata-Torres, M., Reveles-Arredondo, J. and De la Peña (2022). Duplex Surface Treatment on ASTM A-36 Steel by Slide Burnishing and Powder Pack Boriding. Materials Today Communications, 31, 103703. https://doi.org/10.1016/J.MTCOMM.2022.103703

Prakash-Pasupulla, A., Abebe-Agisho, H., Seetharaman, S. and Vijayakumar, S. (2022). Characterization and Analysis of TIG Welded Stainless Steel 304 Alloy Plates Using Radiography and Destructive Testing Techniques. Materials Today: Proceedings, 51, 935-938. https://doi.org/10.1016/J.MATPR.2021.06.305

Rahangmetan, K. A., Wullur, C. W. and Sariman, F. (2020). Effect Variations and Types of Smaw Welding Electrodes on A36 Steel to Tensile Test. Journal of Physics: Conference Series, 1569(3), 032052. https://doi.org/10.1088/1742-6596/1569/3/032052

Ramírez, J. D., Cabezas, K., Jiménez, P., Canelos, R. and Escobar, B. (2020). Calculation of Voltage Distribution along the Insulator Strings of a 500 kV Transmission Line Based on Finite Element Method. Enfoque UTE, 11(3), 1-14. https://doi.org/10.29019/ENFOQUEUTE.V11N3.619

Ramos-Quintero, M., Campozano-Riofrio, R. and Naranjo-Vargas, E. (2022). Análisis y Simulación de Fuerzas en el Trabajo de una Prensa Hidráulica a Planchas de Acero de Distintos Espesores

Aplicadas en Perfiles Estructurales Angulares. Polo Del Conocimiento: Revista Científico - Profesional, 7(2), 1632-1655. https://doi.org/10.23857/pc.v7i2.3670

Rodríguez, M., Urday, E., Pantigoso-Gómez, E. and Andrade-Tacca, C. (2022). Evaluación de Propiedades Mecánicas de un Acero Estructural A-36 en la Formación de Ferritas. Revista Iberoamericana de Ingeniería Mecánica, ISSN 1137-2729, Vol. 26, No 2, 2022, Págs. 47-59, 26(2), 47-59. https://dialnet.unirioja.es/servlet/articulo?codigo=8996231&info=resumen&idioma=ENG

Serrano-Aguiar, C., Calispa-Aguilar, M., Ordoñez-Viñan, M., and Choto-Chariguamán, L. (2021). Efecto de Fisuras en la Tracción de Juntas Soldadas de Acero A36 Mediante Simulación Numérica. Conciencia Digital, 4(4.2), 77-100. https://doi.org/10.33262/concienciadigital.v4i4.2.1948

Serrano, C. and Alban, D. (2022). Evaluation of Mechanical Properties and Metallographic Characterization of ASTM A36 Steel Welded Joints Under the GMAW Process. 1303-5150. https://doi.org/10.48047/nq.2022.20.22.NQ10250

Simbaña, I., Quitiaquez, W., Estupiñán, J., Toapanta-Ramos, F. and Ramírez, L. (2022). Performance Evaluation of a Direct Expansion Solar-assisted Heat Pump by Numerical Simulation of the Throttling Process in the Expansion Device. Revista Técnica "Energía," 19(1), 110-119. https://doi.org/10.37116/REVISTAENERGIA.V19.N1.2022.524

Test Resources. (2024). 315 Universal Test Machines. https://www.testresources.net/test-machines/universal-testing-machines/300-series/315

Vantyghem, G., De Corte, W., Shakour, E. and Amir, O. (2020). 3D Printing of a Post-tensioned Concrete Girder Designed by Topology Optimization. Automation in Construction, 112, 103084. https://doi.org/10.1016/J.AUTCON.2020.103084

Wei, W., Peng, F., Li, Y., Chen, B., Xu, Y. and Wei, Y. (2021). Optimization Design of Extrusion Roller of RP1814 Roller Press Based on ANSYS Workbench. Applied Sciences 2021, Vol. 11, Page 9584, 11(20), 9584. https://doi.org/10.3390/APP11209584

Zhou, T., McBride, K., Linke, S., Song, Z. and Sundmacher, K. (2020). Computer-aided solvent selection and design for efficient chemical processes. Current Opinion in Chemical Engineering, 27, 35-44. https://doi.org/10.1016/J.COCHE.2019.10.007

Board and authors

Lenin E. Cevallos-Robalino, Ph.D.

Lenin Estuardo Cevallos Robalino is a university professor in the Mechatronics Engineering program at Universidad Politécnica Salesiana, Guayaquil campus. He has a solid academic background, he holds a degree in Industrial Engineering (2009), a Master's degree in Nuclear Science and Technology (2014), and a Ph.D. in Sustainable, Nuclear, and Renewable Energy (2019). He completed a postdoctoral fellowship at the Neutron Standards Laboratory of the Center for Energy, Environmental, and Technological Research (CIEMAT) in 2024. His main research areas include neutron detection, dosimetry, gamma spectrometry, and shielding calculations using Monte Carlo methods, in which he has published numerous articles in high-impact international scientific journals and has participated in various scientific conferences and symposiums. He is a member of the Spanish Nuclear Society (since 2017) and the Ecuadorian Association of Radiological Protection (since 2024). Currently, he is a researcher at the Universidad Politécnica Salesiana, Guayaquil campus, where he is part of the Research Group in Micro-Nanotechnology and Nuclear Energy (NANOTECH). Additionally, he serves on the technical and scientific committee of the International Congress of Science, Technology, and Innovation for Society (CITIS) and was the Chairperson in its 2023 and 2024 editions.

María Alejandra De La Cruz Mora, MSc.

Alejandra De la Cruz is a Natural Resources Biotechnology Engineer (2019) from Universidad Politécnica Salesiana and a Master's degree in Industrial Engineering with a specialization in Quality and Productivity (2022) from Universidad San Francisco de Quito. She currently serves as Laboratory Coordinator and Professor in the Biotechnology Program at Universidad Politécnica Salesiana in Guayaquil. Throughout her professional career, she has actively participated in research and development projects in the field of applied sciences to biological resources for both private companies and the public sector, with a focus on optimizing biotechnological processes to obtain high-value-added services and products. Her experience and knowledge have positioned her as an active member of the Research Group in Biotechnology Applications and speaker at the workshop of the International Congress of Science, Technology, and Innovation for Society (CITIS).

Juan Alcides Cárdenas-Tapia, SDB, Ph.D.

He holds a Ph.D. in Education and Society from the University of Barcelona, Spain; a Master's Degree in Research in Didactics, Training, and Educational Assessment from the University of Barcelona, Spain; a Graduate Diploma in Higher Education Evaluation from the Universidad Politécnica Salesiana, Ecuador; a Bachelor's Degree in Educational Sciences with a specialization in Psychopedagogy from the Universidad Politécnica Salesiana, Ecuador; and a specialization in Ecclesiastical Baccalaureate in Theology from the Pontifical Xaverian University of Bogotá, Colombia. He presides over the Publications Council of the Universidad Politécnica Salesiana; he is the main investigator in several research groups, and the author of various scientific publications focused on education. He has held several roles, including Professor at the Universidad Politécnica Salesiana; Rector of the Mario Rizzini Educational Unit; Director of the Salesian Community of Yanuncay-Cuenca; Provincial Delegate for Youth Ministry and member of the Provincial Council; President of the National Council of Salesian Education (CONESA), and National Director of University Ministry.

Daniel Patiño-Vásquez

Software developer with more than 9 years of experience in continuous learning. He has contributed to society and education through research in various areas of computing.

Joe Llerena-Izquierdo

Computer Engineer and university professor at the Universidad Politécnica Salesiana in Guayaquil, Ecuador. He is a Researcher and coordinator of the Research Group on Teaching and Learning of Sciences for Engineering (GIEACI).

Angela Pacheco

Angela Pacheco Flores De Valgaz is a professor-researcher at the Universidad Politécnica Salesiana, specialized in applied biosciences and biodiscovery. Her work focuses on beneficial fungi for crops, phytochemistry, and food contaminants.

Jaime Fabián Vera Chang

He is a professor at the Universidad Técnica Estatal de Quevedo (UTEQ) of the Faculty of Industry and Production Sciences, Food Career, with a degree in Agricultural Engineering from UTEQ, a Master's Degree in Food Processing from Universidad Agraria del Ecuador and a PhD from the Universidad Americana de Europa in Mexico. At UTEQ, he is a professor of the Master's Degree in Agricultural Biotechnology and has held leadership roles in research, being a member of the Technical Research Committee and president of the Research Committee of

the Faculty of Livestock Sciences. In addition, he participates in the international arbitration of scientific articles for prestigious journals and is an external peer evaluator for several institutions.

Luis Humberto Vásquez Cortez

He is a research Professor at the Faculty of Agricultural Sciences of the Agroindustry Career "Universidad Técnica de Babahoyo (Ecuador)" and Universidad Nacional de Cuyo (Argentina). He has two master's degrees in Agroindustry, from the Universidad Técnica de Manabí, including one with a Major in Quality Management and Food Safety from Universidad Laica Eloy Alfaro de Manabí, a Diploma in Higher University Teaching in Mexico, and is currently pursuing a Doctorate in Engineering. of Products and Processes of the Food Industry. He has received an Honoris Causa Doctorate from the Association of Masters, Doctors, Postdoctors of Lima, Peru, and the Unesco Chair for his contribution to the scientific community and for his connection to the conservation of *Theobroma bicolor*. He participates in the international arbitration of articles for prestigious journals and is an external evaluator for several institutions.

María Fernanda Jumbo Tejena

She is an agricultural Engineer graduated from Universidad Técnica Estatal de Quevedo with a solid background in agricultural sciences. She has demonstrated a strong commitment to sustainable development in the agricultural sector. Currently, Maria Fernanda is expanding her knowledge.

Sanyi Lorena Rodríguez Cevallos

Eighth semester student in the Food Engineering Degree at the Faculty of Industry and Production Sciences at Universidad Técnica Estatal de Quevedo. Her passion for scientific research has led her to co-author several articles published in indexed journals. With a deep interest in innovation and development within the food field, Sanyi has become a promising young researcher, contributing significantly to scientific literature from an early age.

Matteo Radice

Professor-Researcher at the Department of Earth Sciences at UEA, where he began his career in 2013 through the Senescyt Prometheus Program. His research focuses on the development of Biotrade products, especially vegetable and essential oils, with a focus on the chemical characterization and bioactivity of secondary metabolites. He has contributed to productive and sustainable development in the Amazon, advising public policies and creating value chains in the cosmetic and natural products sectors for local communities.

Gabriel Usiña

He is a Mechanical Engineer, and he has been working in the industrial field for several years. He holds a master in Mechanical Engineering at Universidad Politécnica Salesiana in 2023.

Cristian Leiva-González

Mechanical Engineer with a Master's degree in Materials, Design and Production, with 10 years of experience in Maintenance and Production in local and multinational companies as well as more than 10 years of experience in university teaching. He is currently teaching and researching at Universidad Politécnica Salesiana

Erika Pilataxi

She received her degree in Business Administration in 2018. She obtained her degree in Mechanical Engineering from Universidad Politécnica Salesiana, in 2020. With experience in the control and transport of hydrocarbons, she works as a laboratorian at Universidad Politécnica Salesiana, where she has a career in mechanical engineering. Her research fields are related to Surface Quality Analysis, Materials Science, and Strength of Materials.

Mayra Comina

PhD in Automation and Robotics from the Polytechnic University of Madrid with Cum Laude honors. She has a Master's Degree in Automation and Robotics from the same university and is a Mechatronics Engineer from Universidad de las Fuerzas Armadas ESPE. She has published articles in international conferences and high-impact journas addressing innovative topics related to Mechatronics.

Alexandra Verdugo

Mechatronics engineer with experience in research, teaching and project development in IoT and cyber-physical systems at Universidad de las Fuerzas Armadas ESPE. She has skills in programming, management of laboratory equipment and leadership of multidisciplinary teams.

Jorge Comina

Civil engineer from Universidad Politécnica Salesiana, he has a master's degree in Structural Calculation from the UDIMA. He has worked as a trainer in various areas of Engineering and has held administrative positions in public companies in Quito.

Walter Verdugo

Systems engineer and professor with advanced degrees in information systems and mathematical methods. He has worked in teaching and research at Universidad Politécnica Salesiana and has held administrative positions. His research focuses on cloud computing and smart cities.

David Saquinga

He is a Mechanical Engineer from the Universidad de las Fuerzas Armadas ESPE and has a Master in Mechanical Design from the Universidad Politécnica del Chimborazo. He currently works as Coordinator of the Electromechanics Course at the Instituto Superior Universitario Sucre

Xavier Vaca

Mechanical Engineer from the Universidad Politécnica Salesiana and has a Master in Computer Aided Manufacturing and Design from the Universidad de las Fuerzas Armadas ESPE. He is a Professor-Researcher at the Engineering, Productivity and Industrial Simulation Research Group (GIIPSI).

Maribel Torres

Petroleum Engineer from the Escuela Politécnica Nacional in 2015; has a Master's in Production and Industrial Operations from the Universidad Politécnica Salesiana in 2022. Her research field is related to Operations Management, Structural Design, Manufacturing Processes, and Simulation.

William Quitiaquez

Mechanical Engineer from the Universidad Politécnica Salesiana in 2011; has a Master's in Energy Management from Universidad Técnica de Cotopaxi, in 2015; a Master of Engineering from the Universidad Pontificia Bolivariana de Medellín, in 2019; holds a Ph.D. in Engineering from the Universidad Pontificia Bolivariana de Medellín, in 2022. He is the coordinator of the Productivity and Industrial Simulation Research Group (GIIPSI) of Universidad Politécnica Salesiana. His research field is related to Renewable Energy Sources, Thermodynamics, Heat Transfer, and Simulation.

Isaac Simbaña

Mechanical Engineer from Universidad Politécnica Salesiana, in 2018; has a Master's Degree in Mathematical Methods and Numerical Simulation in Engineering from the Universidad Politécnica Salesiana in 2022; a Master's Degree in Education from the Universidad Politécnica Salesiana in 2023. He currently

works in the Electromechanical Career at the Instituto Superior Universitario Sucre. His research fields are related to Numerical and Statistical Analysis, as well as Thermodynamics, Manufacturing Processes, Materials Science, and Educational Innovation.

Patricio Quitiaquez

Mechanical Engineer degree from Escuela Politécnica Nacional in 2002; and has Master's Degree in Production Management from the Universidad Técnica de Cotopaxi, in 2007. His research field is related to Operations Management, Structural Design, Manufacturing Processes, and Simulation. He is a member of the Productivity and Industrial Simulation Research Group (GIIPSI) of Universidad Politécnica Salesiana

Jose Luis Ballesteros Lara

PhD in Biomedical and Biotechnological Sciences from the Universidad de Ferrara. He has a Master's Degree in Ethnobiopharmacy and Sustainable Use of Biodiversity from Universidad de Pavia and is an Engineer in Biotechnology from the Universidad Politécnica Salesiana. He is currently Director of the Biotechnology program at Universidad Politécnica Salesiana and coordinator of the Biotechnology Applications Research Group (GIAB). He has published multiple publications in high-impact journals on topics related to biodiscovery and food safety.

Kevin Gabriel Cedeño Vinces

Master's Degree in Industrial Production and Operations from the Universidad Politécnica Salesiana; He also holds a Master in Management of Chemistry Laboratories from Universidad Politécnica del Litroral (ESPOL). He is a Chemical Engineer from University of Guayaquil. He is currently a teaching technician of the Biotechnology degree at Universidad Politécnica Salesiana; he is part of the Research Group on Biotechnology Applications (GIAB) where he has the role of researcher. He has published multiple publications in high-impact journals on topics related to food safety and industrial processes.

Ricardo Salazar

Chemical Engineering degree from the Universidad Central del Ecuador in 2017; has a Master's in industrial production and operations from Universidad Politécnica Salesiana in 2022.;} His research field is related to wastewater treatment plants, in the pharmaceutical sector both in quality control and production

Jairo Jaime-Carvajal

Professor and researcher at UPS, specialized in heavy metals, phytochemistry and bioremediation. His research focuses on the chemical analysis and antioxidant activity of endemic Ecuadorian speciesand on the mitigation of cadmium absorption in cocoa through mycorrhizal symbiosis.

Jaime Naranjo-Moran

Professor and researcher at UPS, with experience in bioremediation, botany, molecular biology and plant biotechnology. His work includes bioprospecting of ericoid mycorrhizae in Ecuador, the study of Na and Pb absorption in cucurbits, and the interaction mechanisms of nematodes with parasites and predators.

Marco Macías

He has a Technical Bachelor's Degree in Industrial Mechanics from Colegio Técnico San José and a Specialist in Machining and Metal Constructions. He is currently a graduate of the Higher Technology Degree in Electromechanics from the Instituto Superior Universitario Sucre

Leonidas Ramírez

He is a Mechanical Engineer from the Escuela Politécnica Nacional and a Master in Mechanics with a specialization in Design from Universidad Técnica de Ambato. He is a Professor-Researcher at the Engineering, Productivity and Industrial Simulation Research Group (GIIPSI) of the Universidad Politécnica Salesiana.